UNIVERSITÀ DEGLI STUDI DI TRIESTE

Dipartimento di Scienze della Vita

XXVIII CICLO DEL DOTTORATO DI RICERCA IN

NEUROSCIENZE E SCIENZE COGNITIVE

Indirizzo Neurobiologia

Adenosine-mediated modulation of muscular nAChRs both transplanted into *Xenopus laevis* oocytes and expressed naturally in skeletal muscle cells

Settore scientifico-disciplinare: BIO/09-Fisiologia

PhD student:
Elisa Ren

Coordinator:
Prof. Walter Gerbino

Supervisor:
Prof. Annalisa Bernareggi

Academic Year 2014 / 2015

CONTENTS

To Giorgio…

Knowledge in its simplest form is a beautiful gift with unpredictable impact.

Seeking it requires no justification.

John Logsdon

ABSTRACT

Adenosine (Ado) is an important nucleoside widely distributed in all living organisms that contributes to the regulation of highly heterogeneous cellular function acting *via* P1-purinergic receptors (P1Rs). The P1Rs belong to the superfamily of G-protein coupled receptor and are divided in 4 subtypes according both to their affinity for Ado (high affinity: A_1R and $A_{2A}R$; low affinity: $A_{2B}R$ and A_3R) and their ability to activate or inhibit adenylyl cyclase (A_1R and A_3 subtypes mainly inhibit adenylyl cyclase activity *via* G_i proteins, whereas A_{2A} and A_{2B} receptors stimulate adenylyl cyclase *via* G_s proteins).

In this study I investigated the purinergic modulation mediated by Ado and P1Rs on the activity of the nicotinic acetylcholine receptors (nAChRs) expressed in skeletal muscle. To do that, I used different electrophysiological approaches.

In the first part of my thesis I analyzed the crosstalk between P1Rs and the embryonic isoform of the nAChRs transplanted into *Xenopus* oocytes after the injection of myotube cell membranes. This approach, the so-called microtransplantation technique, allows the study of ion channels and receptors functionally incorporated into the oolemma, while they are still embedded in their native lipid environment. By using the two-electrode voltage-clamp technique I characterized the effect of Ado and specific ligands for P1Rs on the ACh-induced current desensitization recorded in oocytes after the injection. The desensitization was measured as the time necessary for the current to decay by 10% and 50% from its peak value. For comparison, experiments were also performed on myotubes *in vitro* by using the patch-clamp technique in whole-cell configuration, under similar conditions. The results showed that the purinergic modulation mediated by the P1Rs on the current decay recorded in oocytes was different to that observed in myotubes. In the first case, it was mediated by the A_1R,

whereas in myotubes it was sustained by the $A_{2B}R$ subtype. Thus, the “native” interplay between the two receptors (P1Rs and embryonic nAChRs) was lost after the microtransplantation.

In the second part of my study, the Ado-mediated activity was analyzed at the endplate region of the adult skeletal muscle fiber, where the embryonic nAChRs is replaced by the adult isoform. Here I performed patch clamp recordings in cell-attached configuration to test the effect of Ado and specific P1Rs ligands on the single channel activity of nAChRs. The results demonstrated the capability of the low affinity P1 subtypes to increase the open probability and the mean open time of the channels. This is the first evidence of a possible involvement of postsynaptic P1Rs in affecting the properties of synaptic transmission at the neuromuscular junction.

RIASSUNTO

L'adenosina è un importante nucleoside endogeno che contribuisce alla regolazione di numerosi processi biologici tramite attivazione di recettori di membrana accoppiati a proteine G, denominati recettori purinergici P1. I recettori P1 sono suddivisi in 4 sottotipi (A_1, A_{2A}, A_{2B} e A_3) e la loro classificazione dipende dall'affinità che hanno verso l'agonista endogeno (alta affinità: A_1, A_{2A}; bassa attività: A_{2B}, A_3) e dalla capacità di attivare (A_{2A}, A_{2B},) o inibire (A_1, A_3) l'enzima adenilato ciclasi.

In questa tesi ho studiato la modulazione purinergica mediata da adenosina sull'attività biofisica del recettore acetilcolinico nicotinico espresso nel muscolo scheletrico. Per fare questo ho utilizzato diversi approcci sperimentali.

Nella prima parte della tesi, ho analizzato il crosstalk tra i recettori P1 e recettori acetilcolinici embrionali espressi in membrane cellulari isolate da miotubi e microiniettate in ovociti di rana *Xenopus laevis*. Questa tecnica, denominata tecnica del microtrapianto presenta il vantaggio di studiare recettori e/o canali ionici esogeni "funzionalmente" trapiantati nell'oolemma ancora circondati dal loro ambiente fosfolipidico nativo. Con il voltage-clamp a due elettrodi ho caratterizzato l'effetto dell'adenosina e di specifici ligandi dei recettori P1 sullo stato di desensibilizzazione del recettore nicotinico funzionalmente incorporato nella membrana degli ovociti. La desensibilizzazione è stata misurata come il tempo di decadimento della corrente indotta da ACh al 10% e al 50 % rispetto alla sua ampiezza massima.

Esperimenti analoghi sono stati condotti nei miotubi differenziati *in vitro* con la tecnica del patch-clamp nella configurazione di whole-cell. I risultati hanno dimostrato che la comunicazione tra i due recettori è alterata quando le membrane dei miotubi sono inserite in quelle dell'ovocita. In questo caso, la modulazione è mediata dal recettore P1

del sottotipo A_1, invece nel miotubo dal recettore del sottotipo A_{2B}. La comunicazione nativa tra i due recettori (recettori P1 e recettori nicotinici embrionali) viene quindi persa con il microtrapianto.

Nella seconda parte della tesi, ho analizzato il crosstalk tra recettori P1 e i recettori nicotinici nella giunzione neuromuscolare, dove l'isoforma embrionale del recettore per l'acetilcolina è sostituita con l'isoforma adulta localizzata a livello di placca motrice.
Gli esperimenti sono stati eseguiti con la tecnica del patch-clamp nella configurazione di cell-attached per studiare l'effetto dell'adenosina e dei ligandi per i recettori P1 sull'attività di singolo canale del recettore nicotinico. I risultati hanno dimostrato che l'attivazione dei recettori P1 a bassa affinità è in grado di aumentare la probabilità e il tempo medio di apertura del canale. Questa è la prima evidenza sperimentale di un possibile coinvolgimento dei recettori P1 postsinaptici nella modulazione della trasmissione sinaptica nella giunzione neuromuscolare.

GLOSSARY

α-Btx	α-Bungarotoxin
ACh	Acetylcholine
AChE	Acetylcholinesterase
AChR	Acetylcholine receptor
ADA	Adenosine deaminase
AC	Adenylyl cyclase
ADO	Adenosine
ADP	Adenosine diphosphate
ADK	Adenosine kinase
AMP	Adenosine monophosphate
ANS	Autonomic nervous system
ATP	Adenosine triphosphate
CNS	Central nervous system
cAMP	cyclic Adenosine Monophosphate
cDNA	complementary DNA
ChAT	Choline acetyltransferase
CGRP	Calcitonin gene-related peptide
DAG	Diacylglycerol
DM	Differentiation medium
ENTPD1	Ectonucleoside triphosphate diphosphohydrolase 1
FDB	Flexor digitorum brevis
GABA	γ-Aminobutyric acid
GIRK	G-protein activated inwardly rectifying k^+
GM	Growth medium
GPCR	G-protein coupled receptor
I_{ACh}	Acetylcholine-activated current
IP_3	Inositol 1,4,5-triphosphate
$I_{K,cAMP}$	cAMP-dependent K^+ current
LEMS	Lambert-Eaton myasthenic syndrome
mAChR	Muscarinic acetylcholine receptor
MAPK	Mitogen-activated protein kinase
MS-222	Tricaine methane sulfonate
nAChR	Nicotinic acetylcholine receptor
NMJ	Neuromuscular junction
NSCC	Nonselective cation channels
NT5E	Ecto-5'-nucleotidase
R_m	Membrane input resistance
RT	Room Temperature
PD	Parkinson disease
PLC	Phospholipase C
PKA	cAMP-dependent protein kinase
PKC	C-Protein kinase
PNS	Peripheral nervous system
PTK	Protein tyrosine kinase
V_m	Resting membrane potential
SAH	S-Adenosyl-L-homocysteine

SAC	Stretch-activated channels
Ser	Serine
CM	Culture medium
VAChT	Vesicular ACh transporter
VDCC	Voltage-dependent Ca^{2+} channels
TEA	Tetraethylammonium
Thr	Threonine
TM	Transmembrane domain
Tyr	Tyrosine
TPA	12-O-tetradecanoylphorbol-13-acetate
TTX	Tetrodotoxin
VAChT	Vesicular ACh transporter
TEVC	Two-electrode voltage clamp

CHAPTER 1

INTRODUCTION

1.1 Acetylcholine receptors in skeletal muscle tissue

1.1.1 The neurotransmitter acetylcholine

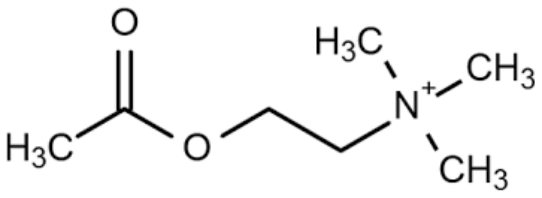

FIGURE 1.1: Structure of acetylcholine.

Acetylcholine (Fig. 1.1), often abbreviated as ACh, is a small, organic molecule that is derivative of choline and acetic acid. It is an excitatory neurotransmitter involved in a wide range of physiological processes both in the central (CNS) and peripheral nervous systems (PNS).

In the autonomic nervous system (ANS) and at the neuromuscular junction level (NMJ), ACh is used to signal muscle movement. On the other hand, ACh performs several different functions based on the different locations of nerve cells in the brain. Some of these functions include the modulation of pain, the regulation of neuroendocrine function, the regulation of REM sleep cycles, and the process of learning and memory formation.

The ACh synthesis takes place in specific neurons also called cholinergic cells, by the choline acetyltransferase (ChAT) the enzyme-catalyzed the condensation of choline and acetyl-coenzyme A. The choline is recycled for ACh synthesis. Following its synthesis,

ACh is transported into storage vesicles by the vesicular ACh transporter (VAChT) in the nerve ending. ACh uptake in the vesicle is driven by a proton-pumping ATPase. Coupled counter transport of H^+ and ACh allows the vesicle to remain isosmotic and electroneutral.

The adult skeletal myofiber is innervated by a single motor axon that terminates and arborizes over a small patch of the muscle fiber membrane, where the neurotransmitter receptors are localized. After the arrival of the action potential at the axon terminal, ACh is expelled into the synaptic cleft as a quantum with a content of about 6000-10000 ACh molecules per vesicle [2]. At the presynaptic membrane the site of synaptic vesicle fusion is known as “active zone” and the release is regulated by voltage-dependent Ca^{2+} channels. ACh diffuses across the synaptic cleft acting on multiple sites including presynaptic and postsynaptic nicotinic and muscarinic receptors.

After the release, the enzyme acetylcholinesterase (AChE) converts ACh into the inactive metabolites acetate and choline. This enzyme is abundant in the synaptic cleft, and its role in rapidly clearing free ACh from the synapse is essential for proper synaptic function. Choline molecules are taken up by the nerve terminal to be recycled into ACh again. Fig. 1.2 shows the typical organization of a NMJ.

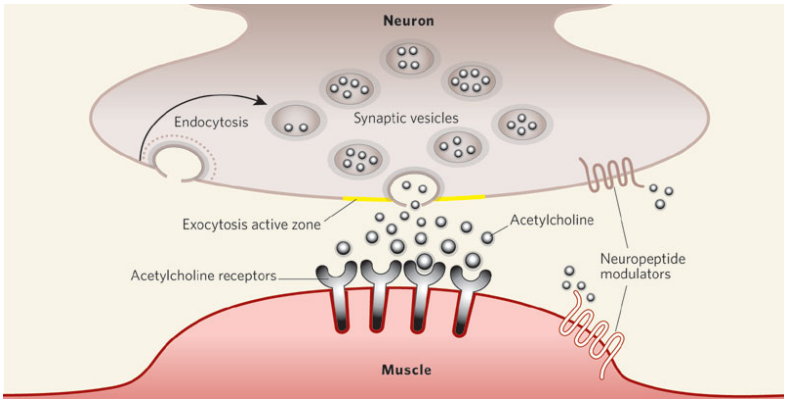

FIGURE 1.2: The neuromuscular junction. The arrival of an action potential triggers the exocytosis of vesicles with the presynaptic terminal and thousands of ACh molecules are released into the synaptic cleft and binds to receptors on the postsynaptic cell [3].

1.1.2 Acetylcholine receptors

ACh transmits the signal binding different acetylcholine receptors (AChRs) belonging to two distinct protein superfamilies: muscarinic AChRs (mAChRs) and nicotinic AChRs (nAChRs), named on the basis of sensitivity to the agonists muscarine and nicotine, respectively.

Muscarinic acetylcholine receptors

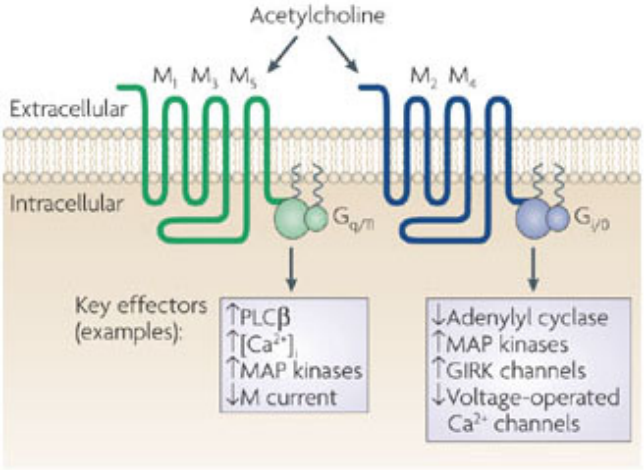

FIGURE 1.3: Structure of different mAChRs that couple to different G-protein families. Distinct mAChRs modulate the activity of a wide array of phospholipases, ion channels, protein kinases and other signaling molecule [4].

mAChRs are described through their interaction with muscarine, a water-soluble toxin derived from the mushroom *Amanita muscaria*. The mAChRs are members of the large family of G-protein coupled receptors (GPCR) and their activation acts as an enzyme to catalyze a cascade of intracellular secondary messenger systems mediating slow metabolic responses. MAChRs are widely distributed throughout the human body and are involved in a variety of physiological functions according to location and receptor subtypes [5]. They are involved in a large number of physiological functions including

heart rate and force, contraction of smooth muscles and the release of neurotransmitters. Based on pharmacological activity, five distinct receptor subtypes (M_1-M_5) have been described, although the exact expression and functional role of all these subtypes has not completely clear.

The M_1, M_3 and M_5 mAChRs selectively couple to G-proteins of the G_q/G_{11} family, allowing the activation of phospholipase C (PLC), generating inositol 1,4,5-triphosphate (IP_3) and diacylglycerol (DAG) eventually leading to an intracellular increase of Ca^{2+} and the activation of protein kinase C (PKC). The remaining two subtypes (M_2 and M_4) are coupled to G_1/G_0-type G-protein and inhibit the adenylate cyclase (AC), thereby decreasing the production of the second messenger cyclic adenosine monophosphate (cAMP) [6].

Interestingly, the expression of mAChR has been described in developing muscle fibers but not in adult innervated muscle; the expression of mAChRs in the course of the neuromuscular junction formation is controlled by nerve-derived signals which inhibit the expression of mAChRs in innervated fibers [7].

Nicotinic acetylcholine receptors

The nAChR is the best characterized member of ionotropic receptors, a group of ion channels that leads the formation of an ion pore across the plasma membrane that mediates a fast synaptic transmission. NAChRs are classified into two subtypes depending on their principal site of expression: muscle-type nicotinic receptors and neuronal-type nicotinic receptors.

The binding of two molecules of ACh results in an extensive conformational change of the receptor that becomes permeated by different cations. Conformational transitions, from the close (non-conducting), to agonist-induced open (ion-conducting), to

desensitized (non-conducting) states, are critical for nAChR functions [8]. The ability of the channel to undergo these transitions is profoundly influenced by the lipid composition of the membrane bilayer [9]. All nAChRs are composed of five subunits, assembled into both heteromeric and homomeric pentamers forming a central pore. Each subunit is comprised of four α-helical transmembrane domains (TM1-TM4), containing an extracellular domain with both the N- and C- terminus, transmembrane and cytoplasmic domains. The pore of the channel is lined by the second transmembrane domain (TM2) from the five co-assembled subunits [10]. The molecular weight of each subunit is about 25 KDa. Genes encoding a total of 17 subunits have been identified: alpha (α1-α10), beta (β1-β4), delta (δ), epsilon (ε) and gamma (γ) [11]. These subunits can assemble with variable stoichiometry, which influences the biophysical and pharmacological properties of the receptors [12]:

- Muscle nicotinic AChRs (adult neuromuscular junction): α1-ε-α1-β1-δ
- Muscle nicotinic AChRs (foetal, extrajunctional, embryonic): α1-γ-α1-β1-δ
- Neuronal nicotinic AChRs (CNS, PNS and developing muscle): (α7)5
- Neuronal and autonomic nicotinic AChRs (ganglion): α3-β4-α3-β4-β4 and α3-β2-α3-β4-α5
- Neuronal and autonomic nicotinic AChRs (brain): α4-β2-α4-β2-β2
- Epithelial and neuronal nicotinic AChRs (cochlea hair cells): (α9)5

The expression of α- subunit is fundamental to allow the ACh to bind the receptor in a proper site. Numerous proteins interact with nAChRs modifying their assembly, trafficking to and from the cell surface and activation by ACh [13]. Moreover, many proteins such as GPCR are known to bind different subunits at specific subcellular localizations and influence the localization of the channels in the cell and in the

membrane; these interactions permit the function of ion channels to be fine-tuned according to both external stimuli and intracellular states [14].

nAChRs in skeletal muscles: from the embryonic to the adult isoform

The muscle-type receptors are synthesized in muscle cells and anchored to the plasma membrane by a 43-KDa protein called rapsyn. The interaction between these two molecules of ACh on each α-subunit allows Na^+, K^+ and Ca^{2+} ions to flow across the membrane, leading to muscle contraction. The current passing across each open channel is very weak, only a few picoamperes (pA; about 10^4 ions/msec).

Two variants of the receptors are found in the skeletal muscle tissue: the mature, junctional or adult isoform located at the endplate, and the immature, extrajunctional, embryonic or fetal isoform expressed in immature and denervated muscle. The embryonic form is composed of α1, β1, δ and γ subunits in a 2:1:1:1 ratio, whereas in the adult form the γ subunits is replaced by the ε subunits in a 2:1:1:1 ratio [1, 15]. The key features of both receptors are shown in Fig. 1.4.

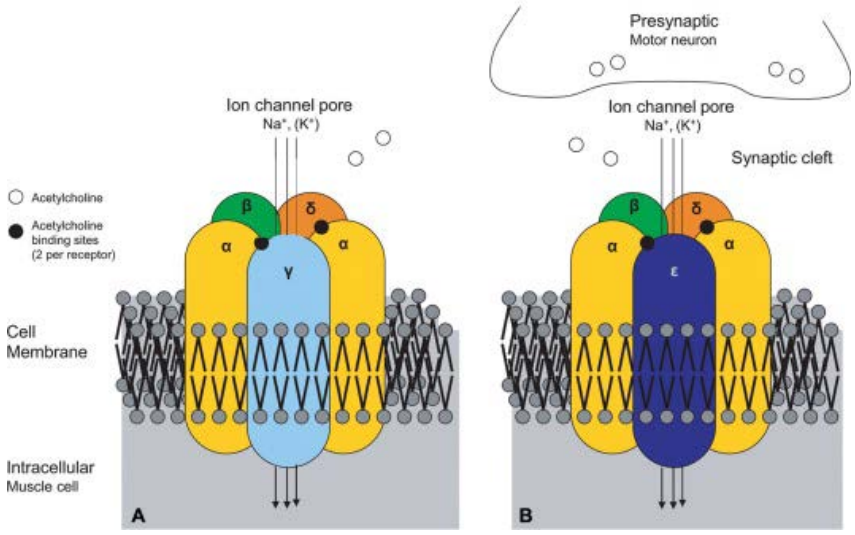

FIGURE 1.4: Structure and arrangement of the embryonic and the adult nAChR. ***A***, in the embryonic isoform, the γ subunit is colored in light blue. ***B***, in the adult isoform, the ε subunit is colored in dark blue (Modified from [16]).

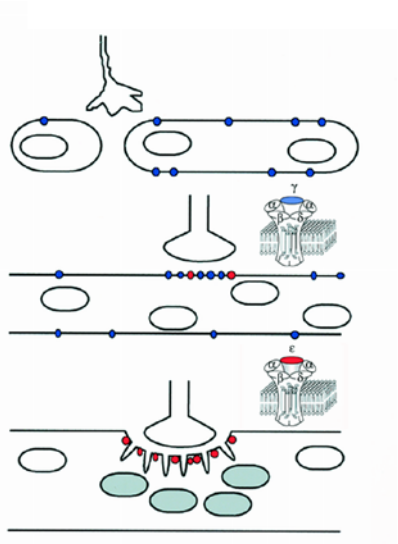

FIGURE 1.5: Distribution of nAChRs in developing adult, mature and denervated muscle [Modified from [1]].

The γ and the ε subunits differ from each other very little in amino acid homology, but the differences are great enough to affect the electrophysiology, pharmacology and the metabolic characteristics of the channel [15]. The fetal isoform containing the γ-subunit shows a long mean open time and a low conductance (6 ms and 35 pS respectively) [17]. The adult or junctional isoform containing the ε-subunit gives rise to the fast-gated, high-conductance channel type (conductance of 50 pS and mean open time of 1 ms) [17]. Moreover, the mature receptors are metabolically stable, with a half-life approximating 2 weeks, whereas the immature receptors have a half-life of less than 24 hours. The myogenesis is the differentiation process that begins with the fusion of precursor myoblasts into multinucleated myotubes leading to the formation of the adult skeletal muscular system. In this period, the expression of the embryonic nAChRs plays essentially two important roles; in the first phase of the myogenic process, the activation of the receptors through the release of ACh or a ACh-like compounds, promotes the fusion of myoblasts into myotubes [18-20]. The receptors are expressed throughout the membrane of the cells (Fig. 1.5). During the synaptogenesis, nAChRs mark specialized membrane sites by forming aggregates known as prepatterned clusters that preconfigures the prospective zone of innervation [21-24]. During the differentiation of *in vitro* mouse myotubes the autocrine activation of prepatterned nAChRs, promotes spontaneous intracellular Ca^{2+} spikes and contractions mimicking the effect of synaptic activity before innervation [25, 26].

Following innervation, muscle cells begin to synthesize the adult form of receptors, and the zone of receptors expression is refined and sharpened, so that nAChR adult isoform expression and clustering is restricted to a nascent synaptic site. The differentiation of the synaptic region depends on neuron-derived signals such as agrin and ARIA/neuregulin. Both increase the synthesis of the nAChRs from the nuclei nearby and prompt the expression of the mature isoform [27]. The nerve-induces electrical activity reduces the expression of the receptors in the extrajunctional area. In addition, signals from the muscle further regulate the differentiation of the presynaptic nerve terminals. The innervation process progresses slowly during fetal life and continues to take place after birth. In rats, it takes about 2 weeks whereas in humans this process takes longer. A child is usually about 2 years old before nerve muscle-contacts are mature [27].

1.1.3 The nicotinic acetylcholine receptor desensitization

As previously described, the activation of nAChRs by ACh, cholinergic agonists or nicotine induces the ion channel opening allowing a postsynaptic current that rises and decays within a few ms [28]. Nevertheless, after prolonged or repeated application of high concentration of the agonists (µM to mM) the receptors can undergo desensitization, a reversible reduction in response with subsequent recovery after the removal of the agonist. This process was first described by Kats and Thesleff in 1957 [29], and referred to as ligand-induced receptor desensitization. In the scheme below the desensitization represents a classical form of allosteric protein behavior, in which the receptor is distributed (in the absence of ligand) between several discrete conformations [30], and the agonist simply increases the probability of transitions between states [31]. Desensitization can also occur without channel activation, thus bypassing the open state [32, 33]:

$$\begin{array}{ccc} \boldsymbol{R + A} & \leftrightarrow & \boldsymbol{AR^*} \\ \updownarrow & & \updownarrow \\ \boldsymbol{D + A} & \leftrightarrow & \boldsymbol{AD} \end{array}$$

A is the agonist; *R*, *R** and *D* are the receptors in the resting, open and desensitized state respectively. In this model, following the agonist (*A*) binding to the resting receptor (*R*) and subsequent receptor activation (*AR**), desensitization arises (when experimental conditions allow it) as agonist-bound desensitized (*AD*) and agonist-free desensitized (*D*) states [34]. The kinetics depend on various factors: time course, amount and type of agonist (e.g. nicotine presents differential ability to desensitize nAChRs if compared to ACh), localization of the receptors in relation to the release site and mechanisms that remove the transmitter from the synaptic cleft. In addition, the intrinsic properties of the nAChR subtypes can have differential susceptibility to desensitization and determine how the current response is shaped [35, 36]. Interestingly, no differences in desensitization have been found between γ- and ε-nAChR channel currents [36]. If the stimulus is strong enough it is possible to have the endocytic downregulation, a ligand-induced internalization of the receptor by which the cell decreases their sensitivity to a specific molecule [37].

The role of nAChR desensitization in normal cholinergic transmission remains unclear. This phenomena has traditionally been referred to in the context of adaptation wherein the receptor system enters in a refractory state in the presence of the ligand and thereby prevents the cell from uncontrolled excitation [37].

The nAChR is susceptible to post-translational modifications both *in vivo* and *in vitro*, such as phosphorylation (on serine and tyrosine residues) and glycosylation, which influence synaptic function by directly modulating the receptor [38, 39]. Phosphorylation can elicit a wide variety of effects ranging from alterations in the level of surface

expression, synaptic targeting and receptor desensitization [40]. It results from the kinase-mediate covalent attachment of the γ-phosphate group of ATP to the hydroxyl group of Serine (Ser), Threonine (Thr) or Tyrosine (Tyr) [40]. Many studies have provided evidence of a nAChR regulation through specific phosphorylation by cAMP-dependent protein kinase (PKA), protein kinase C (PKC), an endogenous protein tyrosine kinase (PTK) and calcium/calmodulin dependent protein kinase (CAMK) [41-43]. Of these, PKA and PKC phosphorylate both Ser and Thr residues and PTK phosphorylates Tyr residues.

PKA phosphorylates γ and δ subunits at a specific amino acid serine 353 and serine 361 respectively [44], leading to an increase in the rate of the desensitization [45, 46]. Agents which increase $[cAMP]_i$ affects the ACh sensitivity of chick myotubes in three different ways: (*i*) an alteration in single-channel conductance; (*ii*) an alteration in the kinetics of the channels or (*iii*) a change in the number of channels capable of being activated [47]. The treatment with forskolin (an AC activator), or with cAMP analogs, increased the phosphorylation and the rate of the nAChR desensitization [46].

PKC phosphorylates different subunits from that observed for PKA changing the gating behavior of the channel [48, 49]. The δ subunit is principally phosphorylated and to a lesser degree also a Ser that resides on the α and γ subunits [50]. Interestingly, stimulation of PKC by 12-O-tetradecanoylphorbol-13-acetate (TPA) accelerates the desensitization of nAChR, hence the decay of ACh-activated current (I_{ACh}) in chick myotubes [48], and induces multiphasic changes of the ACh sensitivity in adult rat muscle fibers [51]. The phosphatidylinositol pathway is also stimulated in muscle cells through both a mAChR pathway and a nAChR pathway [52]. Postsynaptic membranes isolated from the electric organ of *Torpedo californica*, rich in the nAChRs were shown to contain an endogenous and active PTK that phosphorylates the nAChR rapidly and

specifically on the β, γ and δ subunits [50]. The phosphorylation of these three subunits occurs exclusively on Tyr residues. Although, the PTK phosphorylates the β subunit in BC3H1 myocytes [53] and in rat myotubes [54].

The desensitization is a dynamic process that can be modulated by different local factors. One of these is the endogenous peptide substance P, which powerfully facilitates desensitization by binding to an allosteric site distinct from the ACh binding site [55]. Another modulator is Ca^{2+} probably through the activation of PKC or Calcineurin, whose dynamic balance control the recovery process [35]. In primary mouse culture muscle cells, Calcitonin gene-related peptide (CGRP) elevated the intracellular levels of cAMP and increased the phosphorylation and desensitization rate of the nAChR [56]. New findings concerning the modulation of nAChR function and transition between various desensitized states, identified ligands able to bind allosteric sites, including sites located in the transmembrane domain [57].

1.2 Adenosine and the purinergic signalling

The purinergic signalling system, which uses ATP, related nucleotide and adenosine (Ado) as chemical transmitters, appeared very early in evolution and is linked to the fundamentals of the genetic code, bio-energetics and extracellular communication [58]. Release of ATP is detected at all phylogenetic levels, including bacteria, yeast, plants, protozoa and in all multicellular organisms [59]. The evolution of the purinergic system results in the development of different classes of receptors, several pathways for releasing nucleotides and a system controlling the extra- and intracellular levels of purinergic transmitters [58]. Many different receptors are involved in mediating the purinergic transmission: (*i*) ionotropic P2X ATP-gated cationic channels, (*ii*) GPCRs for adenosine (P1-receptors), (*iii*) PY2 receptor for nucleotides (ATP, ADP, UTP, UDP and UDP-sugar) and recently discovered receptors for adenine designated as AdeR or P0 receptors [60, 61]. The purinergic transmission is omnipresent and functionally diverse being involved in both physiological and pathological contexts. ATP and Ado are produced and released by cells in all tissues, and the related purinoreceptors contribute to a wide variety of physiological functions. Those are influenced by different parameters such as: (*i*) the unsteady presence of ligands at receptor sites, significantly varying conformational asset as a function of time and distance from the source of release; (*ii*) the concentration gradient of a ligand simultaneously activating more than one receptor subtype, within different binding affinities; (*iii*) the diverse submembrane compartments in which each ligand operates; (*iv*) the multiple indirect receptors-receptor interaction, and direct homo- or hetero-oligomeric assembly of each receptors subtype [58, 62].

1.2.1 The adenosine

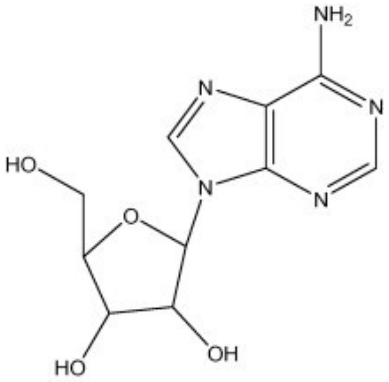

FIGURE 1.6: Structure of adenosine [63].

Ado (Fig. 1.6) is a ubiquitous extracellular signalling molecule that is involved in a variety of basic biological functions, including nucleic acids biosynthesis and the cellular energy metabolism of all living organisms. Much of our understanding of Ado has come through observations of its action in the cardiovascular system where it is both a potent negative ionotropic agent and a coronary vasodilator [64]. However only in 1970 the ability of Ado to regulate cell function *via* occupancy of specific receptors on the cell surface was discovered [65]. The formation of extracellular Ado was first shown to occur in the hypoxic and ischemic heart, thus it was proposed that it served a protective function in the heart against the consequences of metabolically detrimental situations, by decreasing the metabolic demands of the myocardium and increasing coronary blood flow [66]. Other evidence for similarly protective actions has been found in other cellular and organ systems, including brain, kidney, skeletal muscle and adipose tissue [66] and the term of “retaliatory metabolite” is currently used to describe the protective function of Ado [67].

In the SNC, it regulates the release of several neurotransmitters; it plays an important role in controlling the contractile tone of arteries including cerebral arteries, thoracic

aorta, mesenteric and femoral arteries [63], it is an endogenous pain modulator [68], it is involved in in the immune system [69], in the mast cell degranulation [70], asthma [71] in cell growth and apoptosis.

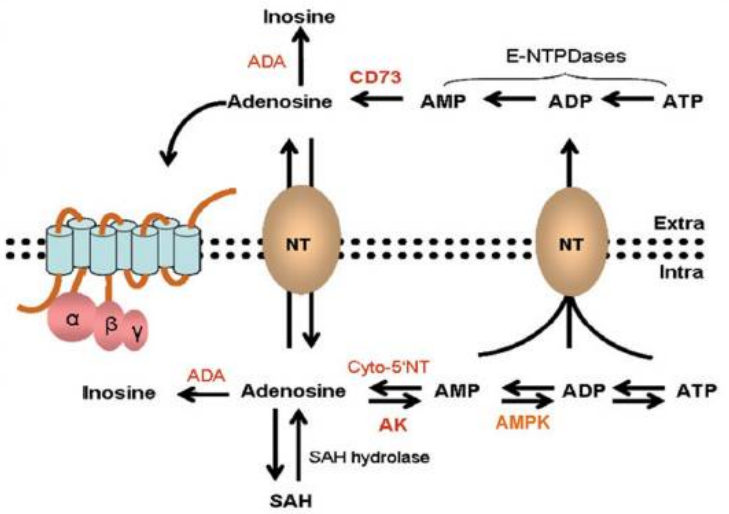

FIGURE 1.7: Adenosine synthesis and metabolic pathways outside and inside the cell [72].

Ado belongs to the purine nucleoside composed of an adenine molecule attached to a ribose sugar moiety *via* a beta-N9-glycosidic bond [73]. Unlike a classical neurotransmitter, Ado is neither stored in synaptic vesicles nor does it act exclusively on synapses. Its release and uptake are mediated by bidirectional nucleoside transporters whereby the direction of transport solely depends on the concentration gradient between the cytoplasm and the extracellular space (Fig. 1.7) [63].

Ado is considered as a neuromodulator affecting neural activity through multiple mechanisms, presynaptically by controlling neurotransmitter release, postsynaptically by hyper- or depolarizing neurons, and on glial cells [74]. It is formed at both intracellular and extracellular sites by two distinct pathways that involve two different substrates, namely AMP and S-adenosyl homocysteine (SAH), and transported across cell membranes by nucleoside transporters [75, 76]. In the intracellular space, Ado can be synthesized *de novo* during purine biosynthesis or produced either by breakdown of

adenosine 5’ phosphates (ATP, ADP, AMP) or by hydrolysis of SAH. In the extracellular space, Ado comes from two different sources (Fig. 1.7). First, it originates from the intracellular pool by means of bidirectional equilibrative and Na^+-dependent concentrative nucleoside transporters to quickly cross the cell membrane [77]. Secondly, it is generated by adenine nucleotide hydrolysis through a controlled two-step enzymatic reaction: first, the conversion of ATP or ADP to AMP by ectonucleoside triphosphate diphosphohydrolase 1 (ENTPD1; also known as CD39), which is followed by AMP hydrolysis to Ado by ecto-5’-nucleotidase (NT5E; also known as CD73).

Interestingly, in the skeletal muscle tissue Chiavegatti et al., (2008) showed evidence for the existence of an extracellular cAMP-adenosine pathway, elicited by the activation of AC followed by the subsequent efflux of the cyclic nucleotide and extracellular generation of Ado [78].

Ado is a very unstable molecule and its half-life is limited by phosphorylation or degradation to inosine catalyzed by adenosine kinase (ADK) and adenosine deaminase (ADA), respectively. The concentration of Ado inside and outside the cell is kept thoroughly under control and it is related to energy consumption. It increases dramatically under metabolically stressful conditions. During hypoxia, ischemia or inflamed environments the intracellular production of Ado reduces tissue injury and promotes repair [79]. In physiological conditions, the extracellular concentration of Ado is about 30-300 nM, it increases during metabolic stress reaching the concentration of 10 µM or even more [80].

1.2.2 The adenosine receptors and their classification

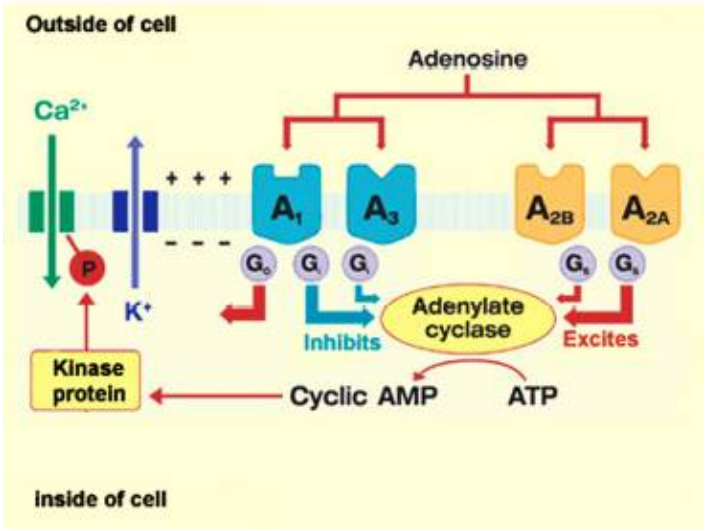

FIGURE 1.8: P1 receptors signaling [72].

The physiological effects of Ado are mediated *via* the activation of purinergic receptors known as P1-receptors (P1Rs). They are classified into four different subtypes named A_1, A_{2A}, A_{2B} and A_3, all belong to GPCR superfamily (Fig. 1.8). Each subtype has been characterized by molecular cloning, agonist activity profile, antagonist activity profile, GPCR and effector systems [63]. Classically, the P1R signalling was based on the effects on cAMP levels in different tissues. Specifically, the A_1 and A_3 subtypes mediate an inhibitory action on adenylyl cyclase via G_i-proteins, and the two A_2 receptors mediate an increase in cAMP acting through the G_s-protein [81]. Apart from that, other pathways, such as PLC, Ca^{2+}, arachidonic acid and mitogen-activated protein kinase (MAPKs), are also relevant [82].

Based on their ligand affinity, P1Rs exhibit high (A_1R: K_i = 73 nM; $A_{2A}R$: K_i = 150 nM, in rodent) or low ($A_{2B}R$: K_i = 5100 nM; A_3R: K_i = 6500 nM in rodent) [83] affinity for the agonist. Activation of A_1R occurs at 0.3–3 nM concentration of Ado, $A_{2A}R$ at 1–20 nM, while A_{2B} or A_3 receptors activation require an agonist concentration larger than 1 μM

[84]. Usually Ado acts in concert with other hormones or neurotransmitters in either an inhibitory or a stimulatory way producing multiple effects within the same cell [85].

P1Rs together with the microenvironment in which they are embedded are described as “purinome”, a molecular complex responsible for the biological effects of extracellular ligands and the coordination of receptor processes [62]. The purinome consists of ectonucleotide-metabolizing enzymes [86], purinergic receptors [87], ectonucleoside transporters [88] and nucleotide channels and transporters [89]. Not recognized dominance subsists among these proteins, but rather they demonstrated tightly concerted actions under physiological conditions, and very often they interact with each other. The alteration of their global and dynamic equilibrium might also be responsible for the appearance/propagation of pathological states [62].

A_1 receptor

The A_1R is the best characterized among P1R family, and it is ubiquitous throughout the entire body. A_1R is abundant and homogeneously distributed in the brain with high abundance in the neocortex, cerebellum, hippocampus and the dorsal horn of the spinal cord. A_1R is also in the adipose tissue, heart muscle, inflammatory cells such as neutrophils [90]. The sequence of amino acid residues is defined by the sequence of a human gene known as ADORA1 and the purified brain A_1R is a monomeric 35- to 36-KDa glycoprotein [85]. This receptor is functionally coupled to members of the pertussis toxin-sensitive family of G proteins: $G_{i1/2/3}$ or G_o protein. Binding of $G_{i1/2/3}$ causes an inhibition of AC and, as consequence, a decrease in the cAMP concentration. A1R also activates potassium channels (including K_{ATP} channels in neurons and the myocardium), blocks transient Ca^{2+} channels and increases intracellular Ca^{2+} and IP_3 levels by PLC [91].

A_{2A} receptor

The A_{2A}R in human is encoded by the ADORA2A gene [92]. The receptor is expressed at high levels in only a few regions of the brain, such as striatum, olfactory tubercle, nucleus accumbens, basal ganglia and caudate putamen, where it is found in pre- and postsynaptic nerve terminal [93]. It is also present in mast cells, airway smooth muscle and circulating leukocytes [94]. A_{2A}R regulates myocardial oxygen consumption and coronary blood flow by vasodilating the coronary arteries, which increase the blood flow to the myocardium [95], it is also an important therapeutic target in Parkinson disease (PD) [94]. A_{2A}Rs are mostly coupled to G_s/G_{olf} proteins [96], thus activating AC which in turn converts ATP into cAMP. Depending on the cell type, A_{2A}R may also signal *via* a pathway independent of heterotrimeric G proteins; such is the case of the activation of the MAPK signaling cascade [97].

A_{2B} receptor

The A_{2B}R in human is encoded by the ADORA2B gene [92]. The receptor also interacts with netrin-1, which in involved in axon elongation [98]. The A_{2B}R, although structurally closely related to the A_{2A}R and positively coupled to AC is functionally very different. Activation of A_{2B}R can also stimulate PLC through a G_s and G_q protein, respectively [82]. The coupling to MAPK has also been described [99]. Among all the P1 receptors, the A_{2B}R has low affinity for its endogenous agonist thus remains silent under physiological conditions while is activated when the extracellular Ado level is high [100]. A_{2B}Rs are highly expressed in gastrointestinal tract, bladder, lung and on the mast cells [101]. A_{2B}Rs are widespread in brain but little is known about their function.

A_3 receptor

A_3R is the most recently discovered P1R. It was identified through molecular cloning from a rat testis cDNA library and its sequence similarity to P1Rs [102]. A_3R is coupled to classical second messenger pathways such as inhibition of AC, stimulation of PLC and mobilization of Ca^{2+} [82]. As $A_{2B}R$, its activation requires a high level of agonist (more than 1 μM, [84]). It is involved in a variety of intracellular signalling pathways and physiological function even if it is less widely distributed than other P1R subtypes. In humans, it is expressed in lung, kidney, mast cells, liver, brain cortex, aorta, testis and heart [103]. Interestingly, A_3R seems to be influenced by metabolites of Ado [104].

A_3R mediates anti-inflammatory, anticancer and anti-ischemic protective effects. This receptor is overexpressed in inflammatory and cancer cells, while low expression is found in normal cells, rendering the A_3R a potential therapeutic target.

Currently, A_3R agonists are being developed for the treatment of inflammatory diseases including rheumatoid arthritis and psoriasis; ophthalmic diseases such as dry eye syndrome and glaucoma; liver diseases such as hepatocellular carcinoma and hepatitis [103] .

1.2.3 P1-receptors: functional receptor-receptors interaction

Recently, many GPCRs have been demonstrated to form receptor-receptor interactions and this multi-receptor complex play a key role in correct receptor maturation, agonist affinity, potency, pharmacology and trafficking to the plasma membrane under both physiological and pathological conditions [105]. Considering the various types of receptors, three principle paths of receptor interaction that contribute to both synergistic and antagonistic effects: (*i*) interactions between ionotropic receptors; (*ii*) interaction

between a metabotropic receptor and an ionotropic receptor; (*iii*) interactions between metabotropic receptors [106].

The modulation of receptor/ion channel can be altered by several proteins such as protein kinases that are linked with P1Rs. More recently, it has become evident that P1Rs can form multimeric or oligomeric structures, even if the monomeric state is sufficient to induce signalling [83]. Through self-association, homo-oligomers ("homomers") can be formed. Hetero-oligomerization leading to "heteromers" may be the consequence of the association between P1Rs and preferred partners, mostly other GPCRs including other P1Rs subtypes [83].

The regulation of Ado levels and P1Rs, their cellular and subcellular localization, signalling pathways have been described in particular in the brain where it is becoming increasingly obvious that the modulatory role of Ado is related to the ability of A_1R and $A_{2A}R$ to heteromerize with themselves as well as with other receptors, such as dopamine, glutamate or γ-Aminobutyric acid (GABA), contributing to a to a fine-tuning of neuronal function, and therefore, to neuroprotection [106, 107].

1.2.4 The purinergic signalling in skeletal muscle

In skeletal muscle, P1Rs are involved in the modulation of blood flow [108], insulin-mediated glucose uptake [109] and in the regulation of contractile force [110]. However, a new emerging role for P1Rs includes the differentiation process either during physiological development or during tissue regeneration in injury/repair processes. Following skeletal muscle injury, an increased level of $A_{2B}R$ is reported in mouse skeletal muscle [111], and a protective role for Ado *via* A_3R was observed in the treatment of post-traumatic human skeletal muscles [112].

P1-receptors in immature skeletal muscle cells

The presence of A_1, A_{2A} and A_{2B} subtypes has been reported in immature skeletal muscle, however their role is still uncertain [113]. The nucleoside Ado is released from immature and adult muscle in response to spontaneous or induced contractions. In primary skeletal muscle cells, the tetanic stimulation rapidly increase the rate of extracellular Ado concentration fivefold more than the muscle at rest [114]. In rat myotubes the activation of A_2R modulates the desensitization rate of nAChR measured as Na^+ influx through the channel [115]. More recently, it has been described an autocrine activation of P1Rs in twitching *in vitro* myotubes that increases the channel openings of nAChRs [116]. The intracellular communication between these receptors contributes to electrical and contractile activity of the cells as well to their tropism before innervation. These aspects represent an important molecular mechanism in the regulation of skeletal muscle differentiation [25].

P1 receptor at neuromuscular junction

The vertebrate NMJ refers as a “tripartite” synapse, made up of three cellular elements: the presynaptic motorneuron, the postsynaptic skeletal muscle fiber and the intimate association with surrounding glial cell, also called perisynaptic Schwann cell. The neuromuscular transmission consists of a series of events confined in a highly specialised contact area where a chemical signal is converted into an electrical one [117]. The way in which the impulse is transmitted to the muscle is principally due to the neurotransmitter ACh that is co-released in the synaptic cleft with ATP.

ATP is released in an activity dependent manner from both nerve and muscle. It activates P2-type purinoreceptors, either ionotropic (P2X) or G-protein coupled (P2Y), and it is also hydrolized by ectonucleotidases to Ado. Ado is involved in modulation of

the ACh release, through P1Rs mainly located at the presynaptic level [118, 119]. However, P1Rs are also present in the postsynaptic membrane and in perisynaptic Schwann cells. Specifically, A_1R localizes in the terminal Schwann cell and nerve terminal whereas the $A_{2A}R$ localizes in the postsynaptic muscle, in the axon and in the nerve terminal [120]. More recent it is has reported the localization of the low affinity A_{2B} and A_3 subtype at the endplate region, but their functional role is still unknown [121].

P1Rs are significant presynaptic autoreceptors that modulate ACh release [122]. Ado in the extracellular environment is known to reduce EPP quantal content and/or vesicle release frequency (miniature endplate potential, MEPPs) in both frog [123] and rodents NMJ [124]. A_1R reduces the release [125], whereas the $A_{2A}R$ increases it [124]. Thus, these high affinity P1Rs act mainly at the presynaptic level. Ado can reach a concentration of the micromolar range under a sustained electrical activity; in this way, it elicits a strong presynaptic protective effect by reducing the synaptic depression [120]. Concerning the low affinity P1R subtypes, neither $A_{2B}Rs$ nor A_3Rs are localized in the Schwann cells, but their expression has been reported in the nerve terminal and at the endplate [121]. Interestingly, these receptors are shown to be more highly expressed in adult muscle than in newborn tissue and they have been observed colocalized perfectly with nAChR clusters [121].

The presence of all P1R subtypes at NMJ level, suggested that the transmitter release modulation is determined by both a complex balance between all P1Rs subtypes in response to a variable amount of Ado concentration in the synaptic cleft [121]. At the moment, very little is known about the role of P1Rs at the post-junctional site. One hypothesis is that they might play some role in short term regulation of neurotransmission, or in long-term modulatory processes.

1.2.5 P1-receptors as drug target

The P1Rs are widely expressed and have been implicated in several biological function, both physiological and pathological, for this reason these receptors are currently investigated as therapeutic targets. Over the past 20 years, medical chemistry effords have generated agonists and antagonists with high affinity (a dissociation constant (Kd) at low nanomolar concentrations) and high selectivity for the variants of the four receptors, so the lack of selective ligands is not a limiting factor for research and drug development on P1R [83]. The greatest challenge in developing P1R ligands for clinical applications is that Ado signalling is so widespread in and exerts a broad spectrum of functions. Medicinal chemistry need to develop novel Ado ligands with refined structural-activity relationship, improved *in vivo* biodistribution and tissue selectivity, which is crucial for druggability [91, 126]. The clinical indications for drugs that are in advanced clinical trials include Parkinson disease (PD), chronic heart failure as well as inflammatory and autoimmune disorders.

In the CNS increasing interest has been focused on $A_{2A}R$ as an important pharmacological target in PD. As discussed above, $A_{2A}R$ are known to be coexpressed with dopaminergic D_2 receptors in striatopallidal GABA neurons, where they form heterodimeric complexex able to decrease the D_2 affinity for dopamin [127]. At this regard, Istradefylline a selective $A_{2A}R$ antagonist was developed and represent a new way for the once-daily oral treatment of PD through a non-dopaminergic mechanism [128].

Ado itself is used clinically for the treatment of supraventricular tachycardia [82], and many clinically used drugs (including dipyridamole and methotrexate) may exert their effects by altering extracellular Ado concentration and signalling. One A_{2A} agonist – regadenoson (Lexiscan: Astellas Pharma)- was approved by the US Food and Drug

Administration (FDA) for myocardial perfusion imaging in patients with suspected coronary artery disease [129]. The presence of P1R in immune system and their expression within inflammatory and tumor environments are interesting as therapeutic target for autoimmune diseases, chronic inflammatory disorders and cancer [130]. In this contest, the A_3R is considered the major target. Other selective P1R agonists and antagonists are available and several trials are currently in progress but the translation of the abundant knownledge of Ado biology to clinical progress has been slow [91].

1.3 *Xenopus laevis* oocytes and the microtransplantation technique

1.3.1 Maintenance of *Xenopus laevis* frog in laboratory

Scientific classification

Kingdom: Animalia
Phylum: Cordata
Class: Amphibia
Order: Anura
Family: Pipidae
Genus: Xenopus
Scientific Name: Xenopus laevis
Common Name: African Clawed Frog
Other Name: Platanna

FIGURE 1.9: *Xenopus laevis* frog (*Xenopus* means "strange foot" and *laevis* means "smooth"; *Left*) and taxonomy (*Right*).

Xenopus laevis (Fig. 1.9), also known as African clawed frog, is native of sub Saharan Africa (Nigeria and Sudan to South Africa), but there are populations introduced in many locations around the world, such as California, Chile and Great Britain. It lives in stagnant ponds, lakes or rivers, where the substrate is usually thick mud. It is almost totally aquatic and spends most of its time underwater, but comes to surface of the water to breathe. *Xenopus laevis* can live 15-16 years in the wild, but the lifespan in captive animals can reach 20-25 years, despite the fact that it is a quite inactive creature. It is considered both carnivorous and scavengers for its habit of feeding living, dead, dying animals or organic waste. Being a nocturnal animal, the vision is not the main sense used to get information from the environment; conversely, to locate food they use sensitive fingers, the acute sense of smell and a developed lateral line system.

The morphology of this frog is unique, lacking in the tongue and visible ears. The body is flattened and multicolored, brown and grey on its back, while the underside is creamy white. Males are smaller (about 5-6 cms long) than females (from 10 to 12 cms) and are sexually mature in 10 to 12 months. Mating is most common in spring and it often takes place during the night, when there are fewer disturbances [131]. *Xenopus laevis* frog is a very suitable non-mammalian animal model for the laboratory because of its short generation time, its longevity in captivity and its ability to adapt to a range of laboratory conditions. The continuous production of oocytes and eggs provides an important source for biological and pharmacological researches [132]. Housing environment for the frogs should ideally constitute a temperature-controlled setting at 16-18°C, and an alternating 12-h light-dark cycle [133]. The animals are an air breathing aquatic frog, so they required to be covered by a sufficient amount of water. They are sensitive to chlorine and chloramine, it is important to ensure that the water in the tanks is free of these reagents [134]. A number of different feeding protocols exist with regard to the laboratory breeding of *Xenopus laevis*. A feeding schedule of 0.2 g of pellet diet per frog once a day is adequate [133].

1.3.2 The biology of oocytes

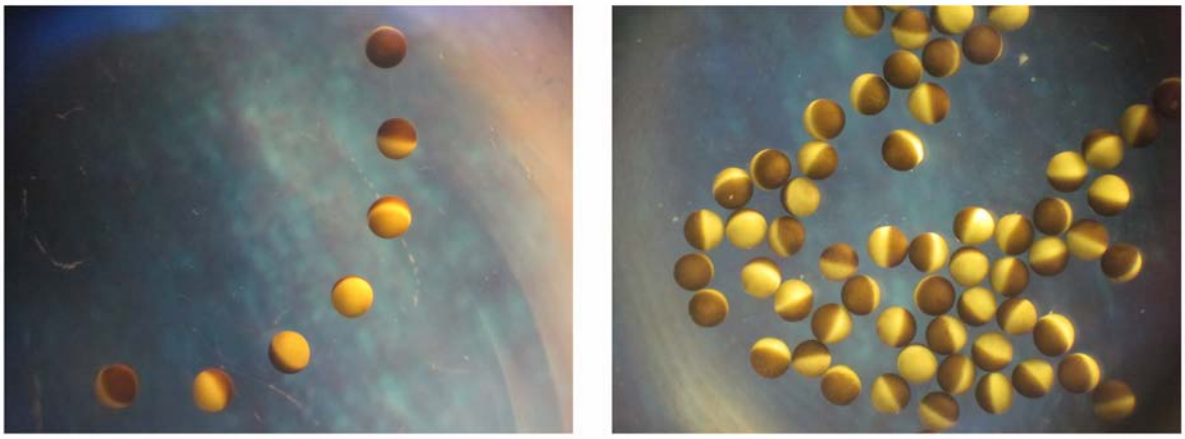

FIGURE 1.10: Defolliculated oocytes of *Xenopus laevis.*

In *Xenopus laevis* frog the gametogenesis can occur year round and is known to be asynchronous, meaning that all stages of oocyte growth are present in the ovary at given time [135]. Six different stages of growth have been carefully described [136] based on their size and the pigmentation which ranges from colorless to marked polarization into two different hemispheres (Fig. 1.10; 1.11). At stage VI these cells are characterized by a two-toned color scheme: the dark-brown animal pole due to pigmented granules containing a high concentration of melanin, and a creamy-colored vegetative pole which are divided by an unpigmented equatorial band. Oocytes at stages V and VI are a very big cell with a diameter around 1.3 mm, and an intracellular volume of 1 µl. The huge nucleus or germinal vesicle is 300-400 nm in diameter and is located in the animal pole, while the vegetal pole contains yolk platelets. The remainder of oocyte consists of cytoplasm that contains about 25 µg of cytoplasmatic protein [137].

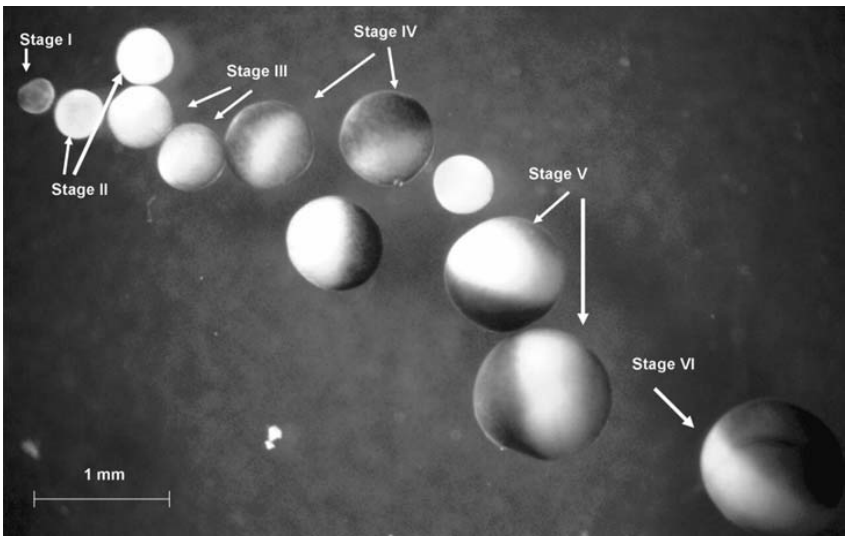

FIGURE 1.11: Different stages of *Xenopus* oocytes development [138].

The process of oogenesis requires about 8 months and arrested at the G_2/M border in the first meiotic prophase [139]. Once the VI stage is reached, the oocytes do not

continue to increase in size but remain at this point for some time before undergoing atresia (death and reabsorption of the oocytes) [137].

The outer surface of the plasma membrane of the oocyte is surrounded by the vitelline membrane, which is a glycoprotein matrix that gives the oocyte some structural rigidity and helps to maintain a spherical shape. In mammals it refers to zona pellucida and it is needed for sperm binding. The vitelline membrane does not interfere with electrophysiological recording because the mesh formed by this matrix is rather large, as consequence small protein and even small molecules such as α-bungarotoxin (α-Btx) can interact with proteins located on the oocyte surface. It is usually removed only for patch clamp recording in cell-attached configuration in order to allow the formation of the gigaohmseal.

The vitelline membrane is in turn surrounded by several layers of follicle cells and thecal tissues [140]. The oocyte is electrically coupled to follicle cells through gap junction, so that electrical events taking place in follicle cells can be detected in the oocyte. For this reason the follicle cell layer is a potential source for many problems, therefore it is removed in order to avoid any possible contamination and this process is called defolliculation.

The ovaries contain upward of 10000 oocytes and expand almost to fill the entire abdominal cavity of sexually mature females. The oocytes are isolated by surgical laparotomy under general anesthesia. Aseptic instruments and a proper surgical environment are required to minimize adverse effects of microbial contamination or other deleterious effects that may affect the oocyte quality and general frog health. The same donors can be used more than once, but it requires an adequate recovery time interval between two surgeries (on the same abdominal side up to 1 year).

1.3.3 Electrical membrane properties of the oocytes

The membrane properties of the oocytes have been well described and change profoundly during the maturation. Passive membrane properties have been shown to be similar in oocytes collected from the same donor, but they tend to vary between different donors. The oocyte surface area has been reported between 18 mm^2 [141] and 20 mm^2 [142] and the capacitance measurements revealed values of 230 nF and 220 nF [143]. The resting membrane potential (V_m) is mainly due to a K^+ diffusion potential as well as the Na^+/K^+-ATPase and present a great variance between different batches ranging from -30 to -70 mV [144]. The defolliculation can change the V_m as a consequence of membrane damage that take several hours to heal [145]. Another area of concern is the trauma caused to the membrane after the impalement with the electrodes during the electrophysiological experiment. After the penetration, the membrane potential undergo to hyperpolarization than gradually recover [146]. In this case the V_m and the membrane resistance are underestimated so it is therefore advisable to wait several minutes after clamping the oocyte prior to the study of ion channel activities. During maturation the surface area increases significantly, resulting in a change of oocyte resistance and capacitance. This variation is attributed to the appearance of microvilli. The capacitance change from ~2 $\mu F/cm^2$ in stage I to ~6-7 $\mu F/cm^2$ in stage V and VI [147]. The input resistance ranges from several 100 kΩ to 2 MΩ and sometime even more [148]. The oocyte itself is equipped with o whole orchestra of endogenous membrane proteins that are fundamental for its physiology [139]. Few examples of endogenous channels present in *Xenopus* oocyte include anion channels (Cl^- channels and organic anions) representing the majority of ion conductances housed by the oolemma, cation channels (K^+, Na^+ and Ca^{2+} channels) including the non-selective and the mechanosensitive cation channels [139].

1.3.4 The purinergic signal in *Xenopus laevis* oocytes

Xenopus ovarian follicles consist of an oocyte surrounded by a vitelline envelope, follicle cells and thecal tissues [140]. Mature follicular oocytes (stage V and VI) are known to possess receptors for Ado and ATP as well as for ACh, serotonin, dopamine, prostaglandins and progesterone [140, 147]. The follicle cell monolayer enveloping the oocyte maintains electrical continuity with follicle cells via cAMP-gated intercellular gap junctions [149]. Three main subtypes of purinergic receptors have been described: (*i*) A_2 receptors responsive to Ado, coupled to cAMP synthesis and opening of K^+ channels (cAMP-dependent K^+ current, $I_{K,cAMP}$) that are sensitive to glibenclamide [150-154]; (*ii*) P2Y receptors responsive to ATP and UTP that operate Cl^- channels generating fast and slow Ca^{2+}-independent currents (F_{Cl} and S_{Cl}) [155, 156]; and (*iii*) a purinergic receptors, referred to as a P3 or novel P1 receptor, that is sensitive to both Ado and ATP and coupled to $I_{K,cAMP}$ generation where Ado and ATP are equipotent agonists (EC_{50} values, 1.9 ± 0.3 µM and 1.7 ± 0.3 µM, respectively) [157, 158]. Ado and ATP do not activate K^+-current in defolliculated oocytes indicating that the receptors for Ado are located in the follicle cells [159]. However, the presence of endogenous P1R in defolliculated oocytes is a matter of debate. Gelerstein et al., [160] demonstrated that Ado elevated cAMP levels both in defolliculated oocytes and in follicular oocytes, suggesting that an adenosine receptor is also located on the oocyte membrane [160]. In contrast, Ado at high micromolar concentration inhibited AC activity in the defolliculated oocyte membrane fraction [161]. These finding suggest the possibility that there are additional endogenous P1R on the oocyte membrane. Keeping this in mind, Kobayashi et al., [162] demonstrated the existence of an endogenous *Xenopus* P1R on the oocyte membrane that couples to G protein-activated inwardly rectifying K^+ (GIRK) channels

expressed exogenously and AC *via* interaction with $G_{i/o}$ proteins. The receptor may be considered an A_1-like P1R due to its unique pharmacological profile [162].

1.3.5 *Xenopus laevis* oocyte as heterologous expression

The definition of *Xenopus* oocytes as eterologous expression system was introduces by Gurdon and collaborators in 1971 [163] as a means to study various aspects of the control of gene expression [163]. Injection of DNA into the oocyte nucleus or mRNA into the cytoplasm let to the expression of functional proteins by the oocytes. The pioneer studies were focused on the expression of protein like globin, interferon and various viral proteins. In the early 80's, Miledi and co-workers demonstrated that several ion channels and receptors could also be expressed in oocytes after the injection of mRNAs isolated from an exogenous tissue [164]. In this novel environment, exogenous proteins could be functionally characterized under well-defined conditions. For example, injection of *Torpedo californica* electric organ mRNA lead to the expression of functional nAChRs [165] while injection of rat or human brain mRNA resulted in the expression of a large number of different voltage- and ligand-gated ion channels, including voltage-gated Na^+ channels, NMDA and non-NMDA subtypes of glutamate receptors, and $GABA_A$ receptors [166, 167].

Two methods with similar efficacies can be used to express functional membrane proteins into oocyte membrane and their functional characterization is performed using electrophysiological recordings (Fig. 1.12): (*i*) the cytoplasmatic injection of mRNAs, as well intranuclear injection of complementary DNAs (cDNA) encoding exogenous ion channels and (*ii*) the cytoplasmatic injection of exogenous plasmamembrane vesicles [168]. The letter approach is also call the microtransplantation technique (see below).

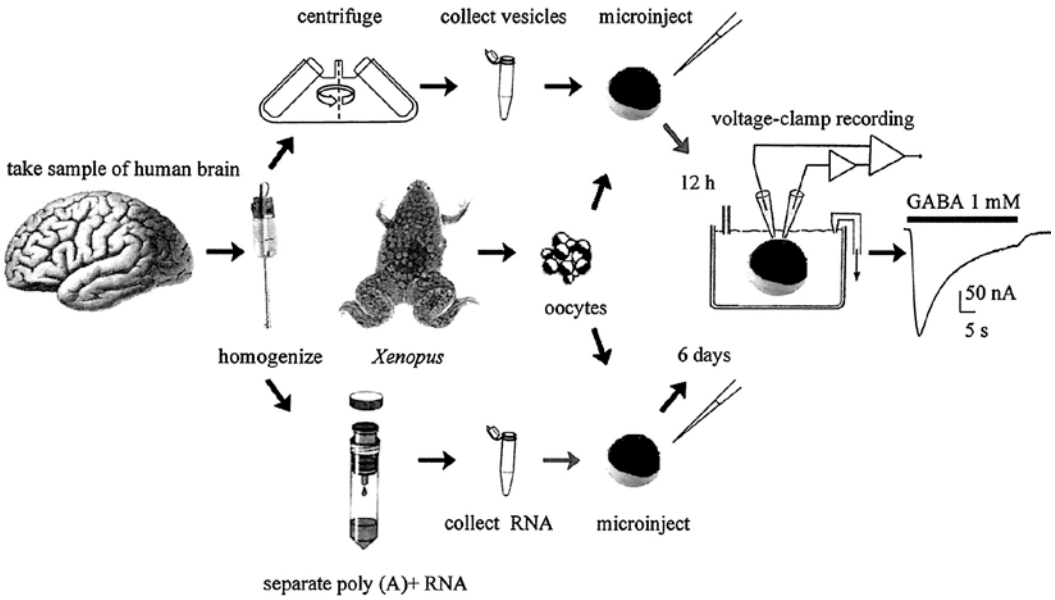

FIGURE 1.12: Transplantation of neurotransmitter receptors from the human brain into *Xenopus* oocyte by injection either cell membranes (*Upper*) or brain mRNA (*Lower*) [169].

The heterologous expression of ion channels and receptors into *Xenopus* oocytes is used by hundreds of laboratories around the world and is considered a powerful instrument for investigating their molecular structure and function. The usefulness of these approached extends from ligand-gated receptors to transporters such as aquaporins [138, 170] in fact the foreign protein expressed in the oocyte is usually biochemically functional, exhibiting the appropriate pharmacological and electrophysiological properties.

Below are listed the main advantages and disadvantages of using the *Xenopus* oocyte as expression system [171, 172]

The technical advantages:

- The translation of exogenous RNA occurs in normal living cell, and is therefore devoid of the artifacts that might be correlated with a cell-free (*in vitro*) system.

- The ovaries of a sexually mature *Xenopus* frog contain thousand oocytes. A small number of viable cells can be isolated from a donor frog and the same animal can be reuses.
- *Xenopus* oocytes show little species specificity for the type of foreign RNA or DNA they can finally translate into membrane proteins.
- Oocytes have a low level of background endogenous channels.
- The robustness and large size (diameter ~1.2-1.3 mm) of the oocytes make them tolerant to repeated impalement of microelectrode and injection pipettes, permitting functional analysis by a number of electrophysiological techniques.
- Foreign proteins are correctly post-translationally modified (e.g., by glycosylation and phosphorylation), and oocytes correctly orient multi-subunit proteins that acquire native activity.

Technical disadvantages

- Oocytes exhibit seasonal variations affecting the levels of protein expression. Some difficulties are known especially during summer.
- The physiological functions of oocytes are optimal at 16-22°C. The biochemical properties of mammalian proteins studied in the system may be therefore questioned.
- The properties of the lipids in oocyte membranes are different from those seen in mammalian cells and this may affect the functional properties of the expressed proteins.
- Expression is transient and there can be significant variation in receptor protein levels seen within (and across) different batches of oocytes.

- The environmental conditions including the cytosolic and extracellular ambient are far from the original one.
- The oocyte's dimension altering the kinetics of macroscopic currents generated by the transmitter. These are generally much slower than the current generated in smaller cells.

1.3.6 The microtransplantation technique

The microtransplantation technique is a very simple and useful approach to study the functional properties of ion channels and receptors present in membranes isolated from different tissues, in particular post-mortem human tissues [169, 173-176]. Plasma membrane vesicles carrying their original neurotransmitter receptors and ionic channels are injected into *Xenopus* oocytes, they fuse with the oolemma together with lipids and any associated native proteins. In this way, they are easily analysed electrophysiologically [168] (Fig. 1.13).

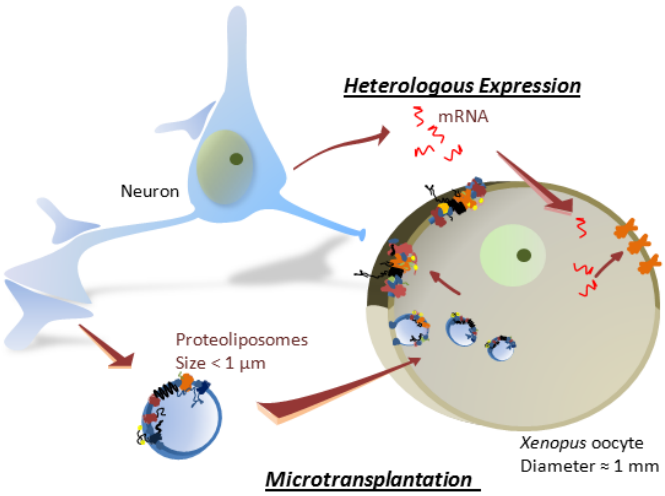

FIGURE 1.13: The microtransplantation technique and the heterologous expression [177].

The microtransplantation technique presents some technical advantages rather than cytoplasmatic injection of mRNAs, or intranuclear injection of complementary DNAs [172, 178]:

- Easier preparation of material to be injected
- Faster functional incorporation of neurotransmitter receptors (few hours *vs* few days).
- More stable preparation because the degradation by RNAase is avoided.
- Small amounts of tissue required and the same aliquots can be used after thawing and freezing many times without many precautions.
- The original ion channels, still embedded in their native cell membrane, are transplanted in the oocyte plasma membrane, overcoming the procedure required to perform protein synthesis and the post-translation modification operated by the oocyte's own machinery.

This method could present some limitations:

- Low level of expression due to their reverse orientation in the oocyte membranes.
- High current amplitude variability not only among oocytes from different frog, but also with the amount of membranes injected.

The incorporation of functional receptors is generally detectable within a few hours after the injection and the current responses lasted for a few days. Concerning the site of injection, the best procedures suggested the injection of the membranes in the vegetal pole or the equator because the neurotransmitter sensitivity resulted to be rather uniform. On the contrary, it results to be quite variable when membranes have been injected into animal pole [172]. Fig. 1.14 shows a certain clustering of receptors in the

vegetal and animal hemispheres when *Torpedo californica* electric-plaque membranes are injected.

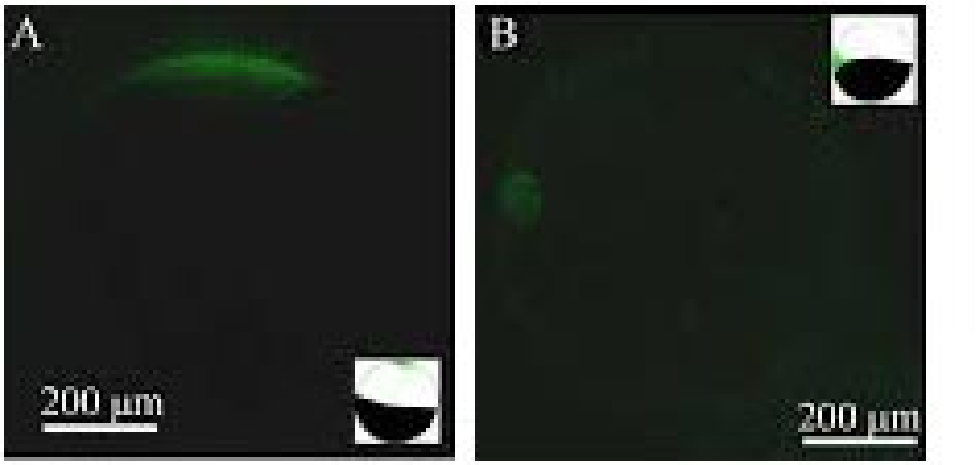

FIGURE 1.14: Confocal images of oocytes expressing nAChR labelled with α-Btx conjugated with Alexa Fluo-488, images were taken 2-3 day after membrane injection. ***A***, Oocyte injected with Torpedo membranes at vegetal pole. ***B***, Oocyte injected with *Torpedo* membranes at equator [Modified from [172]]

The fusion process continues after the peak response has been reached and the prolonged response is not necessarily due to a long life of the protein incorporated in the oocyte membrane. Oocytes show more than one incorporation peak with interval of many hours [179]. Subsequent the injection, a higher density of protein patches are detected near the microinjection site suggests direct fusion of lipoproteosomes with the plasma membrane rather than an indirect such as fusion with the Golgi apparatus and other organelles before the incorporation [180].

This methodology is used by different groups, but very little is known about how the incorporation process takes place. At this regard, Morales et al., [179] reported that the slow fusion of the vesicle does not depend on intracellular Ca^{2+} increase and therefore this process is different from those involved in resealing of disrupted oocyte

membranes or in the fusion of cortical granules with the egg membrane. The same authors suggested that the mechanism of membrane fusion could be accelerated by protein phosphorylation or by incorporation of fusion proteins with membrane before their injection [179].

CHAPTER 2

AIMS OF THE PROJECT

The aim of this thesis was to investigate the role of adenosine (Ado) and purinerigic receptors (P1Rs) in the modulation of the muscular nicotinic acetylcholine receptor (nAChRs) activity.

First, I focused my attention on the embryonic isoform of the nAChRs. In particular, I characterized the desensitization proprieties of nicotinic ACh-evoked currents induced by the presence of P1R ligands. The experiments were performed in oocytes after the injection of membranes isolated from mouse myotubes, and the mouse myotubes cultured *in vitro*. By doing this, I further demonstrated whether the microtransplatation technique could be a suitable approach to study the Ado-mediated modulation of the exogenous receptors/channels incorporated into the oolemma.

Secondly, I investigated the role of P1Rs in the modulation of channel activity of the adult isoform of the nAChRs. To achieve this goal, I performed single channel recordings of the nAChRs located at the endplate region of myofibers, isolated from flexor digitorum brevis of adult mice.

CHAPTER 3

MATERIALS AND METHODS

3.1 *Xenopus laevis* oocytes

3.1.1 Isolation and preparation of oocytes

Animal care and treatment were conducted in conformity with institutional guidelines in compliance with national and international laws and policies (European Economic Community, Council Directive 63/2010 Italian D.L.26/2014). The animals were purchased from Xenopus Express (Ancienne Ecole de Vernassal, Le Bourg, France). They were maintained in a continuous recirculating water system (water temperature 18°C; air temperature 22°C) with a 12-hr light/12-hr dark cycle and fed once a week with 4.7 g/animal pellet diet (AQ3 Expanded, SDS).

Sexually mature female *Xenopus laevis* frogs were fully anaesthetized by immersion in cold 0.17% tricaine methane sulfonate (MS-222) for 15 min and the pieces of ovary were aseptically removed as described elsewhere [178]. A sharp incision, less than 1.5 cms in length, was used and the surgical sites were alternated between left and right ovaries. The follicle cells surrounding the oocytes were manually isolated using fine-tipped forceps and the layer of follicular cells mechanically removed. Oocytes were then treated with 0.5 mg/ml collagenase type I at room temperature for 35 minutes, washed and kept at 16°C in Barth's solution until the experiments.

After the treatment the oocytes were still surrounded by the vitelline membrane, an inner glycoprotein matrix, that did not interfere with the electrophysiological experiments [133]. Under the stereomicroscope, oocytes at stage V and VI were carefully

selected and used for the experiments [136]. The number of oocytes tested is represented as *n*/*frog*, where *n* refers to the number of oocytes tested and *frog* is the number of donor.

3.1.2 Membrane preparation

Cell membranes of mouse myotubes (i28 cells, see below) were isolated according to the protocol described by Miledi et al., [178]. The membranes were suspended in sterile water and kept frozen at −80°C until the injection. The electrophysiological recordings were performed 24 h after the microinjection to let the cell recover from the membrane damage [135].

3.1.3 Microinjection of cell membranes into oocytes

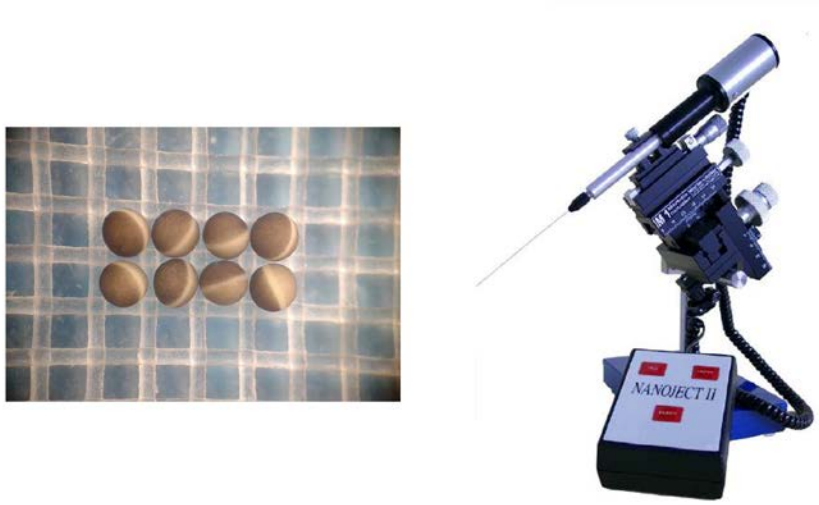

FIGURE 3.1: Oocytes were placed on a net to keep them stable and fix for the microinjection (*Left*). The microinjection of membranes is performed with an automatic nanoinjector (*Right*).

Only oocytes at the stage V-VI were used for the experiments (Fig. 3.1, *Left*). At this stage, the cells appear large with a regular spherical shape and the contrast between the black animal hemisphere and the beige vegetal hemisphere is well defined. The

oocytes were transferred into a Petri dish using a with fire-polished Pasteur pipette to allow undisrupted suction of the cell. The injection needle was produced by a one-stage pull at a specific temperature using a PP-830 vertical puller (Narishige International, Narishige, Japan). The nanoinjector was set on aspiration mode, and the injection needle was calibrated to inject a specific volume of sample (50 nL, Fig. 3.1). The microinjection was performed in the animal hemisphere close to the equatorial band, at an approximately 45-degree angle. The protein concentrations of the sample injected were 1-3 mg/ml. After the injection all oocytes were placed to a glass vial containing Barth's solution and incubated at 16°C.

3.1.4 The two-electrode voltage clamp technique

The two-electrode voltage clamp (TEVC; Fig 3.2) is a conventional electrophysiological technique commonly used to investigate the biophysical properties of membrane proteins (especially ion channels) of large cells such as *Xenopus laevis* oocytes. The technique consists in inserting two microelectrodes at intracellular level: the voltage electrode V_m (voltage membrane sensor) and the current electrode for current injection to adjust the V_m, thus setting the membrane potential at desired values and recording the membrane current to analyze ion channel activities [181].

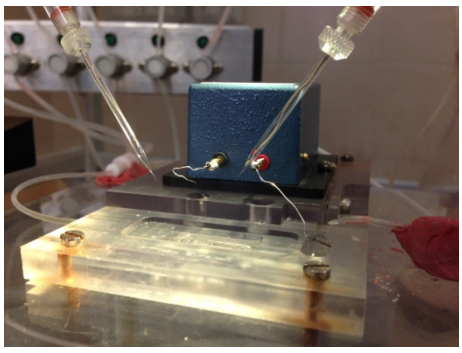

FIGURE 3.2: Recording chamber with two microelectrodes: voltage (*left*) and current (*right*) electrodes and the two bath probes.

The following devises and instruments were used for the TEVC recordings:

- stereo zoom microscope (East German Zeiss, aus Jena) with objective for 6.3x magnification (Fig. 3.3);
- purpose-designed recording chamber (RC-3Z, Warner Instruments, Hamden, CT, USA, Fig. 3.2);
- mechanical macromanipulators for stereo microscope providing movement in three axes (Narishige MMN-1, Tokyo, Japan);
- electrode holders, (voltage electrode and current electrode) with a chloride silver wire for the electrical coupling between the pipette and holder connector (Fig. 3.2). The silver wire was chlorided prior to assembly and use;
- bath probes to maintain a virtual ground in the oocyte perfusate. They were placed close to the silver electrode wires into the recording chamber or into the agar bridge well (Fig. 3.2);
- head stages, which performs the voltage-current conversion;
- the oocyte clamp amplifier (Model OC-725C, Warner Instrument, Hamden, CT, USA);
- Analog & Digital Output Channels (BNC-2090);
- gravity perfusion system (VC-8 perfusion system, Warner Instruments, Hamden, CT, USA);
- suction system (Schego optimal air pump);
- faraday cage, to protect the microscope and the other instruments from external electromagnetic waves are responsible of unwanted artefacts in the electrophysiological recordings;
- pneumatic anti-vibration tables, consisting of a platform designed to reduce vibration normally present in any building (Newport breadboard table);

- personal computer with a dedicate software (WinWCP version 4.1.2 Strathclyde Electrophysiology software) for data acquisition and analyses, kindly provided by Dr John Dempster (Glasgow, United Kingdom).

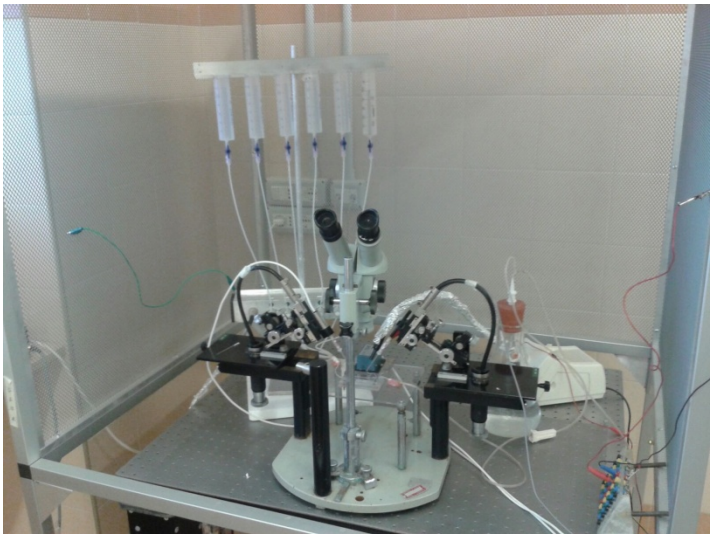

FIGURE 3.3: The two-electrode voltage clamp equipment.

Glass micropipettes were produced from borosilicate glass capillary (Harvard Apparatus, UK) with a vertical electrode puller at two independently selectable temperature setting (L/M-3P-A, List, Darmstadt, F.R.G.). The pipettes were filled with sterile and filtered with KCl (3 M) [182] with a proper syringe with a fine needle, removing the air bubble from the tip of the electrode.

Before the recording, the oocytes ware carefully moved using a fire-polished Pasteur pipette from the vial to the recording chamber to be impaled. During the recordings, they were continuously superfused with Ringer solution (see section: *Solution*) (5-10 ml min-1) at room temperature (22-24°C). All experiments were performed at membrane holding potential -80 mV to drive a large inward current.

The activation of AChR-channels was evoked by ACh at the concentration of 1 mM to open all the channels [183]. The desensitization was measured as a current decay $T_{0.1}$ and $T_{0.5}$, the time necessary for the current to decay by 10% and 50% from its peak value [184, 185]. The resting membrane potential and the membrane input were calculated as described in [186] (see section: *Appendix 1*).

For ACh dose/current response curves, the ACh was repeatedly applied at 5 min intervals, and the half-dissociation constants (EC_{50}) and Hill coefficients (n_h) were estimated by fitting the data to Hill equations [187].

3.2 Cell cultures

3.2.1 Mouse skeletal muscle myotubes

The myotubes used in this study derived from the differentiation of primary murine muscle precursor cells (myoblasts), called i28, established from mouse satellite cells and generously provided by Prof. A. Werning (University of Bonn). Briefly, cells were isolated from the hind-leg of 7-day-old male Balb/c mice killed by cervical dislocation. Muscle tissue was minced and then enzymatically dissociated with collagenase and trypsin, to obtain the cell of interest (for more details see [188]). Myoblast were amplified in the presence of Growth Medium (GM), consisting of HAM'S F-10 containing: 20% fetal bovine serum FBS, L-glutamine 2 mM and 1% penicillin and streptomycin solution (respectively 100 u.i./ml and 100 units/ml).

Myoblasts were trypsinized and routinely seeded at a density of 30000 cells in 90 mm Petri dishes. To perform the experiments, mononucleated myoblasts were plated at a density of 30000-40000 cells in 35-mm matrigel-coated Petri dishes. To induce the differentiation, 1 day after plating, the GM was replaced with a Differentiation Medium

(DM) consisting of DMEM (containing 4500 mg glucose L^{-1} and 110 mg sodium pyruvate L^{-1}, pyridoxine HCl and $NaHCO_3$, without L-glutamine), supplemented with 2% horse serum and L-glutamine, penicillin and streptomycin as above. The differentiation medium was renewed every 3 days to avoid loss of nutrients and growth factors. The electrophysiological experiments were performed on myotubes kept in DM for 4-6 days. Cultures were maintained at 37°C in a humid air atmosphere containing 5% CO_2.

3.2.2 Flexor digitorium brevis myofiber culture

Fresh and cultured dissociated adult mouse myofibers were obtained from dissection of the flexor digitorium brevis (FDB). The FDB muscle were removed from both feet of 1 up to 2 months old male mice killed by cervical dislocation, as approved by local Animal Care Committee and in agreement with the European legislation. Immediately after dissection, FDB muscles were washed in a 35 mm diameter Petri dish containing 2 ml of culture solution (CS, see *Solutions*). Thereafter, myofibers were immediately placed in a small vial containing 3 mg/ml collagenase solubilized in CM. The vial was maintained in ice for 1 hour; it was subsequently incubated at a temperature of 37°C in a humid air atmosphere containing 5% CO_2 and then gently shaken each 20 minutes for approximately 1 hour. This procedure was required in order to perform the enzymatic digestion of the connective tissue that lies on the surface of the muscle. It was therefore necessary to proceed with the mechanical dissociation of the myofibers: FDB muscles were transferred into 35 mm Petri dishes for three consecutive washing (Tyrode 2 ml, CM 2 ml and Tyrode 0.5 ml respectively) and were finally triturated with fire-polished Pasteur pipettes characterized by increasingly fine pore.

Dissociated fibers obtained following this protocol were seeded into 35 mm Petri dishes coated with Matrigel (1 mg/ml, Biosciences). Cell cultures were maintained in 2 ml CM

at 37°C in a humid air atmosphere containing 5% CO_2. Electrophysiological recordings were performed the same day or the day after the isolation.

3.3 The patch-clamp technique

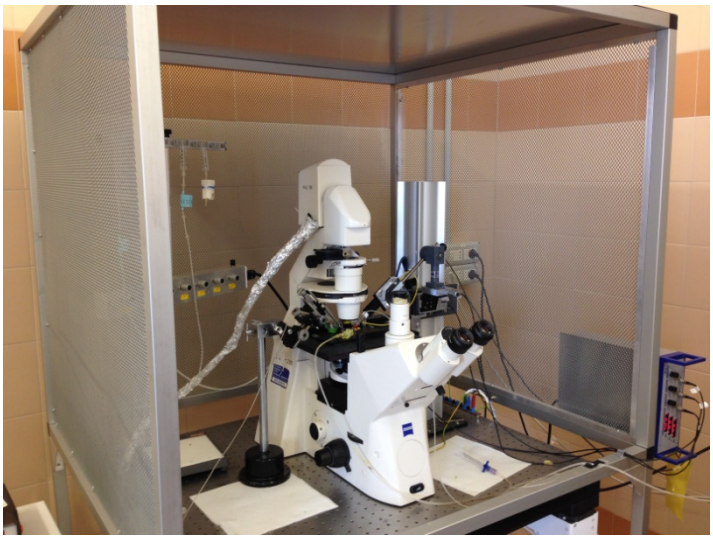

FIGURE 3.4: The electrophysiology patch-clamp equipment.

The patch clamp technique is used to investigate the biophysics properties of ion channels, allowing the recordings both the membrane potential and its variations (current-clamp mode) and the current passing through the cell membrane at a certain voltage values (voltage-clamp mode).

The experimental set-up for patch clamp recordings was organized as follow:

- inverted microscope (Axiovert 100, Zeiss, Germany) with objective for 10x, 20x and 40x magnification, provided with a mechanical stage with dedicated space for 35 mm Petri dishes (Fig. 3.4);
- mechanical macromanipulators and piezoelectric micromanipulators (Physic Instruments, Germany);
- holder (HL-U, Axon Instruments), containing a chloride silver electrode which is inserted into the glass micropipette;

- headstage (CV203BU, Axon Instruments), which performs the voltage-current conversion;
- patch clamp amplifier (Axopatch 200B, Axon Instruments) with switches for the correction of transients and electrode resistance compensation;
- analog-digital / digital-analog converter (Digidata 1231, Axon Instruments);
- a micro-puffing system for local drug delivery (Medical System Corp, Greenvale, NY);
- Faraday cage, to shield the microscope and the other instruments from electromagnetic interferences, which are responsible of unwanted artefacts in the electrophysiological recordings (Fig. 3.4);
- anti-vibration tables, consisting of a platform with minimal mechanical interference (Newport breadboard table; Fig. 3.4);
- personal computer with a dedicate software (Clampex10.3 and Clampfit10.3, Axon Instruments) for electrophysiological experiments acquisition and analysis. For statistical analysis and graph plotting was used Origin7.0 (Microcal Software Northampton, MA, Canada, USA).

All the electrophysiological experiments were performed at room temperature (22-24°C). Glass micropipettes exploited in patch clamp experiments were fabricated from borosilicate glass capillaries (Harvard Apparatus LTD, UK) and produced using a PP-830 Narishige pulling device (Japan) and eventually fire-polished to a final tip resistance when filled with pipette solution.

3.3.1 Whole-cell configuration

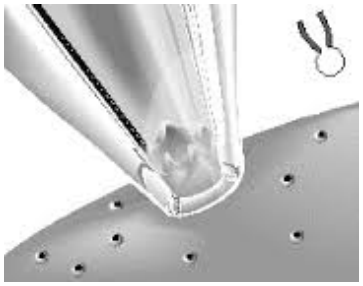

FIGURE 3.5: Whole-cell configuration.

The whole-cell configuration of the patch-clamp was chosen to record the total ACh-induced currents in i28 myotubes (Fig. 3.5). Basic electrical properties of myotubes were evaluated in mouse skeletal differentiated *in vitro* maintained in DM from four to six days.

The mean R_m and the mean membrane capacitance (C_m), measured in voltage clamp in whole-cell configuration, were 1.10 ± 0.16 GΩ (*n* = 10) and 34.42 ± 3.42 pF (*n* = 10), respectively. Resting membrane potential, measured in whole cell configuration immediately after disrupting the patch was – 45.3 ± 2.56 mV (*n* = 10).

Medium-sized multinucleated myotubes were visualized by inverted microscope and selected for the experiments. During recordings, the cells were kept in a normal external solution, NES (see section: *Solutions*). Borosilicate glass patch pipettes were fire-polished to a final resistance of 4-6 MΩ and filled with an intracellular solution that resembled the cytoplasmic ionic composition (see section: *Solution*s).

The activation of AChR-channels was evoked by 100 µM of ACh and recorded at holding potential of -50 mV. As for oocytes, the desensitization was measured as a current decay $T_{0.1}$ and $T_{0.5}$ (time necessary for the current to decay by 10% and 50% from its peak value). Signals were sampled at 50 kHz, filtered at 5 kHz with a low-pass Bessel filter.

3.3.2 Cell-attached configuration

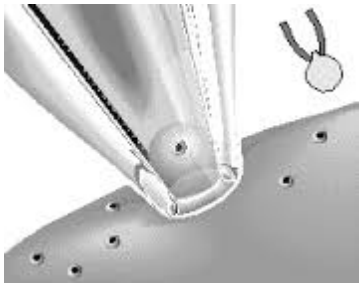

FIGURE 3.6: Cell-attached configuration.

The cell-attached configuration of the patch-clamp allows the study of the single channel activity recorded in the membrane under the pipette (Fig. 3.6). The membrane potential of cell-attached patches ($V_{m.patch}$) is determined by the difference between the membrane resting potential ($V_{m\ cell}$) and the applied potential ($V_{pipette}$). The transmembrane potential is therefore given by:

$$V_{m.patch} = V_{m.cell} - V_{pipette}$$

Myofibers were plated in 35 mm petri dishes coated with matrigel and 2 ml of NES (see section: *Solutions*). Borosilicate glass patch pipettes were fire-polished to a final resistance of 5-8 MΩ and filled with NES plus ACh (200 nM). Signals were sampled at 50 kHz, filtered at 1 kHz with a low-pass Bessel filter. Data were collected immediately after achieving the gigaseal, when the single channel activity was stable. In each cell, the single channel properties were analyzed from at least 300 channel openings. Current amplitude can provide information on single-channel conductance and ion specificity of the channel. To examine with accuracy the mean channel open time, only traces with single openings were considered for the analysis.

The single channel open probability (P_o) was calculated using the formula:

$$P_o = \frac{t_o}{t_i}$$

where t_o is the total open time and t_i is the time interval over which P_o was measured. All recordings were performed at +60 mV pipette potential. Amplitude of channel events was plotted against pipette potential (V_p) at +40, +60, and +80 mV, and the single channel conductance was estimated from the linear regression.

3.4 Radioligand binding

3.4.1 Membrane preparation

Cells were washed with phosphate-buffered saline (PBS), detached from plates in 10 ml of PBS by a scraper, collected and centrifuged for 10 min at 100 *g*. Pellets derived from six plates were pooled and resuspended in 20 ml of ice-cold 50 mM Tris-HCl buffer, pH 7.4, and homogenized in glass potter homigenizer for 10 s. Plasma membranes and cytosolic fraction were separated by centrifugation at 27000 *g* at 4°C for 30 min in a superspeed refrigerated centrifuge (model RC-5B, Sorvall, Wilmingtom, DE, USA). Pellets were resuspended in ice-cold 50 mM Tris-HCl buffer pH 7.4 at 10^8 cells/3 ml and 20 U/ml of adenosine deaminase (ADA) were added. After 30 min incubation at 37°C the membranes were stored in 200 μl aliquots at -80°C. Membrane protein concentrations were measured using the Lowry assay [189].

3.4.2 Receptor binding assay

The P1Rs density (B_{max}) was determined in oocyte membrane aliquots containing 80 μg of proteins and incubated in 200 μl of 50 mM Tris-HCl buffer, pH 7.4, at 25°C for 180 min, according to previous time course experiments. Displacement experiments were performed using 5 nM [^{3}H]DPCPX as radioligand, and saturating concentrations of 100 μM CPA to prevent nonspecific binding to A_1R, following the method of Dalpiaz et al.,

[190]. Separation of bound from free radioligand was performed by rapid filtration through GF/B filters (Whatman, Sigma-Aldrich, Milan, Italy), which were washed three times with ice-cold 50 mM Tris-HCl buffer, pH 7.4. Filter bound radioactivity was measured by scintillation spectrometry after adding of 3 ml Packard Emulsifier Safe (PerkinElmer, Milan, Italy). All the values obtained were the means of three independent experiments performed in duplicate. Data were analyzed by means of nonlinear least-square curve fit (GraphPad Prism 4.0).

3.5 Solutions

3.5.1 Extracellular solution

Xenopus laevis oocytes

Barth solution	
Salt	**Concentration (mM)**
NaCl	88
KCl	1
$Ca(NO_3)_2$	0.33
$CaCl_2$	0.41
$MgSO_4$	0.80
$NaHCO_3$	2.4
HEPES	10
pH 7.4 with NaOH	
Gentamicin (50 µM)	

Ringer solution	
Salt	**Concentration (mM)**
NaCl	88
KCl	1
$CaCl_2$	0.41
HEPES	10
pH 7.4 with NaOH	

Fibre FDB and myotubes in culture

Culture Medium	
Salt	**Concentration (mM)**
NaCl	140
KCl	2.8
$CaCl_2$ (anhydrous)	2
$MgCl_2$ (anhydrous)	0.80
NaH_2PO_4	0.4
$NaCO_3$	12
Glucose	5.5
HEPES	25
10% FBS	
1% PEN-STREP	
Ph 7.4 with NaOH	

Normal external solution (NES)	
Salt	**Concentration (mM)**
NaCl	140
KCl	2.8
$CaCl_2$ (anhydrous)	2
$MgCl_2$ (anhydrous)	2
Glucose	10
HEPES	10
Ph 7.4 with NaOH	

Phosphate buffered saline (PBS)	
Salt	**Concentration (mM)**
NaCl	88
NaH_2PO_4	1.83
Na_2HPO_4	10.6

3.5.2 Solution for electrophysiological recordings

For electrophysiological recordings, the composition of pipette solutions depends on the patch-clamp configuration.

Cell-attached configuration

Pipette solution	
Salt	**Concentration (mM)**
NaCl	140
$CaCl_2$ (anhydrous)	2
$MgCl_2$ (anhydrous)	0.80
Glucose	10
HEPES	10
Ph 7.4 with NaOH	

Whole-cell configuration

Pipette solution	
Salt	**Concentration (mM)**
KCl	120
EGTA	11
$CaCl_2$	1
$MgCl_2$	1
Disodium salt ATP	1
HEPES	10
Ph 7.3 with KOH	

3.5.3 Chemicals

Foetal calf serum was purchased from Life Technologies (Monza MB, Italy) and Matrigel from Becton-Dickinson (Rutherford, NJ, USA). P1R ligands were purchased from Tocris Bioscience (Bristol, United Kingdom) and ADA was from Roche S.p.A. (Milano, Italy). All the other chemicals, unless otherwise stated, were from Sigma (St. Louis, MO, USA).

3.5.4 Statistical analyses

GraphPad Prism 3.0 (GRAPH Pad Software, San Diego, CA, USA) and Origin 7.0 were routinely used for statistical analysis and graph plotting. Differences between data were evaluated by Student's t test (unpaired *t*-test). Data of *n* experiments were expressed as mean ± S.E.M. Data were considered significant at $P < 0.05$.

CHAPTER 4

RESULTS AND DISCUSSION

Most of the results reported in this thesis were obtained in *Xenopus laevis* oocytes isolated from female frogs operated up to 4 times (the time interval between two surgeries was at least 6 months; on the same abdominal side: >1 year).

In the first part of the results I provided an overview of the effects of the multiple laparotomies on the quality of the oocytes, with a special emphasis on the passive electrical properties of the cell membrane (V_m, resting membrane potential; R_m, membrane input resistance), and the ability to incorporate functional exogenous nicotinic acetylcholine receptors (AChRs) into the oolemma.

Xenopus laevis, commonly known as the South African Clawed frog, is a highly adaptable species living in a range of habitats and relatively easy to breed and maintain in the laboratory [191]. Gametogenesis is continuous and occurs year round, so eggs and oocytes can be collected for cellular and biological research. On the other hand, *Xenopus laevis* go through periods of unexplained inefficient poor quality oocytes due to a variety of different factors such as temperature, age and nutrition. This may affect the relative efficiency of the experiment resulting in experimental delays, inability to reproduce data, and ultimately the use of more animals [132]. Many laboratories perform multiple laparotomies on a single frog in order to reduce the number of animals used over the long-term. For electrophysiological purpose, the cells are typically selected based on the pigmentation of the animal hemisphere and the irregular shape [192] but the effect of the surgeries on the quality of the cells has never been investigated in detail.

To evaluate the quality of the oocytes used in my experiments, I compared the V_m and the R_m of oocytes isolated from animals operated one, three and four times. These two parameters have been chosen to provide important information about the oocyte condition in terms of structural and functional integrity of the plasma membrane, which are fundamental in order to perform successful experiments. I found that at the first surgery the V_m and R_m were significantly reduced compared to those at the third and fourth surgery (First: V_m: -31.08 ± 2.10 mV; R_m: 1.19 ± 0.11 MΩ, n = 26/4; Third: V_m: -37.82 ± 0.72 mV; R_m: 1.74 ± 0.06 MΩ n = 165/20; Fourth: V_m: -41.53 ± 1.52 mV; R_m: 1.84 ± 0.15 ΩM, n = 43/5; $^{**}P < 0.01$; $^{***}P < 0.001$; Fig. 4.1).

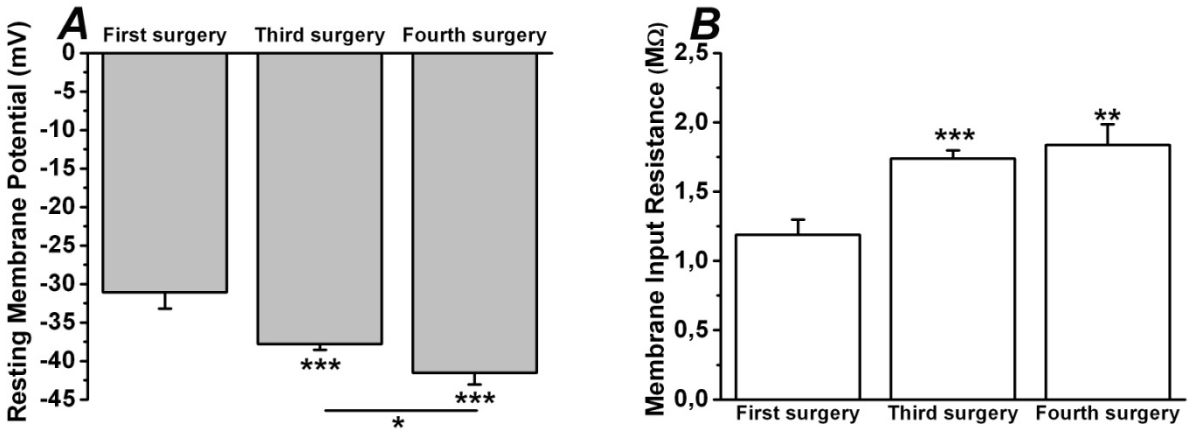

FIGURE 4.1: Effects of multiple laparotomies on the passive electrical membrane properties of *Xenopus* oocytes.

The V_m ***(A)*** and the R_m ***(B)*** are compared among groups of oocytes isolated at the first, third and at the fourth surgery; the V_m is significantly more hyperpolarized at the third and fourth laparotomy, while the R_m increases as surgeries proceed. $^{**}P< 0.01$; $^{***}P< 0.001$.

One of the reasons that may affect the oocyte quality is the poorly understood seasonal variation [142]. In the next series of experiments, I compared the V_m and the R_m recorded through different seasons in oocytes isolated from donors at the third surgery;

Interestingly, the V_m significantly changed becoming particularly hyperpolarized in autumn and spring, while the R_m significantly increased in spring (Fig. 4.2; Table 1).

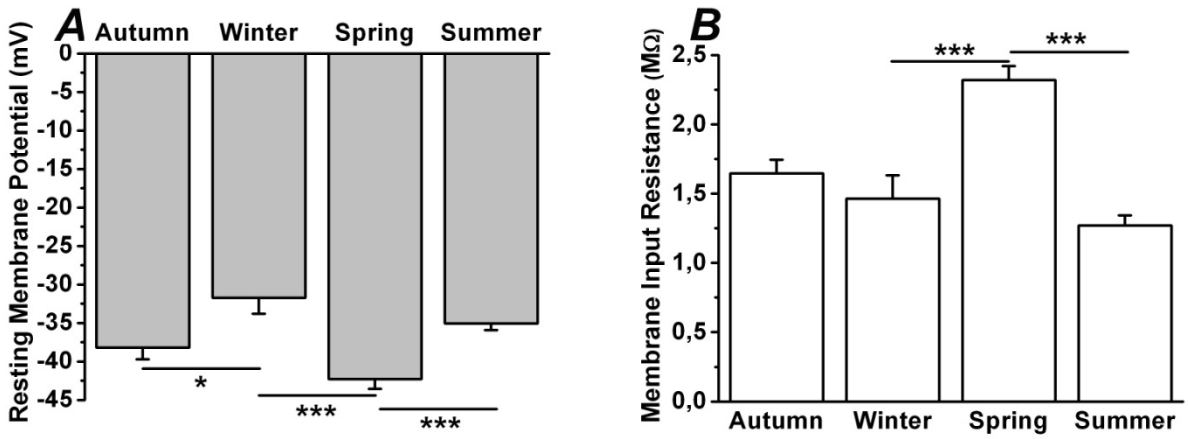

FIGURE 4.2: The effect of seasonal variation on the electrical membrane properties of oocytes. The values of the V_m ***(A)*** and R_m ***(B)*** are compared among groups of oocytes isolated in different seasons. As shown, the V_m is significantly more hyperpolarized during autumn and spring, while the R_m significantly changes in spring. *P < 0.01; ***P < 0.001.

TABLE 1: Averages of the V_m and R_m values recorded in different seasons.

	RMP (mV)	R_m (MΩ)	N/frog
Autumn	-38,19 ± 1,53	1,65 ± 0,09	41/5
Winter	-31,71 ± 2,1	1,46 ± 0,17	21/3
Spring	-42,29 ± 1,24	2,32 ± 0,10	55/7
Summer	-35,04 ± 0,87	1,27 ± 0,07	48/5

Amphibians used for these experiments were kept under a constant light cycles (12 h light/12 h dark). Photoperiod does not seem to play a significant role in oogenesis, but there is only limited information about this effect. Conversely, temperature variations associated with seasonal environmental changes, are strongly correlated with gonadal development and oogenesis in wild frogs. In order to minimize seasonal variation the water is kept constant in a good aquarium filtration/aeration system (18°C) as well as

the air temperature (22°C). Under these conditions the animals are quite capable of continuous gametogenesis and of producing a steady supply of oocytes [192]. The variations of the passive membrane properties could be dependent on the presence of different endogenous channels on the surface of the oocytes that may appear in various combinations. A similar effect is reported for muscarinic receptors where the response of single oocytes to the application of ACh in summer are different from those in winter [193]. Taking into account the housing, husbandry and care of *Xenopus laevis* may not be enough to prevent physiological changes associated with natural biological rhythms.

Xenopus oocytes are a very powerful tool for studying the biophysical properties of exogenous receptors and ion channels. The effect of the laparotomies on the ability of oocytes to incorporate exogenous nAChRs was tested measuring the currents elicited by ACh (I_{ACh}; 1 mM) 24 h after the injection of cell membrane isolated from myotubes (Fig. 4.3). Interestingly, the amplitude was found to significantly increase at the fourth surgery (from 254.11 ± 20.85 nA, *n* = 27/4 at the first surgery to 348.7 ± 30.99 nA, *n* = 54/4 at the fourth surgery).

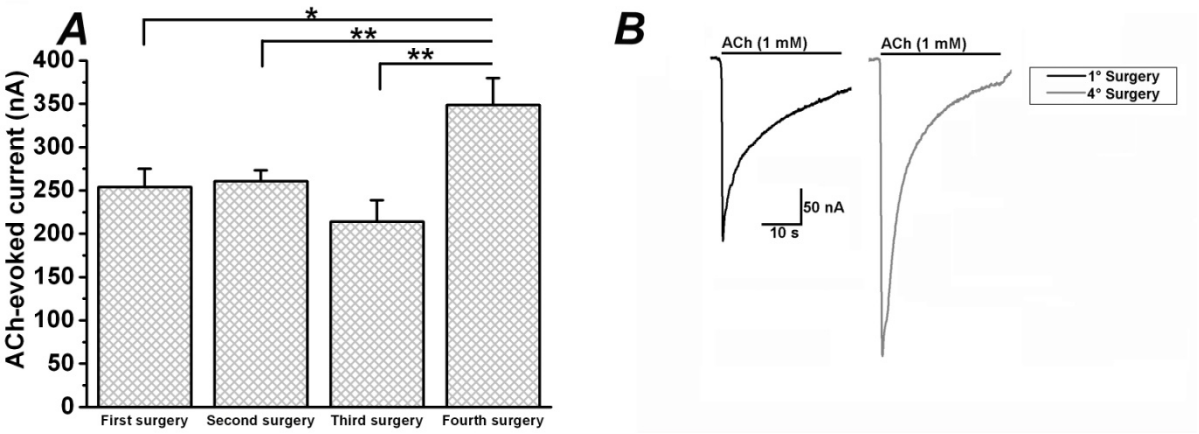

FIGURE 4.3: Functional incorporation of nAChRs in oocytes of frog donors after multiple laparotomies.

A, Averages of I_{ACh} (ACh 1 mM) recorded in oocytes isolated from frog donors at the first up to the fourth surgery. The current significantly increases in oocytes coming from frogs at the fourth laparotomy.

B, representative traces of ACh-currents recorded in two oocytes isolated from frog at the first (I_{ACh}: 250 nA) and the fourth laparotomy (I_{ACh}: 409 nA). *$P < 0.05$, **$P < 0.01$.

Hence the number of nAChRs functional incorporated increases with the number of surgeries. Keeping in mind that the current amplitude could also be depended on the amount of exogenous protein microinjected, it remains to be elucidated what intracellular signals may change in *Xenopus* oocytes isolated in animals under different numbers of laparotomies. It would be interesting to investigate the possibility that these variations can involve factors that promote membrane fusion.

In conclusion, I found that oocytes isolated from animals retain and even improve their capability to incorporate functional nAChRs after the microinjection of the exogenous membranes. These findings support the reuse of the frog to collect the oocytes and consequently the reduction of the number of animals used in the laboratories.

4.1 Functional characterization of the embryonic-type of the nicotinic acetylcholine receptors transplanted into *Xenopus laevis* oocytes

In the second part of my study, I characterized in detail the I_{ACh} recorded in oocytes injected with cell membranes isolated from mouse myotubes. All currents reported in this section were recorded at a holding potential of – 80 mV and they were completely abolished in the presence of the nicotinic cholinergic antagonist α-bungarotoxin (α-Btx 5 µM, *n* = 5/1; Fig. 4.4*A*). The endogenous expression of nAChRs has never been reported in oocytes, however the cells occasionally have native muscarinic cholinergic receptors that increase the membrane conductance to Cl^- and K^+ by a intracellular messenger pathway [146]. Non-injected oocytes never responded to ACh (Fig. 4.4*B*), thus the I_{ACh} recorded in injected oocytes derived from the activation of exogenous nAChRs functionally transplanted into the oolemma.

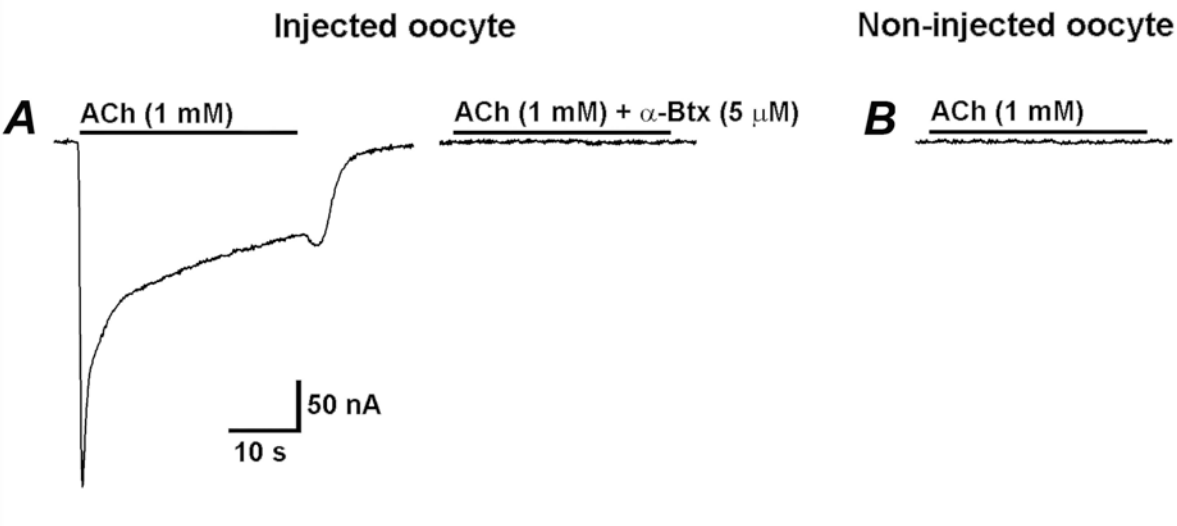

FIGURE 4.4: Functional incorporation of nAChRs into oolemma.
Representative traces showing the response to ACh in oocyte microinjected with muscle membrane ***(A)***, the I_{ACh} was abolished in the presence of α-Btx ***(B)***. In non-injected oocytes ACh did not evoke any current ***(C)***.

The response to ACh recorded in different batches of oocytes was quite variable already 24 hours after the injection (range 53 - 922 nA, *n* = 207/33, Fig. 4.5*A*). The variability could be a consequence of many factors: the diversity of membrane preparations, the frog donors, the number of laparotomies and lag between the microinjection and the experiment [176].

Fig. 4.5*B* shows the time course of the receptor incorporation at different days post-injection in oocytes isolated from the same donor; the responsiveness to ACh after the peak response was reached (in this case 48 hours after injection) was not necessary due to the long life of the protein incorporated in the oocyte membrane but rather to the fusion process that continues also in the following days [179].

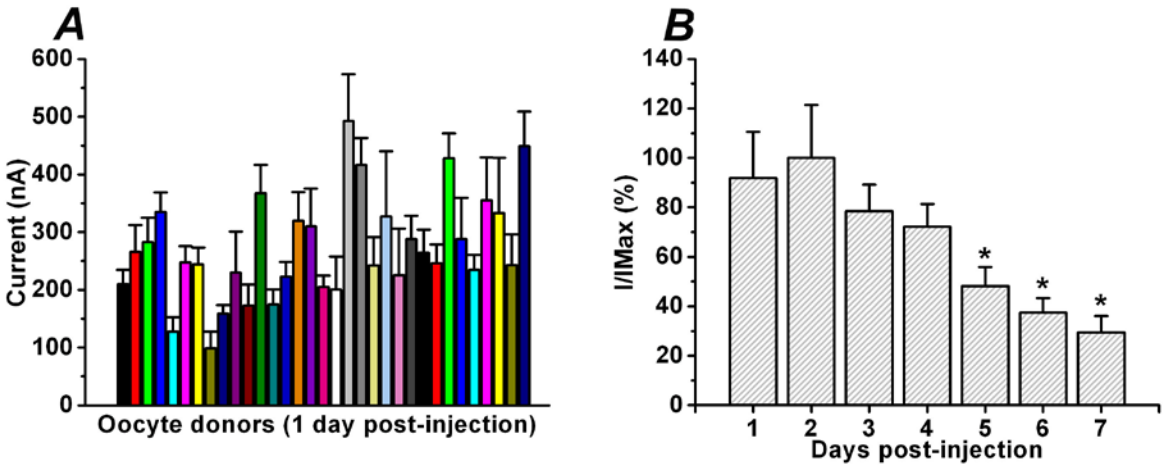

FIGURE 4.5: Time course of nAChR incorporation into oocyte membrane.

A, Comparison of the I_{ACh} amplitudes (ACh 1 mM) among group of oocytes isolated from different donors. All currents were recorded 1 day post-injection (*n* = 107/33). ***B***, Comparison of the I_{ACh} amplitudes obtained in oocytes at different days post-injection. The cells were isolated from same animal. Each histogram represents the % of the amplitudes normalized to the maximal value. *$P < 0.05$ vs the second day post-injection.

The dose–response relationships obtained from 6 oocytes showed a EC_{50} of about 20 ± 4,78 µM and Hill coefficient n_H of 0.99 ± 0.13 (Fig. 4.6), typical of the embryonic isoform of the nAChR [184, 187].

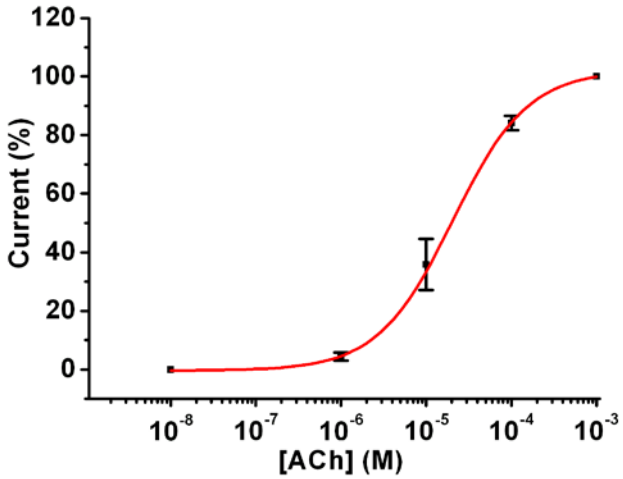

FIGURE 4.6: Dose-response relationship of the nAChRs transplanted into oocytes.
The dose-response obtained in oocytes one day after the injection of the muscle membranes. I_{ACh} is normalized to the maximal response and expressed as % (n = 6/1).

In the next series of experiments I further characterized some of the desensitization properties of I_{ACh}. To that aim I measured and compared the $T_{0.1}$ and $T_{0.5}$ values, which are reliable parameters, to describe two different phases of the decay responses of I_{ACh}. They were estimated as the time necessary for the current to decay by 10% and 50% from the peak [185]. The values recorded in this study were 0.64 ± 0.02 s (range 0.1-1.4 s, n = 154/28) for $T_{0.1}$ and 5.63 ± 0.16 s (range 1.8 - 11.3 s, n = 154/28) for $T_{0.5}$. In Fig. 4.7 the two parameters are plotted *vs* I_{ACh}; the correlation coefficients ($T_{0.1}$: r = 0.095; $T_{0.5}$: r = 0.12) showed that the $T_{0.1}$ and $T_{0.5}$ were independent variables of I_{ACh} amplitude, as reported for the embryonic receptors [184, 185].

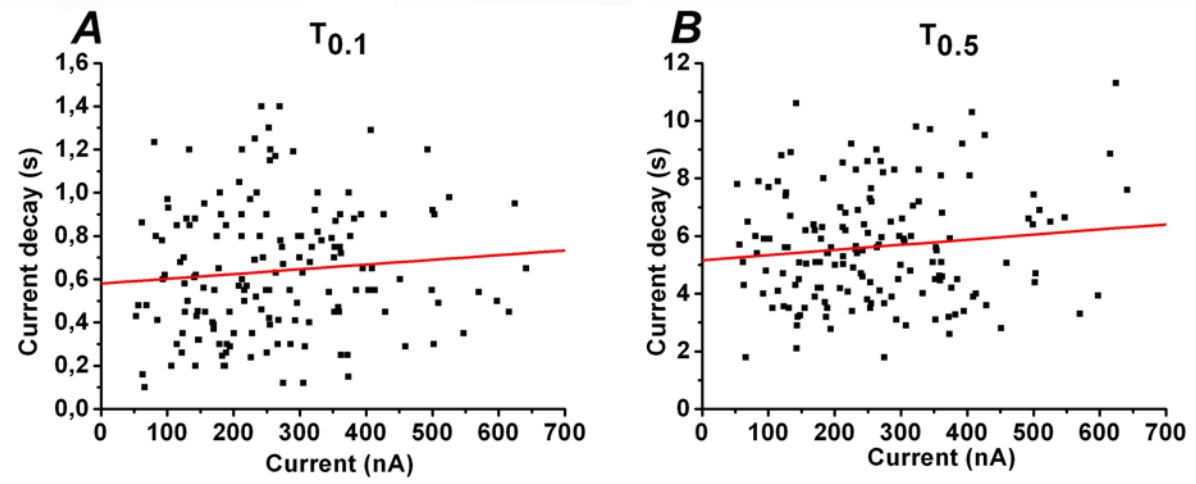

FIGURE 4.7: The ACh-induced current decay is independent from the current amplitude.
Plot of $T_{0.1}$ and $T_{0.5}$ values *vs* I_{ACh} amplitudes (ACh 1 mM) recorded in oocytes after the injection of the myotube membranes (*n* = 154/28). The estimated regression line (red) superimposed on the scatter diagram shows a correlation coefficients of r = 0.095 ($T_{0.1,}$ ***A***) and *r* = 0.12 ($T_{0.5,}$ ***B***).

Fig. 4.8 shows that upon repetitive application of ACh (10 s, intervals of 4 min) the amplitude of the I_{ACh} tended to attenuate and did not fully recover, similarly to what is reported for the embryonic nAChRs transplanted into oocytes after the injection of denervated skeletal muscle membranes [187]. The currents frequently showed a large "wash-kick" (Fig. 4.8*A*), caused to open-channel blockage by high concentration of ACh [194]. The run-down can be a consequence of the desensitization and thus it is regulated by post-translational modifications, such as protein phosphorylation and glycosylation [38]. However, the run-down could be also the effect of the endocytosis of nAChRs from the cell-surface induce by the agonist [195].

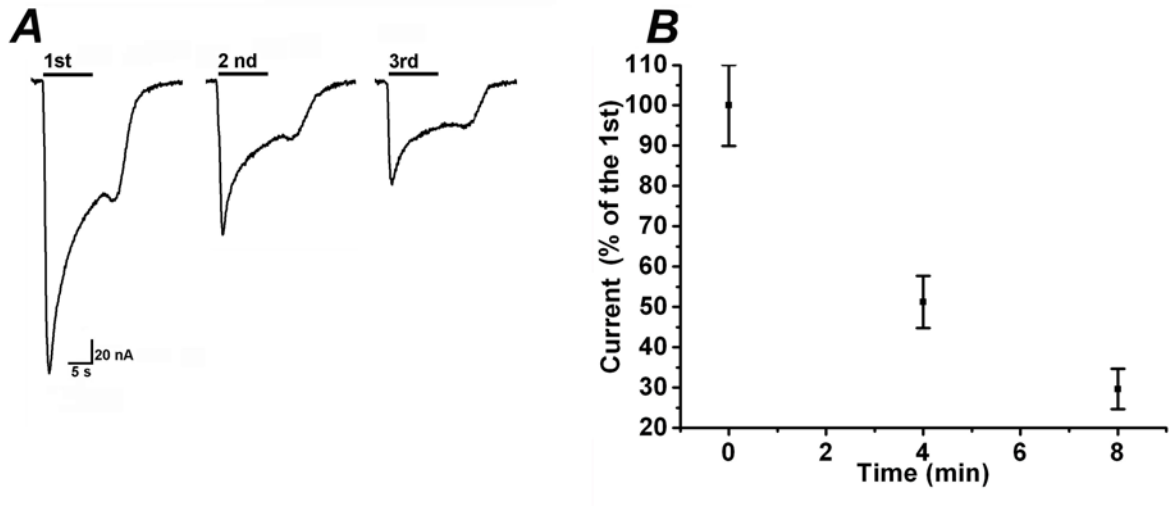

FIGURE 4.8: I_{ACh} run-down recorded in oocytes injected with myotube membranes.
A, Representative traces induced by the 1st, 2nd and 3rd of consecutive ACh applications, 1 day post-injection. ***B***, Averages of I_{ACh} induced by repetitive ACh applications (time interval 4 min, *n* = 8/1, 1 day post-injection). I_{ACh} is expressed as percentage of maximal response (%).

Taken together these results demonstrated that oocytes were able to incorporate functional nAChRs after the injection of cell membranes isolated from the myotubes. The activity of the receptors resembled those reported for the embryonic isoform expressed in the native cells. Furthermore, the injection of the membranes did not affect the V_m and the R_m of the oocytes (non-injected oocytes: V_m = - 41.53 ± 1.51 mV, R_m= 1.83 ± 0.15 MΩ *n* = 43/5; injected oocytes: V_m = - 42.39 ± 1.01 mV, R_m = 1.80 ± 0.07 MΩ, *n* = 101/4, *data not shown*), indicating that the small damage caused by the microinjection did not alter the electrical passive membrane of oocytes.

4.2 Adenosine-mediated modulation of the embryonic-type of the nicotinic acetylcholine receptors

Previous studies carried out in my laboratory demonstrated that the tonic release of Ado from contracting mouse myotubes modulated the single channel activity of the embryonic isoform of the nAChRs. Specifically, the activation of the A_{2B} subtype stimulated AC and increased the mean open time and the open probability of the channels [116]. Here I aimed to investigate whether the transplantation of myotube cell membranes into *Xenopus* oocytes preserved the crosstalk between the two receptors. To do that, the possible purinergic modulation of the nAChRs was evaluated by testing the effect of specific P1Rs ligands on the I_{ACh} desensitization, in particular on the current decay. Part of the results has been compared to those obtained in myotubes under similar experimental condition. To overcome the variability observed in batches of oocytes from different frogs, all results I reported in this section have been compared among cells isolated from the same donor.

4.2.1 Adenosine-mediated effect on the ACh-induced currents

To verify the effect of Ado on the activity of the transplanted nAChRs, the I_{ACh} was recorded in injected oocytes pretreated with the nucleoside. The cells were continuously perfused for about 2-3 minutes (constant flow 5 ml/min) with a Ringer solution containing 100 μM of Ado daily prepared to avoid the rapid degradation of the ligand. This concentration was enough to activate all P1R subtypes [83].

The application of Ado alone did not evoke any current response in non-injected oocytes (*n* = 10/2, *data not shown*) and injected oocytes (*n* = 21/3). In injected cells, as shown in Fig. 4.9*AB*, Ado accelerated the current decay induced by ACh (1 mM); both $T_{0.1}$ and $T_{0.5}$ values resulted significantly reduced compared to those obtained in

untreated cells (Ado: $T_{0.1}$ = 0.69 ± 0.05 s and $T_{0.5}$ = 4.48 ± 0.24 s, *n* = 21/3; Ctrl: $T_{0.1}$ = 1.15 ± 0.10 s and $T_{0.5}$ = 6.54 ± 0.31 s, *n* = 25/3; ****P* < *0.001*).

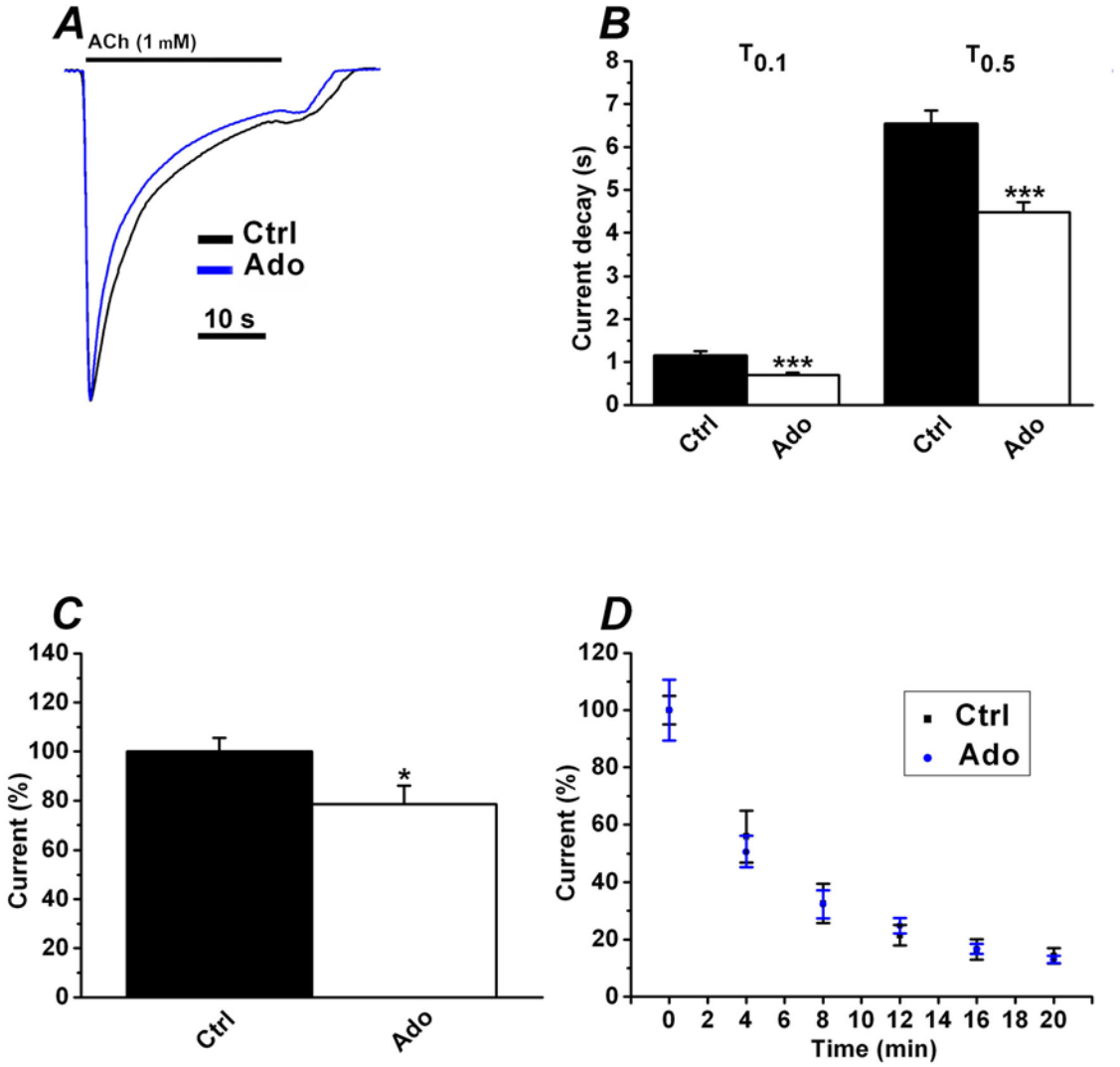

FIGURE 4.9: Adenosine affects the ACh-induced current recorded in oocytes.

A, Superimposed and normalized traces of I_{ACh} recorded in a Ctrl oocyte (*black*) and in an oocyte treated with Ado (100 µM, *blue*) (Ctrl: I_{ACh}= 1017 nA; $T_{0.1}$= 0.97 s and $T_{0.5}$= 6 s; Ado: I_{ACh}= 763 nA, $T_{0.1}$= 0.48 s and $T_{0.5}$= 4 s). ***B***, The histogram represents the averages of $T_{0.1}$ and $T_{0.5}$ in Ctrl oocytes (*n* = 25/3) and oocytes perfused with Ado (*n* = 21/3; ***P* < *0.001*). ***C***, Averages of I_{ACh} amplitude recorded in oocytes before (*n* = 34/3) and after the treatment with Ado (*n* = 27/3: **P* < *0.05*). I_{ACh} was normalized as percentage of maximal response (%) recorded in Ctrl. ***D***, The I_{ACh} run-down (10 s, time interval 4 min) is compared in Ctrl cells (*n* = 6/1) and oocytes treated with Ado (*n* = 5/1). I_{ACh} are normalized to first application of ACh (%).

Furthermore, Ado-treatment affected the I_{ACh} amplitude, which was reduced with respect to the Ctrl (Ado: 78.54 ± 7.59 %, *n* = 27/3; Ctrl: 100 ± 5.63 %, *n* = 34/3; **P* < *0.05,* Fig. 4.9*C*).

The I_{ACh} run-down resulted unaltered (Fig. 4.9*D*; Table 2).

TABLE 2:

Time interval (mins)	I_{ACh} Ctrl (%) (*n= 6*)	I_{ACh} Ado (%) (*n= 5*)
0	100 ± 4.98	100 ± 10.68
4	55.91 ± 8.97	50.62 ± 5.38
8	32.62 ± 6.84	32.29 ± 4.88
12	21.49 ± 3.52	24.79 ± 2.74
16	16.48 ± 3.56	16.74 ± 1.78
20	14.31 ± 2.64	13.01 ± 1.25

Oocytes, like most of the cells, release tonically Ado in the extracellular environment [196]. To investigate if the endogenous release could affect the I_{ACh}, the oocytes were pre-incubated in the presence of ADA (adenosine deaminase, 1 U/ml, 30-60 min) an enzyme that converts Ado into inosine. As shown in Fig. 4.10*BC*, before the treatment the values of $T_{0.1}$ and $T_{0.5}$ were 0.65 ± 0.036 s and 5.55 ± 0.22 s (*n* = 83/10) respectively, whereas in the presence of the enzyme both values significantly increased to 0.76 ± 0.036 s and 7.05 ± 0.28 s (*n* = 97/10 frogs; ***P* < *0.01*, ****P* < *0.001*). Moreover, in ADA-treated cells the amplitude of I_{ACh} increased by about 25% in respect to the Ctrl cells (Ctrl: 100 ± 4.78 %, *n* = 83/10; ADA: 124.71 ± 6.52 %, *n* = 97/10; ***P* < *0.01;* Fig. 4.10*A*). These results were further confirmed by the effect of the non-selective P1R antagonist CGS15943 (100 nM, 20 min, [83]); the blockage of all P1R subtypes tended to enhance the I_{ACh} amplitude of about 12% (Ctrl: 100 ± 4.78 %, *n* = 49/5; CGS15943: 111.61 ± 9.967 %, *n* = 46/5, *data not shown*) and affected the current decay similarly to what was reported in ADA-treated cells (CGS15943: $T_{0.1}$ = 0.73 ±

0.044 s and $T_{0.5}$ = 7.09 ± 0.36 s, *n* = 46/5; Ctrl: $T_{0.1}$ = 0.65 ± 0.043 s and $T_{0.5}$ = 5.70 ± 0.23 s, *n* = 49/5 ***P< 0.01*, *data not shown*).

In the same figure the effect of ADA on I_{ACh} recorded in myotubes is also shown (Fig. 4.10*CDF*). In this case the current was elicited by 100 µM ACh to avoid a desensitization of the channels too fast. Here the treatment with ADA (5 U/mL, 30-60 min) gave the opposite effect; the $T_{0.1}$ and $T_{0.5}$ in untreated cells were 0.11 ± 0.02 s and 0.58 ± 0.05 s (*n* = 12) while in the presence of the enzyme both values were significantly reduced to 0.05 ± 0.008 s and 0.35 ± 0.05 s (*n* = 8) (Fig. 4.10*EF*). Moreover, the I_{ACh} density of ADA-treated myotubes resulted slightly reduced (ADA: 278.63 ± 38.06 pA/pF, *n* = 12; Ctrl: 179.41 ± 30.05 pA/pF, *n* = 8; Fig. 4.10*D*). Note, contracting myotubes release a higher amount of Ado compared to other cells, thus I used ADA 5 times more concentrated than that used for oocytes [116].

The effect of ADA on the ACh-induced whole-cell currents recorded in myotubes was in line to what was previously reported at the single channel level [116]. However, after mictrotransplantation the tonic release of Ado modulated the activity of the nAChRs in a different way.

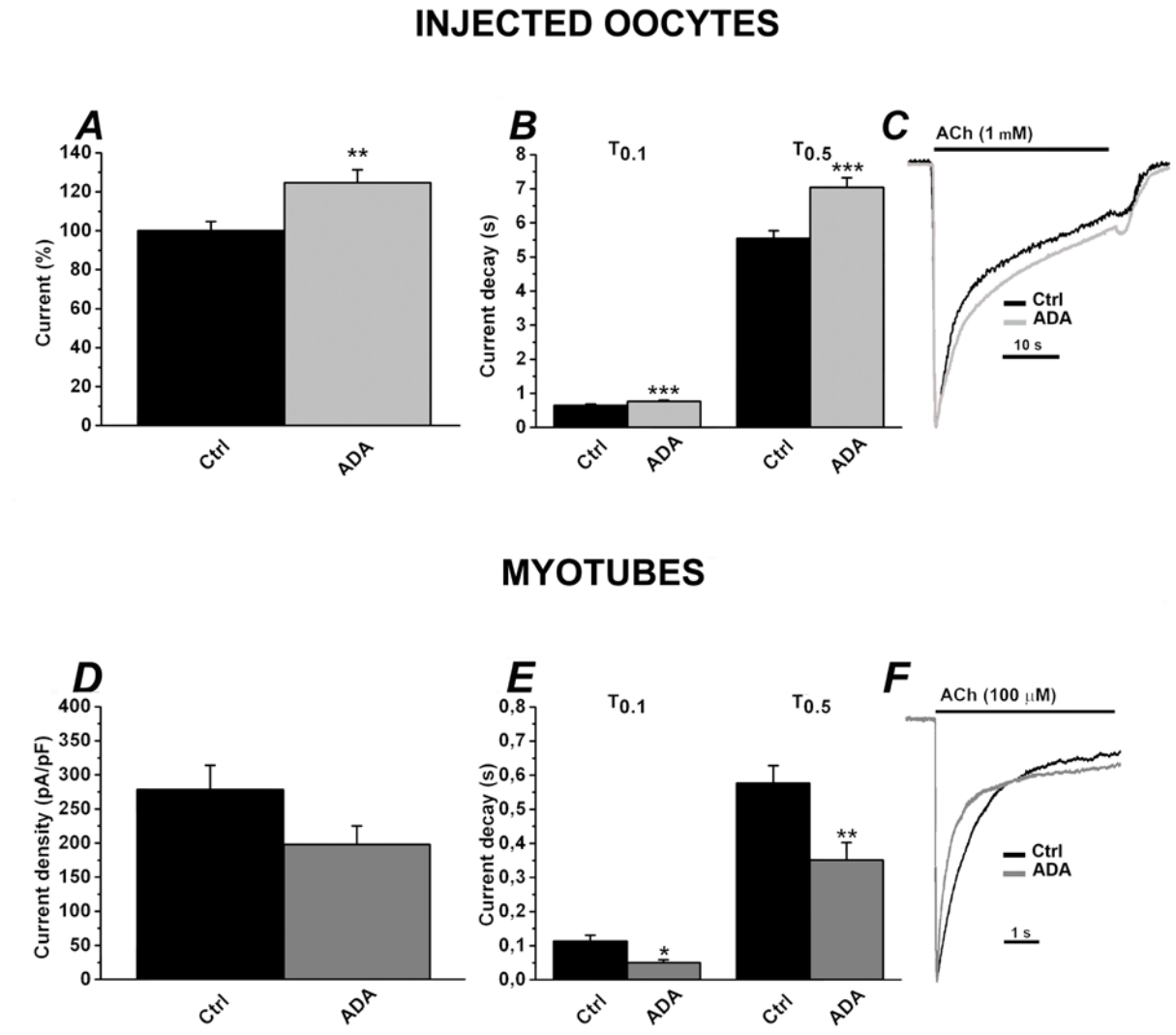

FIGURE 4.10: Endogenous Ado differently affects the ACh-induced currents recorded in oocytes injected with myotube membranes and in mouse myotubes.

A, Averages of I_{ACh} amplitude recorded in Ctrl oocyte (*n* = 83/10) and in oocytes pre-incubated with ADA (1 U/mL, *n* = 97/10; ***P* < *0.01*). I_{ACh} is normalized as percentage of maximal response (%) recorded in the Ctrl. ***B***, $T_{0.1}$ and $T_{0.5}$ values in Ctrl oocyte (*n* = 83/10) and oocytes pre-incubated with ADA (*n* = 97/10; ****P* < *0.001*). ***C***, Superimposed and normalized traces of I_{ACh} recorded in a Ctrl oocyte (*black*) and an oocyte treated with ADA (1 U/mL, l*ight grey*) (Ctrl: I_{ACh}: 231.4 nA, $T_{0.1}$= 0.69 s and $T_{0.5}$= 5.54 s; ADA: I_{ACh}= 353 nA, $T_{0.1}$= 0.75 s and $T_{0.5}$= 8.7 s). ***D***, I_{ACh} density (pA/pF) of I_{ACh} in Ctrl myotubes (*n* = 12) and in myotubes pre-incubated with ADA. ***E***, $T_{0.1}$ and $T_{0.5}$ values in Ctrl (*n* = 12) and ADA-treated myotubes (5 U/mL; *n* = 8; **P* < *0.05*; ***P<0.01*). ***F***, Superimposed and normalized traces of I_{ACh} recorded in Ctrl myotube (*black*) and ADA pre-treated myotube(5 U/mL, *dark grey*) (Ctrl: I_{ACh}= 6860 pA, $T_{0.1}$= 0.12 s and $T_{0.5}$= 0.82 s; ADA: I_{ACh}= 7343 pA, $T_{0.1}$= 0.003 s and $T_{0.5}$= 0.22 s).

4.2.2 Role of P1R subtypes in the modulation of ACh-induced currents

In the next series of experiments I aimed to identify, in more detail, the role of each P1R subtypes in the modulation of the I_{ACh} reported above. Our early study demonstrated that the subtype A_{2B} was the main candidate of the single ACh-channel activity modulation recorded in myotubes [116].

Fig. 4.11*AB* and Fig. 4.12*AB* summarize the effects of the specific A_{2B}R ligands on the I_{ACh} recorded in oocytes after the injection of the myotube membranes. Surprisingly, neither the antagonist MRS1754 (20 nM [197] [198], Ctrl: $T_{0.1}$ = 0,54 ± 0,04 s, $T_{0.5}$ = 4,68 ± 0,31 s, *n* = 48/5; MRS1754: $T_{0.1}$ = 0,64 ± 0,08 s, $T_{0.5}$ = 4,55 ± 0,42 s, *n*= 36/5) nor the agonist BAY60-6583 (100 nM, [199]. ADA: $T_{0.1}$ = 0,75 ± 0,06 s, $T_{0.5}$ = 6,16 ± 0,46 s, *n* = 32/4; BAY60-6583: $T_{0.5}$ = 0,77 ± 0,06 s, $T_{0.5}$ = 5,94 ± 0,51 s, n= 34/4) altered the I_{ACh} decay. Note the agonist was tested in ADA-treated cells to avoid the tonic activation of the P1Rs.

In myotubes in line with previously reported data [116], the ligands for the A_{2B} subtype affected the I_{ACh}; MRS1754 accelerated the current decay (Ctrl: $T_{0.1}$ = 0.11 ± 0.02 s, $T_{0.5}$ = 0.58 ± 0.05 s, *n* = 12; MRS1754: $T_{0.1}$ = 0.09 ± 0.01 s, $T_{0.5}$ = 0.35 ± 0.03 s, *n* = 7; Fig. 4.11*CD*) similarly to ADA, and the agonist elicited the opposite effect when applied in myotubes pretreated in the presence of the enzyme (ADA: $T_{0.1}$ = 0.05 ± 0.008 s, $T_{0.5}$ = 0.35 ± 0.05 s, *n* = 7; BAY60-6583: $T_{0.1}$ = 0.13 ± 0.01 s, $T_{0.5}$ = 0.55 ± 0.01, *n* = 3; *P< *0.01 for $T_{0.1}$. P = 0.052 for $T_{0.5}$;* Fig. 4.12*CD*).

The results suggested that the A_{2B} subtype was not involved in the modulation of nAChRs transplanted in oocytes. Thus, I performed more experiments to find out the possible role of other P1R subtypes.

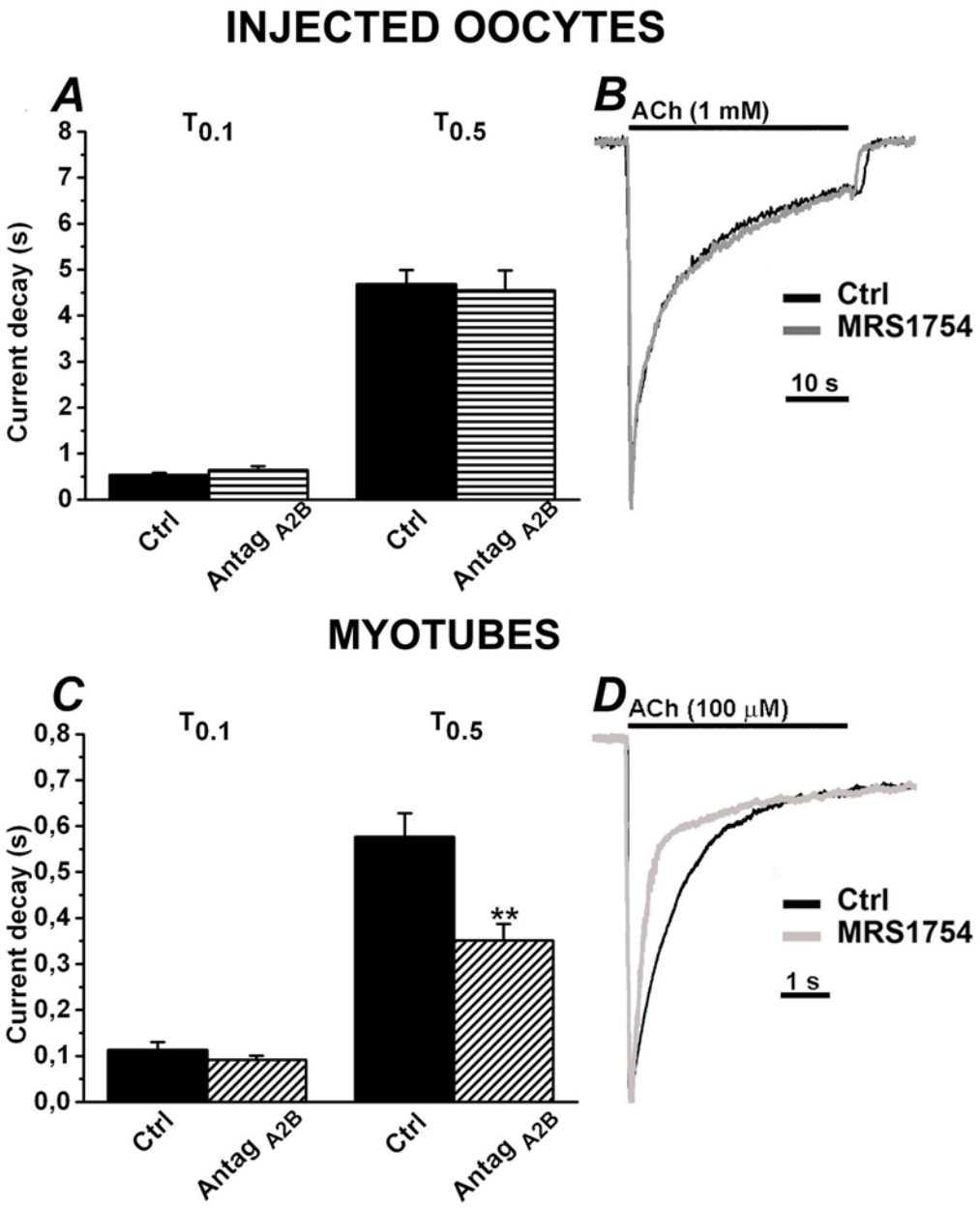

FIGURE 4.11: Effect of the A_{2B} antagonist MRS1754 on the ACh-induced current decay.

A,***C*** $T_{0.1}$ and $T_{0.5}$ values of the I_{ACh} recorded in untreated cells and cells incubated with 20 nM of MRS1754 (***P< 0.001*). ***B***,***D*** Representative traces of I_{ACh} recorded in cells before (*black*) and after (*grey*) the ligand incubation (Ctrl oocyte: I_{ACh}= 185 nA, $T_{0.1}$= 0.2 s and $T_{0.5}$= 3.7 s; MRS1754-treated oocyte: I_{ACh}= 177 nA, $T_{0.1}$= 3.4 s and $T_{0.5}$= 0.15 s; Ctrl myotube: I_{ACh}= 6860 pA, $T_{0.1}$= 0.12 s and $T_{0.5}$= 0.82 s; MRS1754-treated myotube: I_{ACh}= 714 pA, $T_{0.1}$= 0.087 s and $T_{0.5}$= 0.33 s)

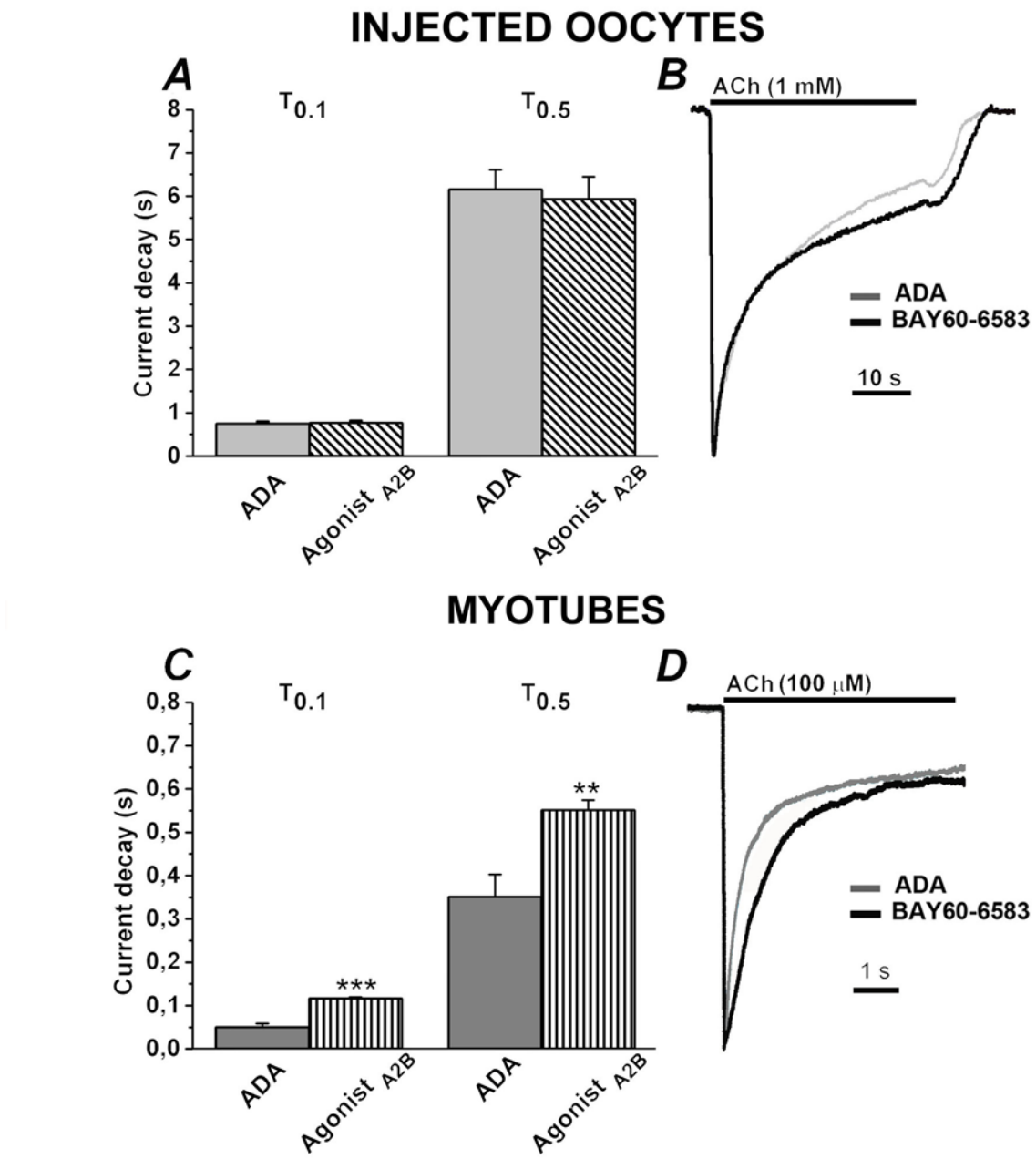

FIGURE 4.12: Effect of the A_{2B} angonist BAY60-6583 on the ACh-induced current decay.

A,***C*** $T_{0.1}$ and $T_{0.5}$ values of the I_{ACh} recorded in ADA-treated cells before (*gray*) and after incubation with 100 nM of BAY60-6583 (*black,**P< 0.001*). ***B***,***D*** Representative traces of I_{ACh} recorded in cells before (*grey*) and after (*black*) the ligand incubation (ADA-treated oocyte: I_{ACh}= 379 nA, $T_{0.1}$= 0.8 s and $T_{0.5}$= 6.7 s; BAY60-6583-treated oocyte: I_{ACh}= 148 nA, $T_{0.1}$= 6.8 s and $T_{0.5}$= 1.05 s; ADA-treated myotubes: I_{ACh}= 7343 pA, $T_{0.1}$= 0.003 s and $T_{0.5}$= 0.22 s; BAY60-6583-treated myotube: I_{ACh}= 2659 pA, $T_{0.1}$= 0.003 s and $T_{0.5}$= 0.22 s)

The antagonists DPCPX (A_1, 20 nM, [83]) ANR94 (A_{2A}, 100 nM, [200]) MRS1334 (A_3, 50 nM, [201]) and the agonists CPA (A_1, 20 nM, [202]), CGS-21680 (A_{2A}, 400 nM, [83]) and AB-MECA (A_3, 400 nM, [203]) were tested in injected oocytes. As before, the agonists were used in cells pretreated with ADA.

As summarized in Fig. 4.13, the only ligands that significantly affected the I_{ACh} were those for the A_1 subtype; indeed, the selective antagonist DPCPX accelerated the decay (Ctrl: $T_{0.1}$ = 0.61 ± 0.04 s, $T_{0.5}$ = 5.30 ± 0.26 s, *n* = 42/4; DPCPX: $T_{0.1}$= 0.69 ± 0.04 s, $T_{0.5}$ = 6.51 ± 0.26 s, *n* = 49/4, ***P < 0.01*; Fig. 4.13*AB*) while the agonist CPA restored the effect induced by the treatment with ADA (ADA: $T_{0.1}$ = 0.73 ± 0.07 s, $T_{0.5}$ = 5.56 ± 0.44 s, *n*= 15/3; CPA: $T_{0.1}$ = 0.61 ± 0.07 s, $T_{0.5}$ = 4.08 ± 0.31 s, *n* = 14/3, ***P < 0.01*; Fig. *4.13CD*).

The negligible role of the A_{2A}, A_{2B} and A_3 subtypes in the modulation of the I_{ACh} decay recorded in oocytes, and the strong effect of the A_1R ligands, suggested the A_1 subtype as a major candidate of the crosstalk between nAChRs and P1Rs in oocytes.

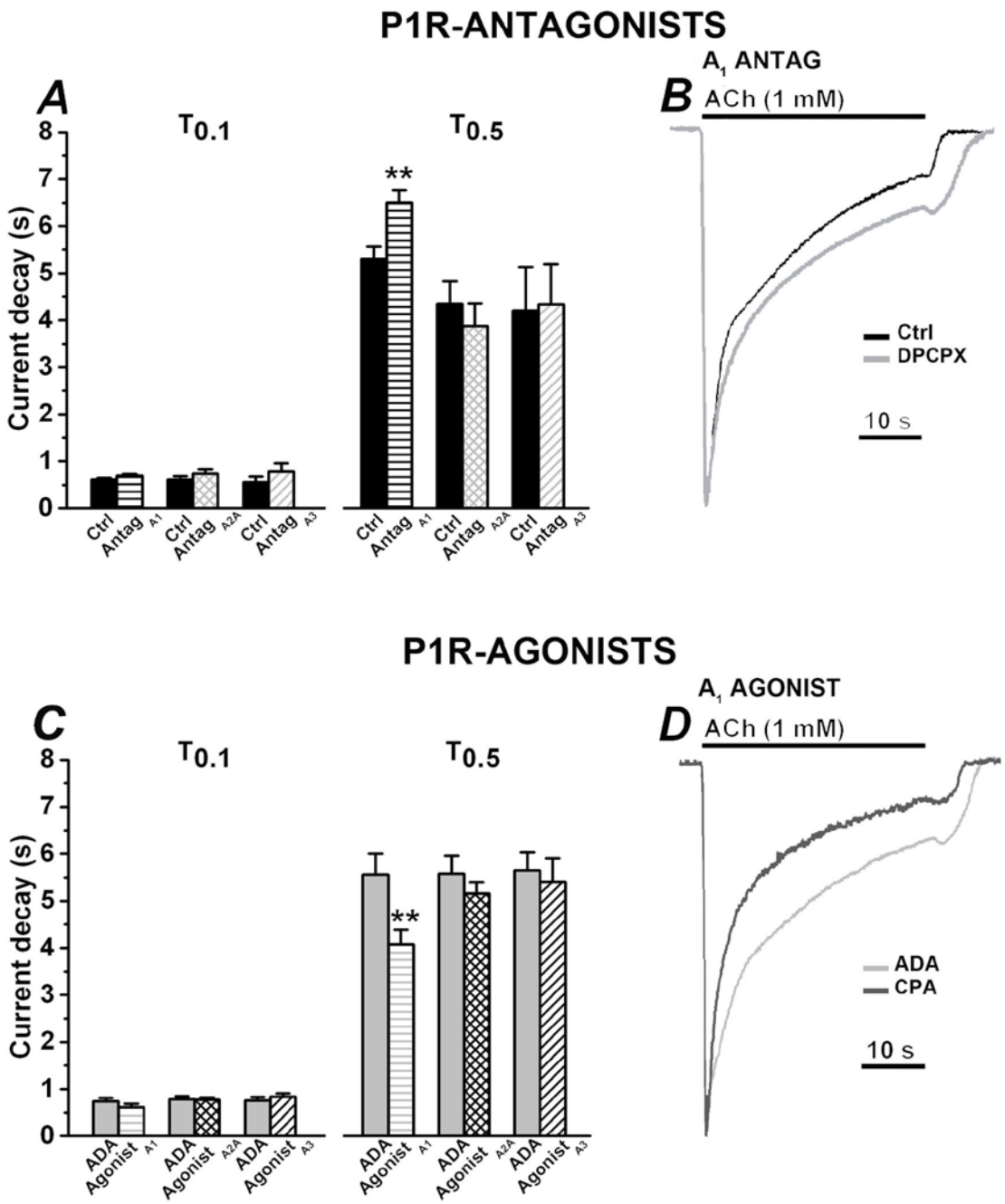

FIGURE 4.13: Effect of selective P1R subtype ligands on the ACh-induced current decay recorded in oocyte.

A, $T_{0.1}$ and $T_{0.5}$ values of Ctrl oocytes and pre-incubated with selective A_1 (DPCPX 20 nM), A_{2A} (ANR94 100 nM) and A_3 (MRS1334 50 nM) receptor antagonists (Ctrl *vs* A_1 antagonist ***P < 0.001*, *n > 40*). ***B***, Superimposed and normalized traces of I_{ACh} recorded in two oocytes, in the absence (*black*) and in the presence (*grey*) of DPCPX (Ctrl: I_{ACh}= 597 nA, $T_{0.1}$= 0.5 s and $T_{0.5}$= 3.93 s; DPCPX: I_{ACh}= 432 nA, $T_{0.1}$= 0.55 s and $T_{0.5}$= 6.5 s). ***C***, $T_{0.1}$ and $T_{0.5}$ values of ADA-treated oocytes before and after treatment with selective A_1 (CPA 20 nM), A_{2A} (CGS-21680 400 nM) and A_3 (AB-MECA 500 nM) receptor antagonists (ADA *vs* A_1 agonist ***P <0.01*, *n > 10*). ***D***, Superimposed and normalized traces of I_{ACh} recorded in two ADA-treated oocytes before (*light grey*) and after the A_1 agonist incubation (*dark grey*, CPA 20 nM)(ADA: I_{ACh}= 224 nA, $T_{0.1}$= 0.4 s and $T_{0.5}$= 6.8 s; CPA: I_{ACh}= 212.6 nA, $T_{0.1}$= 0.3 s and $T_{0.5}$= 2.4 s).

4.2.3 Role of adenylyl cyclase in the modulation of the ACh-induced currents recorded in oocytes

The most characterized mechanism to classify P1Rs subtypes is their effect on adenylyl cyclase activity (AC) [204]. As previously mentioned, the A_1 subtype decreases the activity of the enzyme in most of the cells, including muscle cells [113].

I investigated the role of the AC activity in the crosstalk between nAChRs and P1Rs by testing the effect of the inhibitor NKY 80. NKY80 exhibits greater affinity for AC5 (IC_{50} = 8.3 µM) but it is strongly associated also to the AC6 isoform, whereas its affinity has not been investigated [205]. However, it is possible that NKY-80 blocks both AC5 and AC6 with similar affinity [206].

In mice the AC5 protein is detectable in different organs, including skeletal muscle [207]. AC6 is expressed in developing mouse skeletal muscle and its expression declines dramatically in the postnatal period. On the other hand, very little is known about the AC isoforms present in oocyte plasma membrane. Some authors reported the presence of the AC isoforms AC7, AC2, and AC4, which are regulated by the subunits βγ of the G protein and they are involved in the oocyte maturation process [208]. At the moment the presence of other isoforms in oocyte membrane cannot be excluded.

The effect of AC inhibition on the I_{ACh} decay was analyzed in injected-oocytes after 20 mins of pre-incubation with NKY80 (20 µM); the inhibitor accelerated the decay of the currents from $T_{0.1}$ = 1.16 ± 0.18 s and 6.78 ± 0.50 s (*n* = 9/1) measured in the Ctrl cells, to $T_{0.1}$ = 0.57 ± 0.19 s and $T_{0.5}$ = 4.22 ± 0.68 s measured in the oocytes after the treatment (*n* = 5/1; Note the *P < 0.0579* for the $T_{0.1}$; **P < 0.05 vs* Ctrl; Fig. 4.14). Curiously, the inhibition of AC 5/6 resembled the same effect of Ado (Ado: $T_{0.1}$ = 0.69 ± 0.06 s, $T_{0.5}$ = 4.64 ± 0.38 s, *n* = 11/1) while the pre-treatment with NKY80 in the

presence of Ado did not further change the values of $T_{0.1}$ and $T_{0.5}$ ($T_{0.1}$ = 0.83 ± 0.15 s, $T_{0.5}$ = 4.02 ± 0.51 s; *n* = 11/1). Thus, the inhibition of AC 5/6 produced an effect similar to that observed in Ado-treated cells (Fig. 29*AB*).

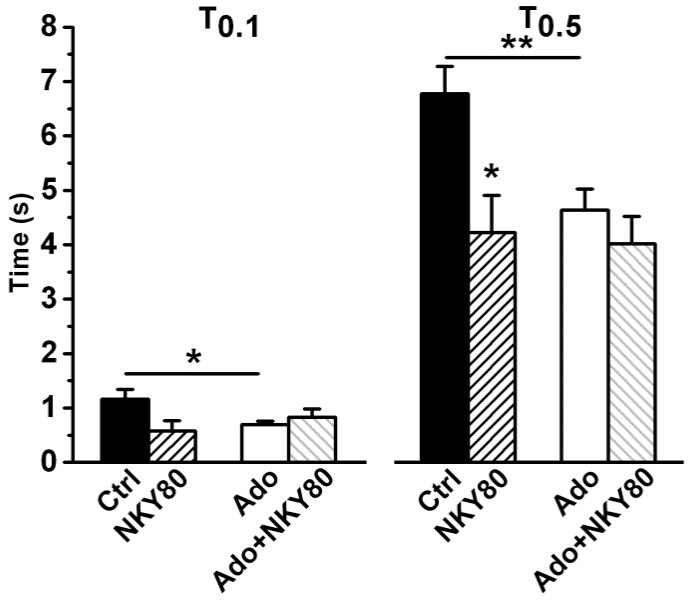

FIGURE 4.14: Effect of the selective adenylyl cyclase inhibition NKY80 of the ACh-induced current decay recorded in injected oocyte.
Comparison of the $T_{0.1}$ and $T_{0.5}$ values in Ctrl oocytes (*n* = 9/1) and oocytes pre-incubated with selective AC5/6 inhibitor (*n* = 5/1, NKY80 20 µM, **P* < *0.05 vs* Ctrl), or in Ado-treated oocytes in the absence (Ado, *n* = 11/1) and in the presence of NKY80 (*n* = 11/1).

My results suggested the A_1 receptor subtype as the candidate for the Ado-mediated effect of the I_{ACh} recorded in injected oocytes. This receptor acts mainly via G_i protein, through the inhibition of the 1, 5 and 6 isoforms of the AC [209]. Accordingly, my data showed that the inhibition of AC 5/6 induced the acceleration of the I_{ACh} decay, similarly to Ado and CPA. Although the involvement of the AC inhibition I reported represented an indirect approach to study the pathway associated to ACh-channel modulation induced by Ado/A1R, it anyhow suggested an involvement of the AC/cAMP pathway.

4.2.4 Expression of A_1R in *Xenopus* oocytes

The results reported in this section have been obtained thanks to the collaboration with Dr. Barbara Pavan (Department of Life Sciences and Biotechnology, University of Ferrara, Italy).

The presence of endogenous P1Rs in the oocyte membrane is still unclear. Purinergic receptors activated by Ado were described many years ago in the follicular cells surrounding the oocytes; when stimulated, these receptors increase the AC activity eliciting a cyclic AMP-mediated outward K^+ current [150, 210]. This current disappears after the defolliculation [159]. The presence of P1Rs in the oocyte membrane is reported in Kobayashi et al. [161]; the receptor described by the Authors inhibits the AC and shares some pharmacological proprieties with the A_1 subtype.

To further investigated the presence of endogenous A1 receptors in the oocyte membrane the 5 nM [^{3}H]DPCPX radioligand saturation binding assay was used to detect the expression of the receptor in folliculated, defolliculated and in injected oocyte membranes.

In Fig. 4.15 the B_{max} values are compared among these three groups of cells. The value in non-injected folliculated oocytes was B_{max} = 19.57 ± 2.60 fmol/mg membrane protein (*n* = 3, ***P < 0.01 vs* defolliculated), in non-injected defolliculated oocytes B_{max} = 11.9 ± 0.73 fmol/mg membrane protein (*n* = 3), and in injected oocytes B_{max} = 57.48 ± 1.69 fmol/mg membrane protein (n = 3, ****P < 0.001 vs defolliculated*). All oocytes used in this experiment were isolated from the same frog.

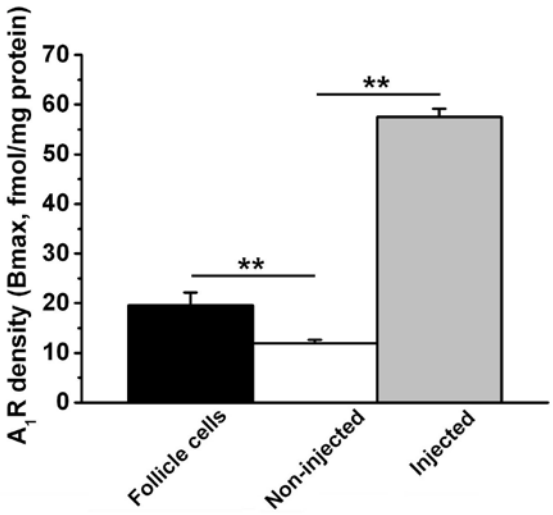

FIGURE 4.15: A_1R expression oocytes.
A_1R was detected by [^{3}]DPCPX radioligand saturation binding assay. The expression of A_1R density (B_{max}) increased significantly in oocytes injected with myotubes membranes (data kindly provided by Barbara Pavan).

A_1R expression was significantly increased in oocyte plasma membrane after the injection of the myotubes membranes. Thus, these receptors likely derived from the transplantation of the exogenous membranes. However, A_1Rs were also detected in non-injected cells but their expression was significantly reduced after defolliculation.

4.2.5 Discussion

Combined, the above results on Ado-mediated modulation of exogenous nAChRs indicate a negligible physiological role of the A_{2A}, A_{2B} and A_3 subtypes and strongly suggests the A_1 subtype as a major candidate in the crosstalk modulation in the *Xenopus* oocytes. These findings reveal that the interplay between P1Rs and the embryonic nAChRs is altered when the receptors are transplanted into the oocyte membrane.

The classification of A_1 and A_{2B} receptors is based on their ability to act on AC activity in an opposite way; in most of the cells the A_1 subtype inhibits the AC whereas A_{2B} stimulates the enzyme activity [83]. In oocytes, the effect of Ado on the ACh-induced currents resembles that observed in the presence of the AC inhibitor. MRS1754, the A_{2B} antagonist, also inhibits the AC activity [116] and increased the rate of I_{ACh} decay recorded in myotubes. Taken together, these results suggest the involvement of the AC/cAMP pathway in the Ado-mediated modulation of AChR activity, either in injected oocytes or myotubes.

The acceleration of the I_{ACh} decay could be caused by an enhanced rate of the receptor phosphorylation [211]. It remains to be clarified as to whether the results could be due to a direct action of protein kinases, or to protein kinases action on regulatory proteins that in turn control nAChR function. As reported by many Authors, Ado and the P1R subtypes activate many and often unpredictable signal transduction cascades [83]. At the moment, the involvement of other pathways cannot be excluded.

Here I found the expression of endogenous A1Rs. Most of them disappear after defolliculation, as reported by other Authors [212]. Thus, I can exclude their involvement in the Ado-mediated modulation of the AChRs. However, some of them remain after the removal of the follicular cells.

The endogenous P1R (A_1-like adenosine receptor) reported by Kobayashi et al., [162] inhibits the AC and share some pharmacological proprieties with the A_1 subtype. Specifically, it is blocked by DPCPX (IC_{50} = 18 nM) but is activated by a concentration of CPA (EC_{50} = 96 nM) higher than that used in my experiments (20 nM). Most of the A_1Rs detected in injected oocytes were likely exogenous, thus those transplanted into oolemma after the injection of the myotube membranes.

The “native” modulation by the A_{2B} subtype on the ACh-induced currents recorded in myotubes is lost when the myotube membranes are transplanted into the oolemma. In this case the activation of the A_1 subtype is predominant over the A_{2B} subtype. Ion channels and receptors together with their native microenvironment form a complex network including intermolecular and intramolecular cooperation and communication systems to determine receptor functioning [62]. My results suggest an alteration of the dynamic equilibrium in the crosstalk and cooperation network between the embryonic nAChRs and A_{2B} subtypes that result in a different termination of the purinergic signalling. Another explanation could be related due to a different distribution/colocalization of P1Rs subtypes with embryonic nAChRs after the isolation and incorporation of exogenous myotube membrane into the oolemma.

4.3 Adenosine-mediated modulation of the adult-type of the nicotinic acetylcholine receptors

In this part of the study I investigated whether the interplay between the P1-receptors and the nAChRs is preserved at the endplate region of the adult muscle fibers. To address this issue two approaches have been used: a direct recording of ACh-activated single channel currents recorded at the motor end plate and the analysis of the time course of the miniature endplate currents (MEPC) which mainly reflects the postsynaptic events. The letter part of the study it was performed by Dr. Arthur Giniatullin from the University of Kazan in collaboration with Prof. Rashid Giniatullin of University of Eastern Finland, Kuopio.

During skeletal muscle development with the arrival of the nerve and the release of trophic factors, the embryonic nAChRs (α2βγδ) is replaced by the adult isoform by the substitution of the γ subunit with the ε subunit (α2βγε). The switch of the subunit confers to the channel a higher conductance and the reduction of the mean open time in respect to the embryonic isoform. Moreover, after innervation, the receptors are clustered only at the endplate region and not spread along the cells as in immature muscle (for a review see [27]). In this study, the single channel analysis of the nAChRs was performed at the motor endplate region of adult mouse FDB fibers at rest, 24 h after the dissociation (Fig. 4.16*A*). The intrapipette solution containing ACh 200 nM was chosen in order to avoid nicotinic receptors desensitization (Fig. 4.16*B*). In this condition, the mean open time of channels was 1.93 ± 0.068 ms (n = 48), the open probability P_o = 0.0047 ± 0.00073 (n = 48) and the conductance 60.84 ± 1.97 pS (n = 25). These values resembled those typical for the adult isoform of the receptor [17].

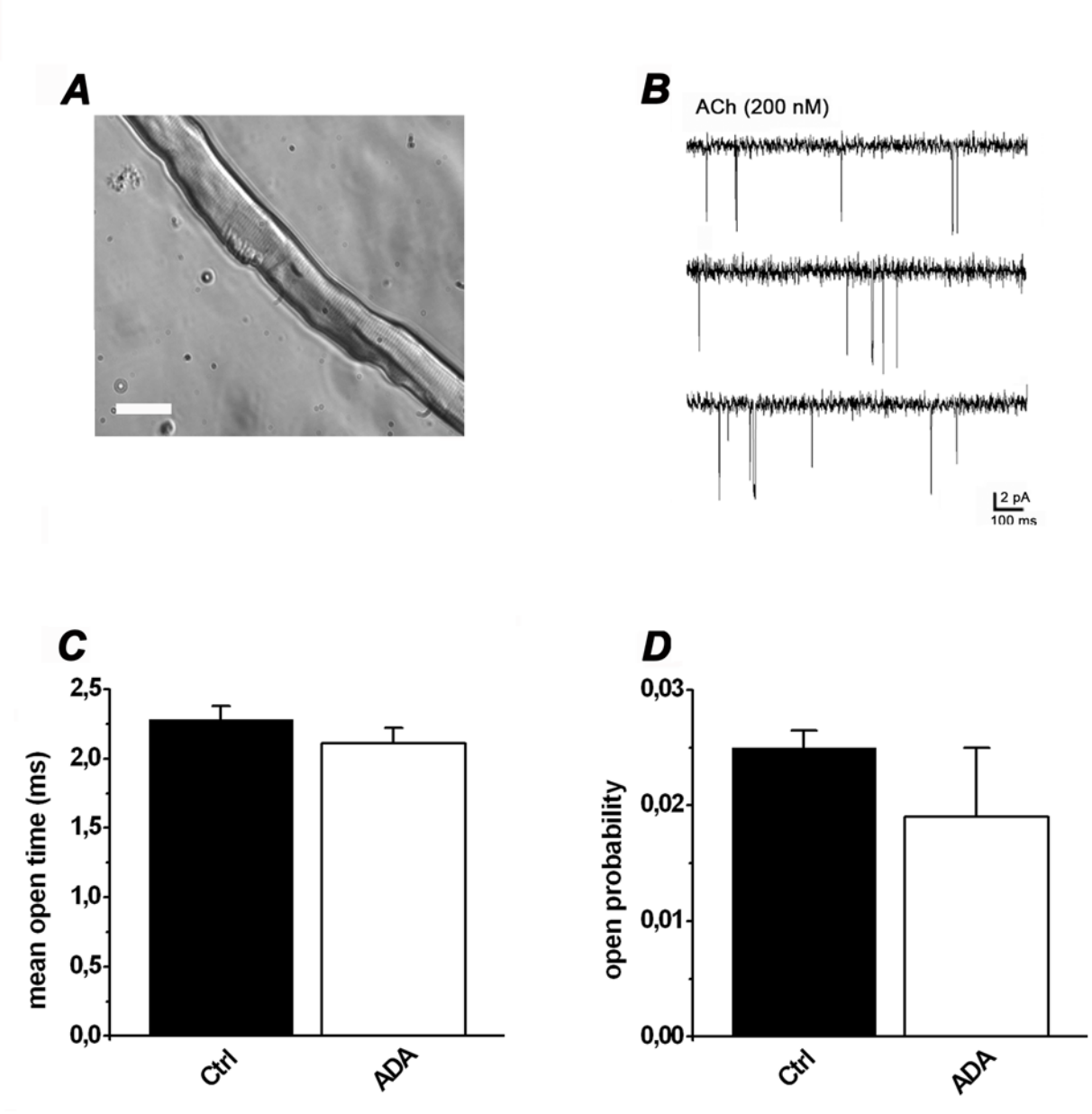

FIGURE 4.16: The endogenous adenosine does not affect the single channel activity of the nAChR recorded at the adult motor endplate in isolated muscle fibers in the resting conditions.
A, Example of mouse *FDB* fiber isolated from a P30 animal (scale 30 µm). ***B***, Example of the single channel activity evoked by 200 nM of ACh and recorded at the endplate. ***CD***, Averages of the mean open time and open probability of channels recorded before (Ctrl) and after the treatment with the enzyme adenosine deaminase (ADA 5 U/mL) to remove all extracellular adenosine. Holding pipette potential +60 mV.

To verifier whether the endogenous Ado could affect the properties of the nAChRs as previously reported, the activity of the ACh-channels was analyzed in fibers before and

after incubation in the presence of 5 U/ml of ADA (30-60 minutes). Contrary to the embryonic isoform of the nAChRs expressed in contracting myotubes [116], at the adult endplate the treatment with the enzyme did not alter the mean open time and the P_o (Ctrl: 2.28 ± 0.1 ms, 0.025 ± 0.0015, *n* = 7; ADA: 2.11 ± 0.11 ms, 0.019 ± 0.006, *n* = 7, Fig. 36*CD*) of the channels. This was an expected result, since the main sources of Ado were missing (lack of muscle contractions, nerve terminal and Schwann cell).

A series of experiments were performed to investigate whether the activation of the P1-receptors could have some effect on the channel activity. To reach this goal, exogenous Ado and other more stable and specific ligands were applied to cells and the results were compared to those obtained in non-treated cells, as shown in Fig. 4.17*A*. When cells were continuously perfused with 100 μM of Ado (15-30 minutes) the mean open time of the AChR-channels significantly increased (Ctrl: 1.93 ± 0.067 ms, *n* = 48; Ado: 2.29 ± 0.17 ms, *n* = 8, **P < 0.05;* Fig. 4.17*AC*) and the P_o slightly increased (Ctrl: 0.0047 ± 0.00068, *n* = 48; Ado: 0.007 ± 0.0029, *n* = 8; Fig. 4.17*AC*). In line with this, when the cells were incubated with NECA (5'-N-Ethylcarboxamidoadenosine, 100 μM for about 20-30 minutes) a more stable and non-specific P1-receptor agonist [213], both parameters significantly increased (NECA: 2.21 ± 0.064 ms and 0.012 ± 0.0028, *n* = 54, ***P > 0.01*, **P > 0.05* respectively, Fig. 4.17*AC*). Either Ado or NECA did not alter the current amplitude of the channels (Ctrl: 5.82 ± 0.17 pA, *n* = 45; Ado: 5.39 ± 0.27 pA, *n* = 6; NECA: 5.67 ± 0.13 pA, *n* = 52, Fig. 4.17*B*).

These results supported a crosstalk between the Ado/P1-receptors and the AChR-channel at the endplate region of the adult fibers.

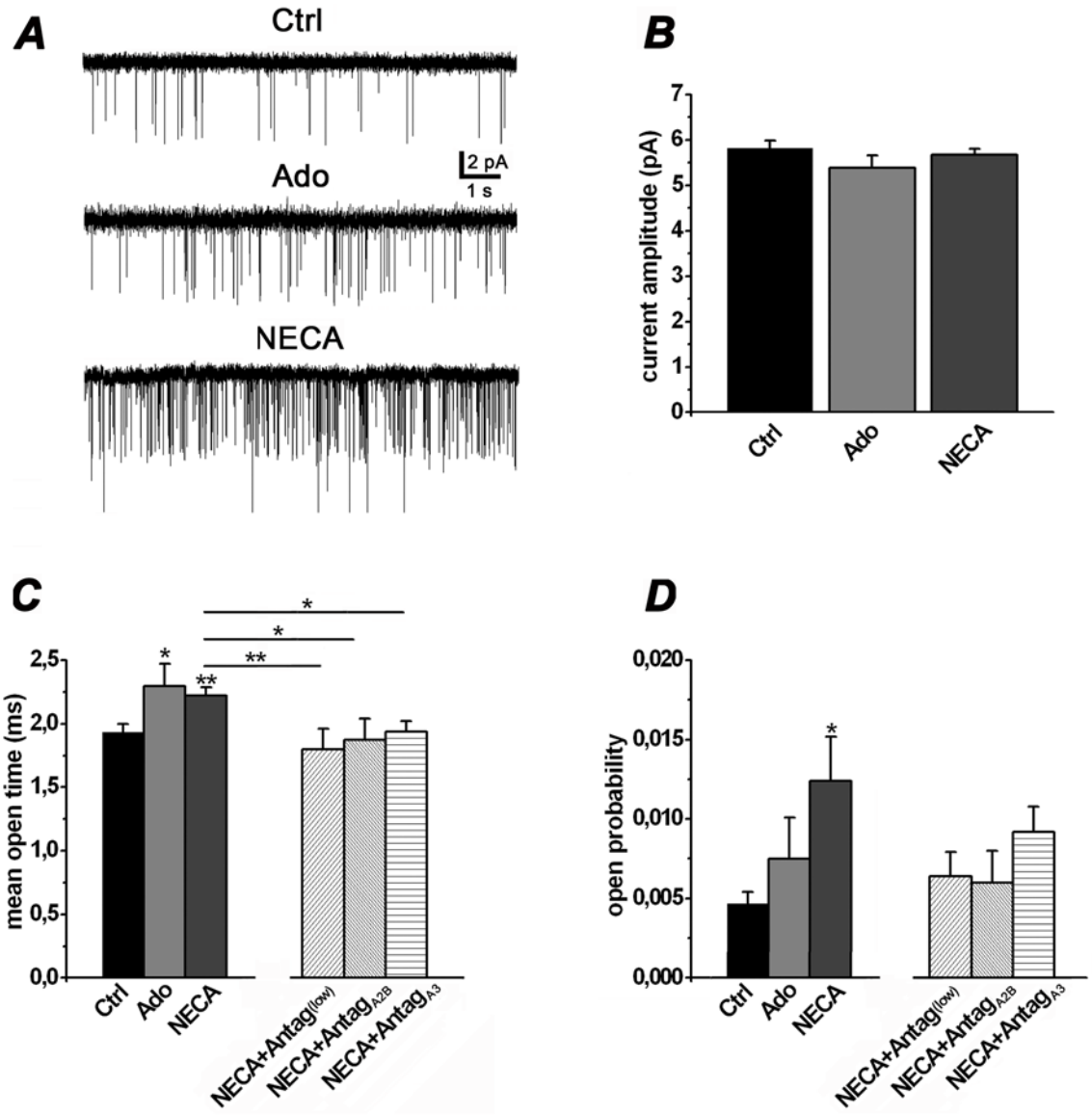

FIGURE 4.17: P1-receptor modulation of the nACh-channels recorded at the adult motor endplate. ***A***, Single channel activity recorded at the endplate of a non-treated fiber (Ctrl) and two fibers incubated with adenosine (Ado 100 µM) and NECA (100 µM). ***B***, Averages of the ACh-current amplitudes recorded in Ctrl and after the treatment with the two P1-receptor agonists. ***CD***, Comparison of the mean open time and open probability averages in non-treated cells (*n* = 48) cells incubated with adenosine (Ado 100 µM, *n* = 8), NECA alone (100 µM, *n* = 54) or in the presence of the antagonists for the low affinity P1-receptors (NECA + $Antag_{low}$: NECA 100 µM + MRS1754 20 nM, A_{2B} antagonist + MRS1334 50 nM, A_3 antagonist, *n* = 14). The antagonists were applied also separately in the presence of NECA (*n* = 9 and *n* = 11, respectively). *$P < 0.05$, **$P < 0.01$. Holding pipette potential +60 mV.

The P1-receptor low affinity subtypes expressed in mouse are activated by micromolar range of NECA and selectively inhibited by nanomolar range of MRS1754 (A_{2B} antagonist: K_i= 5100 nM, [83]) and MRS1334 (A_3 antagonist: K_i= 6500 nM, [83]). To explore more in detail the role of those receptors in the ion channel modulation reported above, the nAChR-channels activity was recorded in fibers incubated with NECA (100 μM) and two antagonists for the A_{2B} and A_3 subtypes (20 nM MRS1754, 50 nM MRS1334). In Fig. 4.17*CD* are showed the results: in the presence of the antagonists, the effect of NECA was almost abolished and the values of the mean open time and the P_o were similar to those obtained in untreated cells ($Antag_{low}$: 1.8 ± 0.16 ms and 0.0064 ± 0.00015, *n* = 14, respectively, Fig. 4.17*CD*). A similar effect was also observed when the antagonists were applied separately ($Antag_{A2B}$: 1.87 ± 0.16 ms, and 0.006 ± 0.002, *n* = 9; $Antag_{A3}$: 1.94 ± 0.08 and 0.0093 ± 0.00016, *n* = 11; Fig. 4.17*CD*).

Thanks to collaboration with dr. Arthur Giniatullin and Prof. Rashid Giniatullin the potential postsynaptic action of Ado was also tested in a more physiological conditions. Application of 100 μM Ado at the NMJ of mouse diaphragm largely reduced the frequency of MEPCs (0.67 ± 0.09 s-1 versus 1.24 ± 0.3 s-1 in Ctrl *n* = 6; *P = 0.03*) in agreement with previous studies [214]. However, the decay time constant (τ) was increased from control 536 ± 17 μs to 595 ± 13 μs, respectively, (*n* = 6; **P > 0.05*) Thus, recording on natural synaptic events indicated the slowing effect of Ado which is consistent with increased open time of single channels in isolated fibers.

4.3.1 Discussion

During skeletal muscle development with the arrival of the nerve and the release of trophic factors, the embryonic nAChRs (α2βγδ) is replaced by the adult isoform by the

substitution of the γ subunit with the ε subunit (α2βγε). The switch of the subunit confers to the channel a higher conductance and the reduction of the mean open time in respect to the embryonic isoform. Moreover, after innervation, the receptors are clustered only at the endplate region and not spread along the cells as in immature muscle (for a review see [27]). At the neuromuscular junction, the main source of Ado is that coming from the nerve terminal by the degradation of ATP. Ado and ATP are the two important autocrine modulators of the synaptic activity [119]. ATP, co-released with ACh by the exocytosis of the synaptic vesicles, modulates the synaptic activity by binding the pre- and postsynaptic P2-receptors [215]. ATP is also converted into Ado by the ectoenzymes, which modulates the release of the synaptic vesicles through P1-receptors expressed presynaptically [214, 216]. The role of P1Rs that are localized on the presynaptic membrane is principally associated to a complex balance between the activation/inhibition of A_1 and A_{2A} subtypes that modulate the neurotransmitter release. On the other hand very little is known about the function of P1Rs expressed on the postsynaptic membrane and how they could be involved in controlling the plasticity of synapses [121].

In this study I found the interplay communication between P1Rs and the adult isoform of nAChRs expressed at the endplate of adult mouse skeletal muscle fibers and among all P1Rs subtypes the pharmacological investigations pointed out a prevalent role of A_{2B}Rs.

The properties of the adult nAChRs were first analyzed before and after incubation with ADA in order to explore the effect of endogenous Ado in cultured isolated myofibers. The removal of extracellular Ado did not result in any change in the mean open time and the P_o of the nACh-channel openings. This result could have been expected

because at NMJ the Ado is usually released in an activity dependent manner from both nerve and muscle. In isolated myofibers the main sources of Ado were missing (lack of muscle contractions, nerve terminal and Schwann cell), and the concentration of the agonist might be too low to have a tonically effect. To explore more clearly the role of the P1R, the nAChR-channel activity was recorded in myofibers treated with both exogenous Ado and the non-selective agonist NECA. Under this experimental condition the amplitude of single channels remained unchanged compared with Ctrl. Beside this both NECA and the natural agonist Ado significantly prolonged the mean open time and increased the P_o of the adult even if NECA appeared to have a more potent effect that Ado in particular on P_o.

It was mentioned before that, the four P1R subtypes are present in the motor endings. Concerning the high affinity subtypes, the A_1R localizes in the terminal Schwann cell and nerve terminal whereas the $A_{2A}R$ localizes in the postsynaptic muscle, in the axon and in the nerve terminal [120]. In addition the expression of the low affinity P1R subtypes has been reported in the nerve terminal and muscle cells where they have been observed to coincide perfectly with nAChR clusters [121]. To inquire into in detail the role of the low affinity P1R subtypes (A_{2B} and A_3) the single nAChR-channel activity was recorded in fibers incubated with subtype-selective antagonists for the A_{2B} (MRS1754) and A_3 subtypes (MRS1334). In order to study the effect resulting from a highly selective subtype inhibition, these ligands were always used in the presence of NECA that produce a robust stimulation of all P1Rs. In this condition the values of the mean open time and the P_o were significantly reduced similar to those obtained in Ctrl cells. Interestingly, when the antagonists were applied separately the specific inhibition of the A_{2B} and A_3 subtype indicate the A_{2B} as the principal candidate in the Ado-mediated modulation.

Thanks to collaboration with Dr. Arthur Giniatullin and Prof. Rashid Giniatullin, the role of P1Rs was also tested on the isolated phrenic nerve diaphragm preparation considered a more physiological condition. The P1Rs appeared to be involved in spontaneous released because the frequency of MEPCs in mouse NMJ was significantly decreased by non-selective agonist Ado. This result confirms previous knowledge about the involvement of presynaptic P1Rs in the inhibition/potentiation of ACh release [123, 124]. Moreover, they assayed the role of P1Rs at postsynaptic level. Ado shows to delay the decay of I_{ACh}, confirming the results obtained with isolated myofibers where the stimulation of P1Rs prolonged the mean open time of nicotinic single channels.

These results suggest that the nicotinic channels are principally modulated when the content of Ado increased over the micromolar concentration.

P1Rs activate different pathways within the cells but they have been principally linked to the activation/inhibition of AC that in turn can activate other signaling cascade. New findings about the role of protein kinases in muscle fibers proposed PKA and PKC as a key modulator for the trafficking, clustering and stability of nAChRs on membrane surface [217, 218]. However, it is unclear whether this process is a direct consequence of receptor phosphorylation or an indirect effect induced by phosphorylation of other protein by PKA and PKC [217, 218].

In summary, my results supported a new role of the P1Rs and in particular for the A_{2B} subtype at the endplate of the skeletal muscle cells. It remained to clarifier which are events associated to the intercellular pathway and whether the purinergic signaling could play other functions related to nAChRs such as the clustering and the stability of the endplate. These questions raise a stimulating possibility for further studies.

CHAPTER 5

CONCLUSIONS AND FUTURE DIRECTIONS

The purinergic signalling system is omnipresent and remarkably functionally diverse it appears to be one of the most primitive and widespread chemical messengers in the animal and plant kingdoms [59]. The purinome is a biological compartment made up of submembrane microdomains at the plasmalemma level, which are important for the coordination of the effects of extracellular purine and pyrimidine ligands [62]. It contains the molecular network able to ensure correct intracellular trafficking and fast communication among ligands, receptors, reuptake systems, degrading enzyme and signalling protein [62].

The major advantage of the microtransplantation technique is that receptors/ion channels are analyzed in their native microenvironment in which they are embedded. By doing this, once incorporated into oolemma the membrane proteins preserved the original properties. Here I used this technique as a tool to verify if the “native” crosstalk between the purinergic receptors and the nAChRs observed in myotubes was preserved once the myotube membranes were injected into oocytes. Surprisingly, I found that in oocytes the adenosinergic modulation of the nAChR activity was different from that of the native tissues. This discrepancy could be due to the procedure for isolating the cell membranes, which may alter the global and dynamic equilibrium that discipline the signalling mechanism between A_{2B}Rs-nAChRs.

Fig. 5.1 shows a model which explains how the native Ado-mediated modulation of nAChRs is lost once the myotube membranes are injected into *Xenopus* oocyte: in the upper part of the figure, the extracellular Ado released by contracting myotubes

promotes the activation of P1Rs allowing the activation of different intracellular pathways, principally linked to the AC/PKA-related signalling. Among the P1R subtypes, the A_{2B} subtype was found to promote activation of the AC, the enhancement of cAMP [116] and the consequent activation of PKA that in turn may modulate the channel activity probably *via* phosphorylation. On the contrary, when the myotube membranes are isolated and injected into *Xenopus* oocytes, in this new environment the A_1 subtype activity plays the major modulatory role over the A_{2B}Rs, indicating that the original crosstalk is not preserved anymore. The action of A_1R is usually linked to the AC inhibition, which inhibits the PKA that in turn affects the nAChRs function both directly or through other regulatory proteins. Likely, the “new” modulation is a consequence of the endogenous “A1-like receptors” expressed by the oocytes [162]. However, at the moment, the role of the exogenous A_1R cannot be totally excluded.

In conclusion, it is important to reconsider the microtransplatation technique as approach for studying the adenosinergic modulation of the transplanted receptors/ion channels. The oocyte is equipped with endogenous receptors that could contaminate and complicate the interpretation of the results.

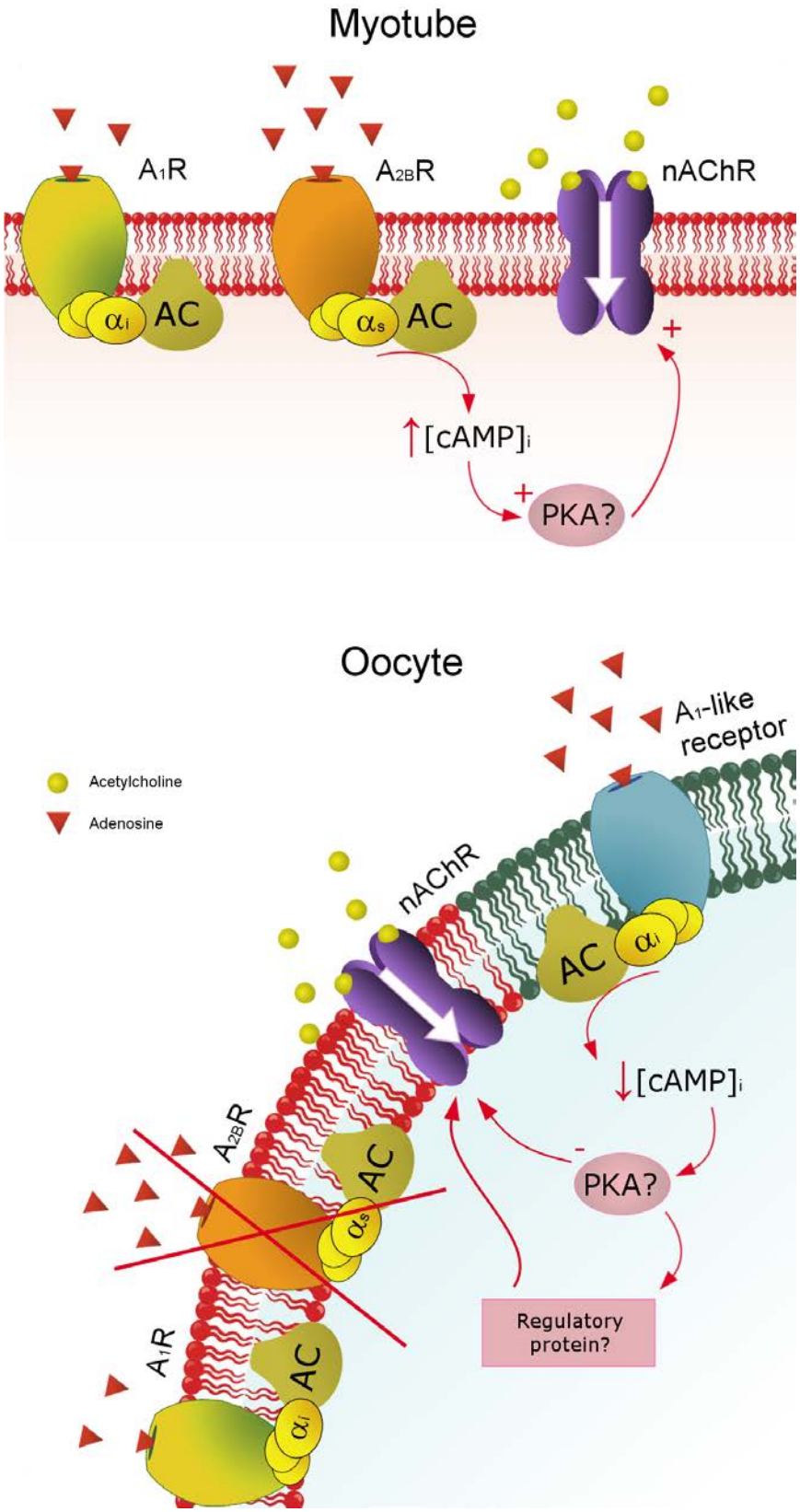

FIGURE 5.1: Proposed mechanisms for Ado-mediated modulation after the microtransplantation of myotube cell membranes into *Xenopus* oocytes.

In the latter part of my study I investigate the role of Ado/P1Rs in the channel modulation of the nAChRs located at the motor endplate region. My results underline a new role of the adenosinergic signalling *via* postsynaptic low affinity P1Rs at the neuromuscular junction. My outcome proposes the prevalent role of A_{2B}Rs and further studies are needed to characterize the signalling mechanism involved in such modulation.

Nowadays, P1R subtypes are potential therapeutic targets and selective agonists and antagonists have been introduced for the therapy of many neurological disorders [59]. The knowledge of their interactions and allosteric modulations is of great interest for developing new therapeutic drugs. For instance, the A_{2A}R is considered an important pharmacological target for PD treatment, and a drug called Istradefylline is currently of interest for the treatment of motor complications in this disease [219]. Most skeletal muscle diseases are characterized by dysfunction of the synaptic transmission. For instance, in the Lambert-Eaton myasthenic syndrome the quantal release of ACh is impaired, giving the clinical symptoms of muscle weakness, diminished reflexes and autonomic symptoms. In myasthenia *gravis* there is a defect of the nAChR activity. In addition, traumatic peripheral nerve injuries gives either partial or complete muscle denervation and an appropriate therapy could help to maintain a basal electrical activity and so delay or avoid the muscle fibrosis and atrophy that begins immediately after denervation.

APPENDIX 1

PUBLISHED RESULTS

The following work was performed parallel with the main project of my thesis and is a result of the collaboration with prof. Giuliano Zabucchi and his colleagues from the University of Trieste.

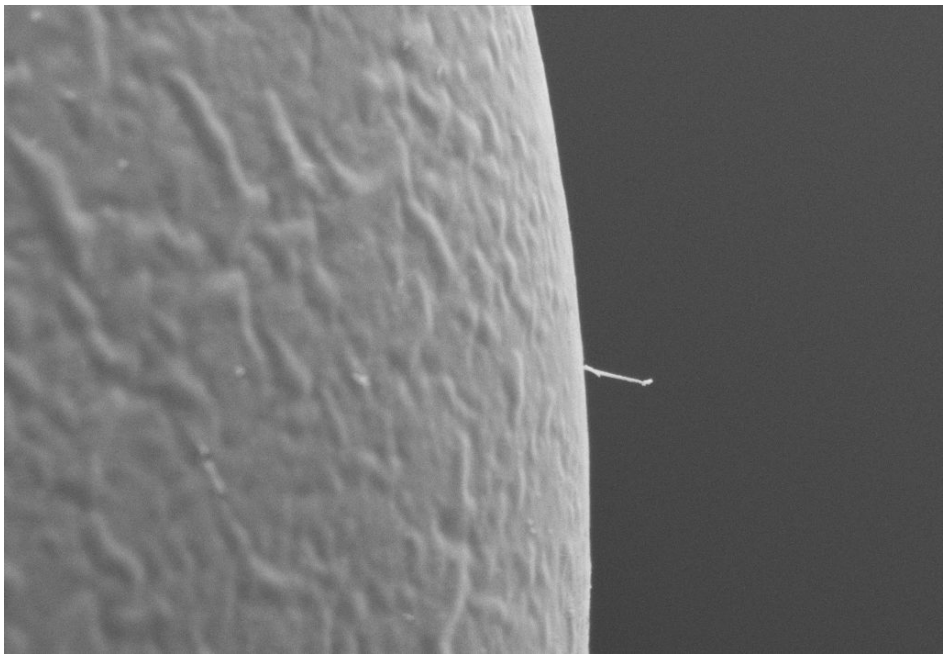

BLUE ASBESTOS

Xenopus laevis oocyte observed by scanning electron microscope (SEM).

Blue asbestos, commonly known as crocidolite can be seen impaled into vitelline membrane of the *Xenopus laevis* oocyte. It looks hair-like, long and straight and it is thought to be the most toxic variety of mineral fibers. Its nickname arose from its unique gray-blue color. Crocidolite is a sneaky, silent and invisible enemy that strikes after a while with very severe asbestos-related diseases including the lung cancer mesothelioma.

OXFORD
SOT | Society of Toxicology
www.toxsci.oxfordjournals.org

TOXICOLOGICAL SCIENCES, 145(2), 2015, 263–272

doi: 10.1093/toxsci/kfv050
Advance Access Publication Date: March 4, 2015
Research Article

Xenopus laevis Oocytes as a Model System for Studying the Interaction Between Asbestos Fibres and Cell Membranes

Annalisa Bernareggi*,†, Elisa Ren*,†, Violetta Borelli*, Francesca Vita*, Andrew Constanti‡, and Giuliano Zabucchi*,[1]

*Department of Life Sciences; †Centre for Neuroscience B.R.A.I.N., University of Trieste, 34127 Trieste, Italy; and ‡Department of Pharmacology, UCL School of Pharmacy, London, UK WC1N 1AX

[1]To whom correspondence should be addressed at Department of Life Sciences, University of Trieste, via Valerio, 28/1, 34127 Trieste, Italy. Fax: +39 040 5584023. E-mail: zabucchi@units.it.

ABSTRACT

The mode of interaction of asbestos fibres with cell membranes is still debatable. One reason is the lack of a suitable and convenient cellular model to investigate the causes of asbestos toxicity. We studied the interaction of asbestos fibres with *Xenopus laevis* oocytes, using electrophysiological and morphological methods. Oocytes are large single cells, with a limited ability to endocytose molecular ligands; we therefore considered these cells to be a good model for investigating the nature of asbestos/membrane interactions. Electrophysiological recordings were performed to compare the passive electrical membrane properties, and those induced by applying positive or negative voltage steps, in untreated oocytes and those exposed to asbestos fibre suspensions. Ultrastructural analysis visualized in detail, any morphological changes of the surface membrane caused by the fibre treatment. Our results demonstrate that Amosite and Crocidolite-type asbestos fibres significantly modify the properties of the membrane, starting soon after exposure. Cells were routinely depolarized, their input resistance decreased, and the slow outward currents evoked by step depolarizations were dramatically enhanced. Reducing the availability of surface iron contained in the structure of the fibres with cation chelators, abolished these effects. Ultrastructural analysis of the fibre-exposed oocytes showed no evidence of phagocytic events. Our results demonstrate that asbestos fibres modify the oocyte membrane, and we propose that these cells represent a viable model for studying the asbestos/cell membrane interaction. Our findings also open the possibly for finding specific competitors capable of hindering the asbestos–cell membrane interaction as a means of tackling the long-standing asbestos toxicity problem.

Key words: asbestos fibres; Crocidolite; Amosite; *Xenopus* oocytes; two-microelectrode voltage-clamp; electron microscopy

Asbestos is a silicate consisting of thin, fibrous needle-like crystals that was used widely for fire, heat, electrical, and building insulation. Different types of asbestos are recognized, including Amosite (Amos), Crocidolite (Croc), and Chrysotile. The discovery that asbestos fibre inhalation can lead to severe forms of lung disease, led to its general ban across the world; nevertheless, asbestos-related diseases are still evident in the 21st century, sometimes long after original asbestos exposure. The mechanisms underlying its repertoire of biological cellular effects are still not completely understood, although fibre morphology and chemical composition are recognized to be important factors (Boulanger *et al.*, 2014).

The interaction between asbestos fibres and cell membranes has been analyzed since the 1980s (Brody and Hill, 1983; Brody *et al.*, 1983; Elferink and Kelters, 1991; Gendek and Brody, 1990; Iguchi and Kojo, 1989). It has been reported that Chrysotile can induce red blood cell lysis (Brody *et al.*, 1983), suggesting that the fibres can affect the cell membrane properties

independently of any endocytic process. Asbestos fibres can also be found free in the cytosol of macrophages (Palomäki *et al.*, 2011) or within the phagosomes, protruding from them into the cytosol (Blake *et al.*, 2007; Johnson and Davies, 1983), but they were also found in the nuclear compartment, suggesting a passive piercing (Johnson and Davies, 1983; Malorni *et al.*, 1990). Other findings obtained by studying carcinoma and mesothelial cells in culture supported this possibility (Andolfi *et al.*, 2013; Malorni *et al.*, 1990), even if in the latter case, the fibre entry into the cell appears to be dependent on the phagocytic process (Liu *et al.*, 2000).

In general terms, it is thought that the first interaction between macrophages and asbestos fibres is realized through a phagocytic process which does not exclude the possibility that the ingested fibres can exit from the phagosome into the cytosol and even enter the nuclear compartment. Nor can it be excluded that a contemporaneous passive entry of fibres through the cell membrane also occurs. Moreover, by comparing the effect of different asbestos fibre types on a macrophage cell line, it was concluded that different fibres can cause different changes in electrophysiological features of the cell (Gormley and Wright, 1980; Gormley *et al.*, 1978). Despite the results obtained in all these reports, the mechanism of interaction of asbestos fibres with cell phospholipid membranes and the influence that this has on the cell membrane and intracellular organelle properties is still a matter of debate. The problem of whether asbestos fibres can exert their harmful effects through a phagocytic-dependent process and/or by passively piercing or adsorbing onto the bilayer remains to be clarified. It seems that the lack of a simple, convenient, and reproducible cellular model by which to study asbestos/cell membrane interactions makes it difficult to investigate this topic in detail, and to possibly find specific "competitors" capable of hindering the asbestos–cell interaction as a new therapeutic approach for tackling the long-standing asbestos toxicity problem.

In this article, we describe the setting up of a model employing *Xenopus laevis* oocytes (XLOs) for investigating the cellular interaction of asbestos fibres. Using this method, we show here for the first time, that standard Amos and Croc-type asbestos fibres significantly modify the electrophysiological properties of the XLO plasma membrane starting very shortly after exposure. Morphological analysis of the fibre-exposed oocytes by both optical and electron microscopy excluded the possibility that these changes could be due to phagocytic events. We propose that this method can be a viable model for studying the asbestos/cell membrane interaction.

MATERIALS AND METHODS

Ethical approval and oocyte isolation. Animal care and treatment were conducted in conformity with institutional guidelines in compliance with national and international laws and policies (European Economic Community, Council Directive 63/2010 Italian D.L.26/2014). Adult female *X. laevis* frogs were fully anaesthetized by immersion in cold 0.17% MS-222 for 15 min, and the pieces of ovary were aseptically removed according to the protocol described by Miledi *et al.* (2006). Follicles were isolated manually using fine-tipped forceps and the layer of follicular cells mechanically removed. The cells were treated with 0.5 mg/ml collagenase type I (Sigma) at room temperature for 35 min, and then kept at 16°C in Barth's medium (NaCl 88 mM, KCl 1 mM, $Ca(NO_3)_2$ 0.33 mM, $CaCl_2$ 0.41 mM, $MgSO_4$ 0.80 mM, $NaHCO_3$ 2.4 mM, HEPES 10 mM, adjusted to pH 7.4 with NaOH, containing gentamicin [50 μg/ml]). The electrophysiological recordings were performed 24 h after the treatment to let the cell recover from the membrane damage induced by the collagenase (Dascal *et al.*, 1984). Oocytes at stage VI were carefully selected under an optical microscope and used for the electrophysiological recordings.

Asbestos fibre suspensions. Analytical Standard UICC samples of Amos and Croc were obtained from SPI-CHEM, West Chester, Pennsylvania, re-suspended in PBS at a final concentration of 10 mg/ml, and stored at 4°C until use. The number of fibres was evaluated after adequate dilutions in a Thoma counting chamber. Wollastonite (Wolla), used as a control particulate, being a nonasbestos silicate powder, was a kind gift of Bal-Co SpA (Sassuolo, MO, Italy). The fibre size parameters of the asbestos UICC standard have been described in detail by Kohyama *et al.* (1996). Briefly, our standard fibres spanned from 0.5 to 100 μm in length and from 0.1 to 1.2 μm in width. The reference batches of the standard samples were as follows: Amos South African 12172-73-502703-AB and Croc South African 12001-28-402704-AB. Wolla characterization in length distribution (from <16 to >96 μm, the 16-32 form being the most represented) was reported by Governa *et al.* (1998).

Scanning and transmission electron microscopy. The procedure to analyze the samples by scanning electron microscope (SEM) was previously described elsewhere (Andolfi *et al.*, 2013). Control and treated oocytes were fixed with 2.5% glutaraldehyde (Serva, Heidelberg, Germany) in Ringer's solution at room temperature for 20 min, rinsed in Ringer, and postfixed in 1% osmium tetroxide in PBS for 30 min. Afterwards, samples rinsed in Ringer were dehydrated in ascending ethanol concentrations (35%, 50%, 70%, 90%, and 100%) and transferred in 100% ethanol to a critical point dryer (Bal-Tec; EM Technology and Application, Furstentum, Liechtenstein) and dried through CO_2. Coverslips were mounted on aluminum sample stubs and gold coated by sputtering (Edwards S150A apparatus; Edwards High Vacuum, Crawley, West Sussex, United Kingdom). SEM images were obtained using a Leica Stereoscan 430i SEM (Leica Cambridge Ltd, Cambridge, United Kingdom). For each sample observed by SEM, many photomicrographs at different magnifications were stored. SEM, imaging was performed at a range of accelerating voltages of 20 kV, working distance of 17–18 mm, and beam currents of 0.08–0.1 nA were used.

The procedure for preparing the samples to be analyzed by transmission electron microscope (TEM) was described elsewhere (Trevisan *et al.*, 2014). Ten oocytes incubated in Ringer's solution or in Ringer containing asbestos fibres (15 μg/ml) for 60 min were fixed for 30 min at room temperature in a solution of 1.5% glutaraldehyde in 0.1 M sodium cacodylate buffer (pH 7.4) containing 0.03 M $CaCl_2$. As previously described, samples were washed twice with sodium cacodylate buffer (pH 7.4) and then postfixed with 1% OsO_4 for 1 h at 4°C. Postfixed cells were dehydrated with a graded ethanol series ending with 100% ethanol and then embedded in Dow epoxy resin (DER332; Unione Chimica Europea, Milan, Italy) and DER732 (Serva). Ultrathin sections were prepared with an Ultrathome III (Pharmacia-LKB, Uppsala, Sweden) and double stained with lead citrate and uranyl acetate. Sometimes, identification of the asbestos fibres was difficult due to the extrusion of electron-dense granules or granule fragments from treated oocytes and to the small size of the fibres capable of interacting with the oocyte surface. Accordingly, to show that what we were observing was really asbestos, we analyzed its

appearance at a very high TEM magnification (from 56 K to 89 K). In the case of true asbestos, the fibre could show a specific band-like discontinuity in the electron density and a non-round appearance of the section (not shown). This can probably be ascribed to superimposed layers of the silicate and/or to a heterogeneous distribution of iron (Croc and Amos contain a large amount of iron) within the fibre itself. This analysis was carried out in all the cases of the structure pinpointed by arrows in the Figures 1–7.

Electrophysiological recordings. Ten-fifteen oocytes in a 1.5-ml Eppendorf tube were incubated in 1 ml of Ringer's solution containing 5–20 μg/ml asbestos fibres under continuous mixing (wheel, 10 revolutions/min). At the indicated times (5–120 min), one oocyte was taken, and its electrophysiological properties were recorded for about 10 min. The two-microelectrode voltage clamp technique was used to investigate the effects of applying asbestos fibre suspensions (in Ringer's solution) on the electrical membrane properties of the oocytes. Glass microelectrodes with a resistance of 0.5–2 MΩ were filled with 3 M KCl (Miledi, 1982). During the recordings, the cells were continuously superfused with a Ringer's solution containing NaCl 115 mM, KCl 2 mM, $CaCl_2$ 1.8 mM, HEPES 5 mM, adjusted to pH 7.4 with NaOH, in a purpose-designed recording chamber (RC-3Z, Warner Instruments, Hamden, Connecticut) at room temperature (23°C). The Ringer's solution was applied using a constant perfusion system (7 ml/min, VC-8 perfusion system, Warner Instruments), and the flux speed was routinely controlled and maintained constant during each set of experiments (for further details, see Bernareggi *et al.*, 2011).

The resting membrane potentials (RPs) of the oocytes were recorded 3–5 min after impalement, when the values were more stable, and oocytes with a resting potential lower that −20 mV were excluded from the analysis. The membrane input resistances (R_m) were estimated either from the values of the recorded RP, holding potential ($V_h = -80$ mV), and holding current (I_h) by the equation $R_m = (V_h - RP)/I_h$ (Dascal *et al.*, 1984) or from the slope of *I*–*V* relationships measured at −80, −70, −60, −50, and −40 mV. To reduce the variability of the frog's donors, the results were compared among oocytes of the same batches (Englund *et al.*, 2014).

Two-voltage clamp protocols were used. A linear voltage ramp protocol: oocytes were held at −40 mV and a linear voltage ramp from −80 to 20 mV (1 s) was applied. A step protocol: from a holding potential of −40 mV, oocytes were clamped for 3 s from −80 to +50 mV in 10 mV increments.

In a series of experiments, Croc suspended in Ringer was injected inside the cells (50 nl per cell) by using a Nanoject II (Drummont, Pennsylvania), and a group of cells of the same batch was injected with the same volume of Ringer. In this case, the electrophysiological recordings were performed 30 min after the treatment to let the membrane recover from the injection. Data acquisition and analyses were performed by WinWCP version 4.1.2 Strathclyde Electrophysiology software, kindly provided by Dr John Dempster (Glasgow, United Kingdom). Prism 3.0 and Origin 7 were used for the statistic analysis (unpaired *t*-test). All values are expressed as mean ± SEM. *p* Values <.05 were considered as significant.

Treatment of Croc fibres. Inactivation of asbestos electrical charges contributed by surface iron was carried out by following the methods described elsewhere (Governa *et al.*, 1999; Gulumian, 2005). Briefly, 0.75 mg of Amos or Croc fibres were incubated under continuous mixing in 0.5 ml final volume for 2 h at room temperature in Ca^{2+} free Ringer's solution alone (control) or containing the iron chelator 1 mM deferoxiamine (DFO) B or the chelators 1 mM ethylenediaminetetraacetic acid (EDTA), or 1.5 mM ammonium ferric citrate (AFC). Thereafter, the fibres were extensively washed in 10 ml Ca^{2+}-free Ringer 3-fold and re-suspended in the same solution at the concentration of 1 mg/ml.

For microinjection, 2 ml of the Croc fibres (1 mg/ml in Ca^{2+} free Ringer solution) were filtered firstly through BD Falcon filters (2-fold 100 μm pore and 2-fold 70 μm). For improving the filtration process, drops of Ringer's solution were continuously added to a final volume of 3.25 ml. The fibre suspension was finally brought up to a concentration of 0.6 mg/ml. We calculated that 50 nl injection of this suspension should result in an intracellular concentration of approximately 30–40 μg/ml of Croc (assuming that, the diameter of the oocyte is 1–1.3 mm, the final volume is about 1 μl), which is higher than that reached in Croc-treated oocytes, as judged from the morphological evidence showing that only some fibres were found to interact with XLOs.

RESULTS

Application of Asbestos Suspensions Affects the Membrane Properties of the Xenopus Oocytes

To test whether application of asbestos fibre suspensions could affect the oocyte cell membrane, we first analyzed the effects on the passive electrical membrane properties of the oocytes, comparing the RP and R_m of control oocyte cells with those exposed to asbestos fibre suspensions, using a standard two-microelectrode voltage clamp technique. Before the recordings, the oocytes were incubated in Ringer's solution (Ctrl, nontreated oocytes) or in the presence of Amos or Croc asbestos. Moreover, some records were performed in the presence of Wolla, a safer fibre mineral often used as an asbestos replacement (Maxim and McConnell, 2005). In all cases, the concentration of the fibres was 10–15 μg/ml (re-suspended in Ringer's solution), and the cells were slightly mixed during the entire period of incubation (for 5–120 min) to avoid sedimentation.

A summary of these results is presented in Figure 1. In control condition (Ctrl), the mean values of the RP and R_m resembled those typical of mature stage oocytes (RP = −38.50 ± 0.82 mV, $R_m = -0.95 \pm 0.03$ MΩ; $n = 102$, Dascal *et al.*, 1984), whereas after asbestos exposure, both parameters significantly changed relative to control (Figs. 1A and 1B). In Amos- and Croc-treated oocytes, there was a significant depolarization of the RP followed by a reduction of the R_m (Amos: RP = −34.03 ± 1.06 mV, $R_m = 0.79 \pm 0.03$ MΩ, $n = 68$, $p < .01$, $p < .001$; Croc: RP = −31.38 ± 0.71 mV, $R_m = 0.66 \pm 0.03$ MΩ, $n = 84$, $p < .001$). All these changes were well evident after 5–10 min of incubation, suggesting a very rapid effect of the fibres on the cell membrane; after 5 min of incubation 58% and 64% of the cells were already responsive to the treatment with Amos and Croc, respectively. In contrast, after exposure to Wolla, we did not observe any significant effects on the cell membrane properties (Wolla: RP = −38 ± 1.17 mV, $R_m = 1.07 \pm 0.09$ MΩ, $n = 7$, $p > .05$). At the low concentration of 5 μg/ml Croc, there was already a significant depolarization of the RP followed by a reduction of the R_m (−29 ± 1.46 mV, 0.59 ± 0.04 MΩ, $n = 10$, $p < .001$). In Amos, a similar effect was observed at a higher concentration (15 μg/ml: RP = −27.17 ± 3.31 mV, $p < .01$; $R_m = 0.64 \pm 0.02$ MΩ, $n = 5$, $p < .05$) and in both cases, at the concentration of 20 μg/ml, most oocytes displayed a RP lower than −20 mV and it was

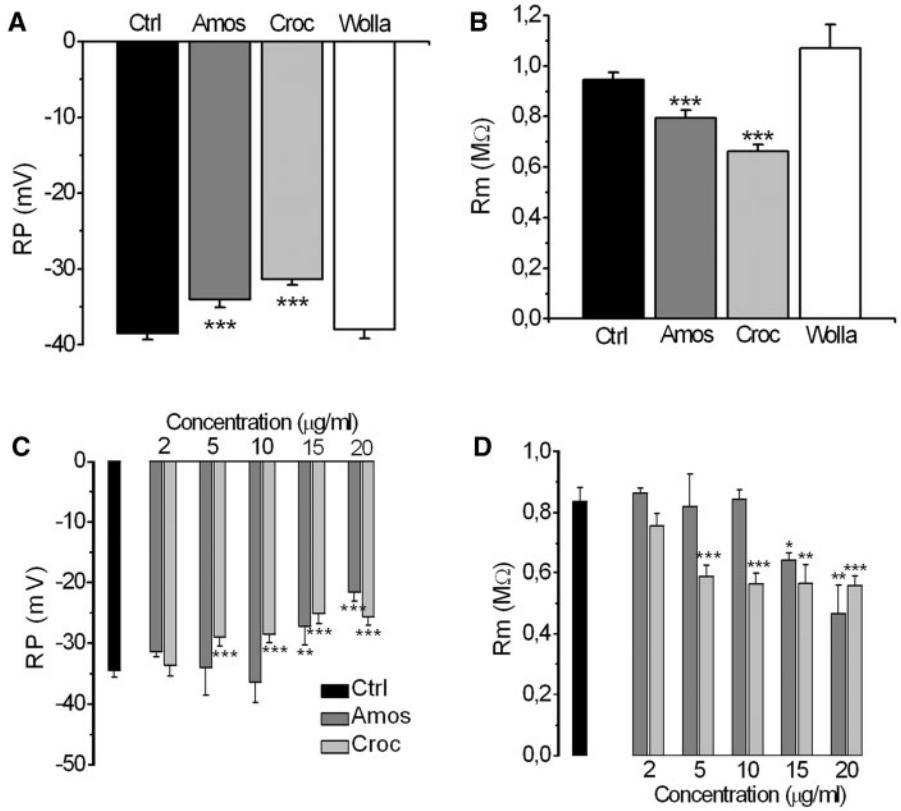

FIG. 1. Comparison of the effects of Amos, Croc, and Wolla on the electrical membrane properties of oocytes. A, Mean ± SEM of the RP and B, the R_m recorded in nontreated (Ctrl), Amos, Croc, and Wolla-treated oocytes (10–15 μg/ml, from 5 to 120 min). C, Mean ± SEM of the RP recorded in Ctrl versus asbestos-treated oocytes at different concentrations of Amos or Croc and D, mean ± SEM of the R_m recorded in the same oocytes. Note the significant decrease in the RP and R_m of oocytes exposed to the higher concentrations of Amos or Croc asbestos but not Wolla. Ctrl: $n = 102$; Amos: $n = 68$; Croc: $n = 84$; Wolla: $n = 7$ ($^*p < .05$; $^{**}p < .01$;$^{***}p < .001$ vs Ctrl).

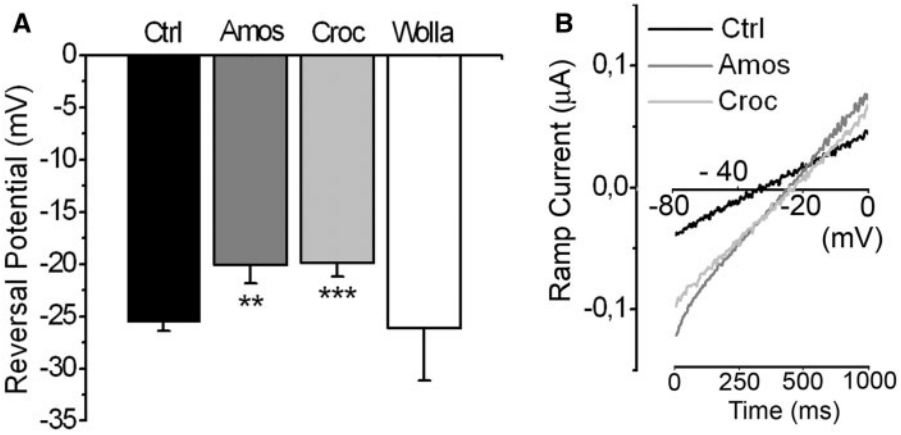

FIG. 2. Effect of Amos and Croc fibre suspensions on the ramp currents recorded in oocytes. A, Histograms showing the mean ± SEM of the zero current reversal potential shift of the currents induced by a voltage ramp from −80 to 0 mV in nontreated (Ctrl) and Amos-, Croc-, and Wolla-treated oocytes (10–15 μg/ml; time interval 1000 ms, holding potential = −40 mV) (significantly different $^{**}p < .01$; $^{***}p < .001$ vs Ctrl). Ctrl: $n = 54$; Amos: $n = 22$; Croc: $n = 46$; Wolla: $n = 9$. In B, example of the ramp current–voltage (*I–V*) traces recorded in three oocytes in the absence (Ctrl) or in the presence of Amos or Croc (15 μg/ml). Note the intersection of the *I–V* lines at around −20 mV (see text).

impossible to voltage clamp the cell (Figs. 1C and 1D). To analyze in detail the effect of the interaction between the asbestos fibres and the membrane, we initially performed a ramp voltage protocol to record the instantaneous (voltage independent) or rapidly activating currents and then a voltage step protocol to record the slower voltage-activated currents. Interestingly, when a 1-s voltage ramp protocol was applied to the oocytes (from −80 to 20 mV; Fig. 2), the zero current reversal potential of the ramp currents was found to be significantly shifted to a more depolarized level in asbestos-treated oocytes (10–15 μg/ml); in Amos-treated oocytes it reversed at −20.10 ± 1.75 mV ($n = 22$; $p < .01$), in Croc-treated oocytes at −19.87 ± 1.3 mV ($n = 46$; $p < .001$), whereas in Ctrl the current reversed at −25.55 ± 0.89 mV ($n = 49$). In Wolla, the reversal

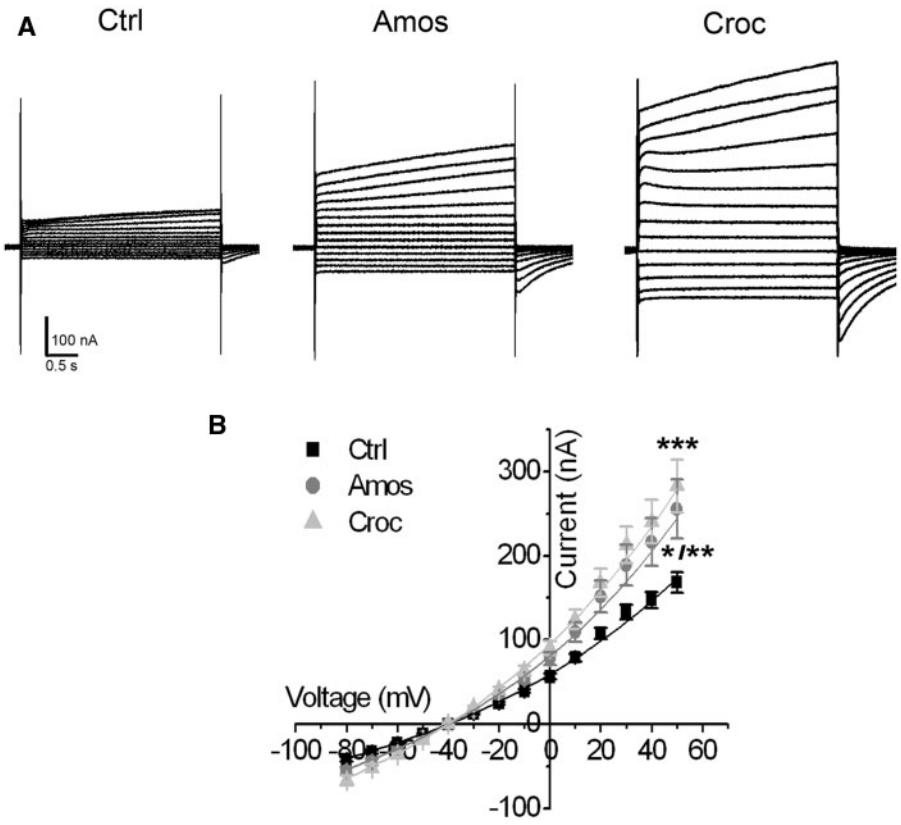

FIG. 3. Effect of Amos and Croc asbestos fibre suspensions on membrane currents activated by voltage steps. A, Examples of currents induced by depolarizing steps (from −80 to +50 mV, 10 mV steps, 3 s) from a holding potential of −40 mV. B, Steady-state current–voltage relationships. Note, Amos and Croc asbestos fibre suspensions dramatically increased the amplitude of the slow outward rectifying membrane current (and rebound inward tail current), as well as increasing the resting leak conductance at the holding potential (significantly different Amos: */**$p < .05/.01$ vs Ctrl; Croc: ***$p < .001$ vs Ctrl at all voltage steps). Ctrl: $n = 90$; Amos: $n = 63$; Croc: $n = 84$.

potential remained unaltered (−26.11 ± 5.01, $n = 9$; $p > .05$) (Fig. 2A). In Figure 2B are shown the typical ramp current traces recorded in Ctrl condition and after the treatment with Amos or Croc asbestos; the current/voltage relations were linear and their slope tended to increase after the treatments (indicating an increase in membrane conductance) along with a shift in the zero current reversal potential to a more depolarized level.

Figure 3A shows typical current traces recorded from oocytes following application of different voltage clamp steps (from −80 to + 50 mV; holding potential = −40 mV), in a Ctrl and asbestos-treated cells (10–15 μg/ml); Figure 3B summarizes the *I–V* relationships obtained at the steady state. Surprisingly, in Amos and particularly Croc-treated cells, there was a dramatic increase of the outward rectification (and corresponding inward tail current).

A second set of experiments was performed by microinjecting 50 nl of a Croc suspension per cell (0.6 mg/ml, for more details, see "Methods") directly inside the cells. In this case, the recordings were made 30 min after the injection and the measurements compared with those obtained in oocytes injected with Ringer's solution (see "Methods"). In parallel, oocytes of the same batch were incubated with the same solution containing asbestos or Ringer's solution. The results reported in Figure 4 clearly show that the presence of Croc fibres inside the cells did not affect the electrical membrane properties.

To test whether the changes in oocyte electrical membrane properties we observed were due to the presence/release of fibre surface iron (Pollastri *et al.*, 2014), we carried out a series of experiments in which Croc was applied in presence of agents capable of modifying the activity of surface iron; namely, the iron chelator DFO, and also the chelators EDTA or AFC. We found that all treatments were able to abolish the effects of Croc on the passive membrane properties (Figs. 5A and 5B) and to partially reduce the enhancing effect on the voltage-dependent slow outward rectifying currents activated by the voltage ramp and voltage step protocols, respectively (Figs. 5C and 5D).

Asbestos Fibres Can Modify the Surface Morphology of the Xenopus Oocytes

Figures 6A and 6D show the appearance of control untreated XLOs viewed under a SEM. The eggs were oriented on the stub with the animal pole facing upward. The surface of the vitelline envelope (VE) appeared to be covered by many putative "pores," separated by filamentous structures, giving a vein-like appearance. Each pore was surrounded by an elevated edge. In some samples, a few granules (probably cortical granules) were rarely found bound onto the external surface. Underneath the external envelope, the plasma membrane microvilli (MV) were evident (inset in Fig. 6A). We think it possible that these pore-like structures may derive from an interaction between the MV of the underlying plasma membrane and the inner surface of the envelope (Larabell and Chandler, 1989). After 30 min of incubation with 15 μg/ml Amos followed by careful washes, the appearance of the VE clearly changed. A few Amos fibres, mainly short, having a length of approximately 5–15 μm, were seen to be attached to the egg surface and some of them were frequently found in the process of penetrating/piercing the envelope (arrow in Fig. 6B). Many, if not all the pore-like

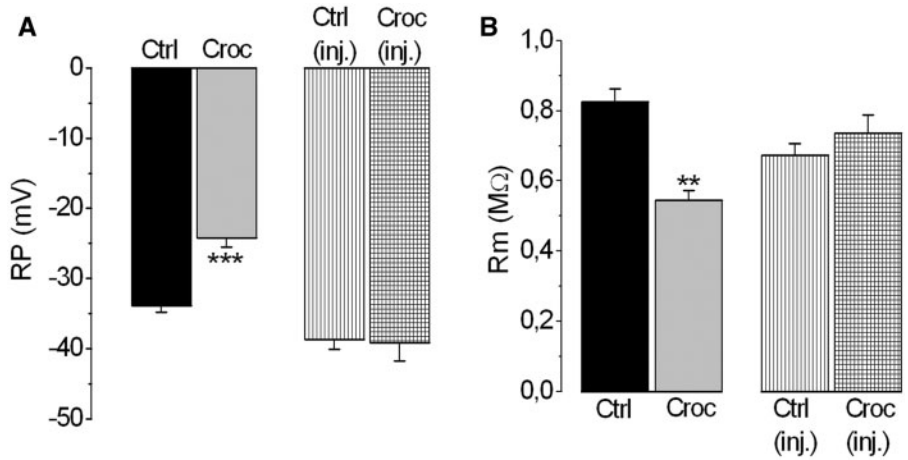

FIG. 4. Intracellular microinjection of Croc does not affect the electrical membrane properties of the oocyte. A, Mean ± SEM of the RP recorded in nontreated (Ctrl) versus (external) Croc-treated oocytes, and oocytes injected with Ringer (Ctrl inj.) or oocytes injected with Croc in Ringer's solution (Croc inj.). B, Mean ± SEM of the R_m recorded in the same oocytes (significantly different $^{**}p < .01$, $^{***}p < .001$ vs Ctrl). Ctrl: $n = 22$; Croc: $n = 5$; Ctrl (inj.): $n = 7$; Croc (inj.): $n = 10$.

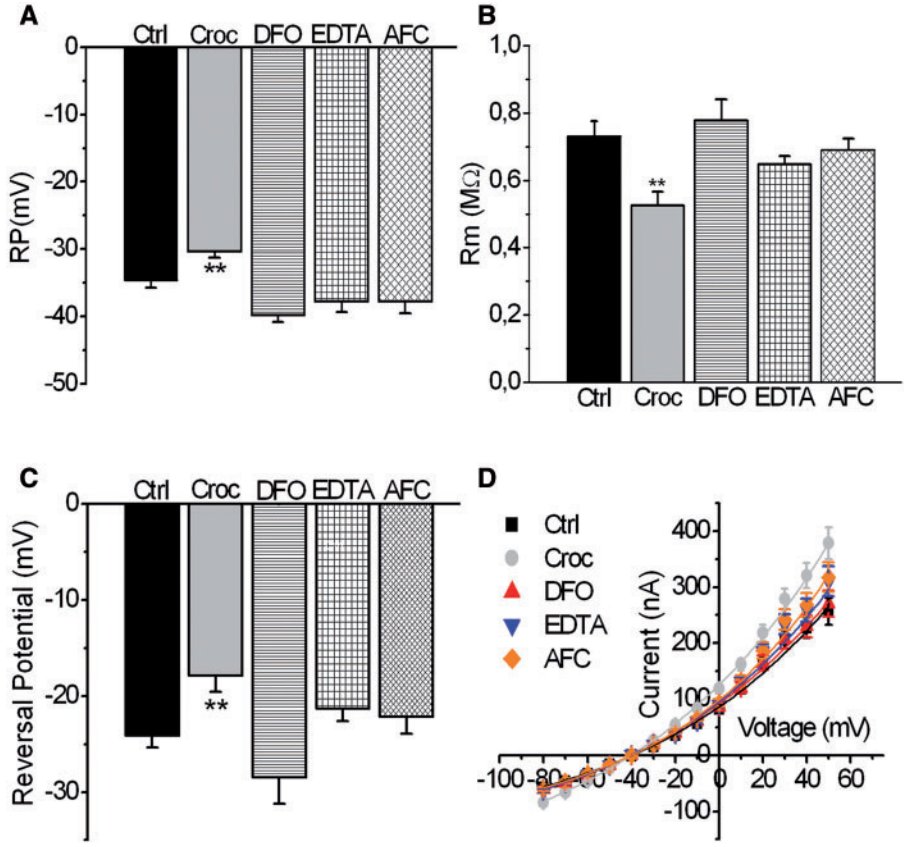

FIG. 5. DFO, EDTA, or AFC treatment abolishes the effect of Croc suspension fibres on the membrane properties of the oocytes. A, Mean ± SEM of the RP and B, the R_m recorded in nontreated oocytes (Ctrl) and Croc-treated oocytes in the absence or in the presence of DFO, EDTA, or AFC. In C and D, the effect of Croc treatment on the zero current reversal potential and slow voltage-activated current (see text). Ctrl: $n = 17$; Croc: $n = 14$, DFO: $n = 23$; AFC: $n = 21$ (significantly different $^{**}p < .01$ vs Ctrl).

structures appeared closed without the surrounding edge and, on the whole, the envelope surface appeared smoother with respect to the control eggs (Fig. 6E). Granules, clouding around and associated with the interacting fibres were frequently found (arrowhead in Fig. 6B). The incubation with Croc fibres (15 μg/ml) also induced some evident morphological changes (Fig. 6C). Patches of pores remained open, but these were surrounded by many sites of closed pores. Also in this case, many secreted granules were found on the envelope surface. Interestingly, in all the asbestos-treated samples the typical surface "veins" found in the untreated samples were notably less evident. To better define the dramatic effects exerted by the fibres on the pore morphology, we examined these structures at a higher magnification. Figure 6D shows that the pores in

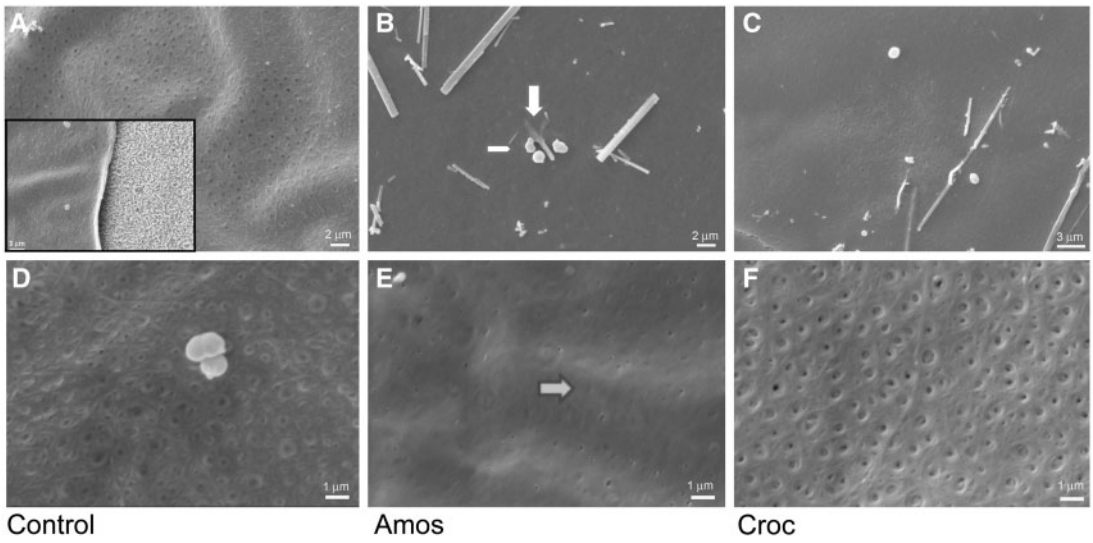

FIG. 6. Appearance of XLOs observed under a SEM. Oocytes were incubated for 30 min under continuous mixing in Ringer's solution at room temperature. A, D, Control untreated oocytes, original magnification ×10 000 and 25 000, respectively. The inset in A (boxed, original magnification ×10 000) shows the plasma membrane MV underneath the external envelope. B, E, Amos-treated oocytes, original magnification ×10 000 and 25 000, respectively; C, F, Croc-treated oocytes, original magnification ×10 000 and 25 000, respectively. Arrows in B show some short Amos fibres penetrating/piercing the envelope. Arrowhead in B shows some granules around the interacting fibres.

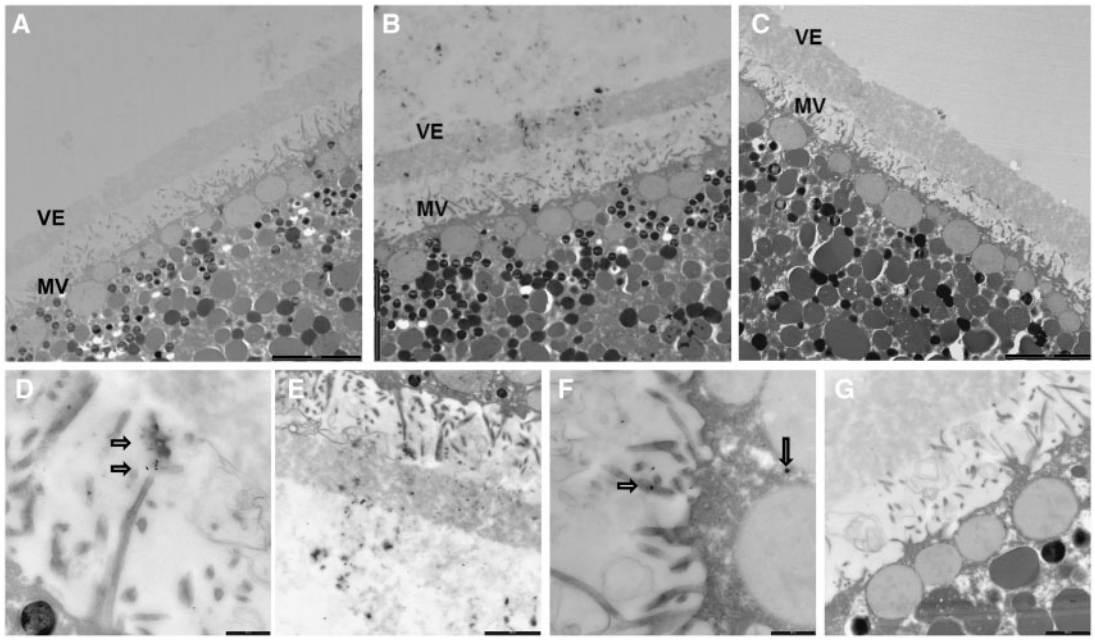

FIG. 7. Appearance of XLOs observed under a TEM. Oocytes were treated as indicated in the legend to Figure 6. A, Untreated oocytes, bar = 5 μm; B, Amos (15 μg/ml)-treated oocytes, bar = 5 μm; C, Croc-treated oocytes, bar = 5 μm; D, E, Amos-treated oocytes, bars = 0.5 and 2 μm, respectively; F, G, Croc-treated oocytes, bars = 0.5 and 1 μm, respectively. Arrows in D and in F show sections of Amos and Croc fibres in contact with plasma membrane MV.

untreated samples were different from those in asbestos-treated oocytes (Figs. 6E and 6F). The stronger effect was confirmed for Amos-treated oocytes. In this case, most, if not all the pores appeared closed and the veins were missing, making the envelope surface smooth in appearance (Fig. 6E). Croc-treated cells were examined in those sites where the pores were open. These pores appeared enlarged without the surrounding edge. Veins were evident within these sites, but were lacking in the surrounding sites. These findings were confirmed in three separate experiments.

Other information derived from the analysis of the oocyte sections was obtained using a TEM at higher magnification. Figure 7 shows that specific changes were found in the interspace between the VE and the plasma membrane MV. The morphology of Amos (Figs. 7B and 7E) and Croc (Figs. 7C and 7G) treated samples were clearly affected. The main effect involved the MV which appeared thickened and more numerous with respect to control, and the presence of many membrane vesicles in the interspace between the cell membrane and the external envelope, suggesting membrane damage. A detailed

analysis on higher magnification revealed that some Amos (Fig. 7D) and Croc (Fig. 7F) fibres were in contact with the MV (arrows) suggesting that the VE cannot represent a barrier for the movement of the fibres through the oocyte membrane. In the hundreds of sections of asbestos-treated oocytes that we analyzed, we never observed any evidence of a phagocytic process occurring; all the fibres, which came into contact with the cell membrane were free and not included in any type of vacuole, but simply adsorbed on the plasma membrane. Sometimes, electron-dense structures seemed to be ingested by the oocytes, however, when observed at very high magnification, they did not show the typical appearance of true asbestos fibres (see "Methods" section), but were frequently identified as "pigmented granules" (Fig. 7B), which were probably undergoing cell extrusion. The analysis with the TEM gave the same results in three separate experiments.

DISCUSSION

The results reported in this study are in line with what was previously reported in the literature, where a change in both the RP and R_m was observed in the murine macrophage cell line P388D1 treated with Amos and Croc (Gormley and Wright, 1980). In addition, we found here a dose-dependent effect, which was more evident in Croc-treated than in Amos-treated cells. These unexpected changes in the passive electrical properties of the cell, suggested a direct interaction of asbestos fibres with the oocyte cell membrane, which then somehow affected the ionic permeability. As concentrations equal or lower than 15 μg/ml did not compromise the survival of the cells, we attempted to further characterize the nature of such changes.

Two further features of XLOs that facilitates their use as a model for studying the biophysical changes of the cell membrane after asbestos, is their low expression of endogenous ion channels (Englund *et al.*, 2014) and their large size, that allows the microinjection of material directly inside the cell, without impairing the membrane properties (Miledi *et al.*, 2006). It is well known that at rest, the oocyte cell membrane is mainly permeable to K^+, Cl^-, and in part Na^+ and the values of the equilibrium potentials of these ions are −95, −28, and +61 mV, respectively (recorded with KCl microelectrodes) (Costa *et al.*, 1989). Under our conditions, the intersection of the ramp current–voltage (*I–V*) traces at more positive value than that found in Ctrl indicates a relatively positive ionic equilibrium potential of the asbestos-induced conductance change. The zero current reversal potential was at approximately −20 mV, more depolarized than in Ctrl or Wolla-treated cells, suggesting thus an increased permeability to Cl^- and/or cations.

As previously reported, oocytes have several types of voltage-sensitive ion channels, but normally their activity is low (Englund *et al.*, 2014). Indeed, in nontreated oocytes the ramp protocol, from −80 to 0 mV and the *I–V* relationships obtained from the voltage step protocol were essentially linear confirming a low expression of endogenous voltage-gated channels, whereas in the presence of asbestos there was a significant slow time-dependent outward rectification at more positive potentials, followed by a rebound inward tail current on stepping back to the holding potential. We did not investigate the nature of this outward rectification, but it is likely to involve either a K^+ or Cl^- ion conductance (or both), as reported elsewhere (Lu *et al.*, 1990; Miledi, 1982; Voets *et al.*, 1996). Interestingly, when Croc fibres were injected inside the cells no effect on the electrical membrane properties was observed excluding a possible minuscule interaction of asbestos fibres.

Asbestos minerals are known to contain iron, magnesium, and calcium within their molecular structure, with a core of SiO_2. The toxicity of asbestos, in particular Croc and Amos, is often correlated with the presence and/or release of Fe^{2+} and Fe^{3+} from the asbestos fibre surface which may then be important in initiating toxic inflammatory cascades (Aust *et al.*, 2011; Liu *et al.*, 2013); this suggests that surface charges due to iron present on the Croc fibres were indeed important in mediating effects on the oocytes. Interestingly, Croc and Amos asbestos fibres also have negative surface charges in aqueous solution, which is the so-called "zeta potential" (Pollastri *et al.*, 2014). The negative surface zeta potential reported for Croc depends on the presence of the positive charge carried by Fe^{2+} and Fe^{3+} within the molecular structure of the mineral, and it has been recently postulated to be one of the causes for the tumorigenic effect of asbestos (Pollastri *et al.*, 2014). The existence of the zeta potential could conceivably change the electric field of the cell membrane following adsorption onto the cell surface, and thereby alter the function of adjacent ion channels. Moreover, mobilization of surface iron away from the fibres is reported to promote the formation of ROS, which can activate nonselective cationic endogenous currents in oocytes (Duprat *et al.*, 1995). We propose that both surface charge mechanisms could explain our observed results.

Taken together, these results support a direct interaction of the fibres with the cell membranes, as confirmed also by our findings obtained from ultrastructural analysis. The morphological analysis of asbestos-treated oocytes showed a direct interaction of the fibres with the plasma membrane of the oocyte that cannot be hindered by the VE. Moreover, the fibres could clearly affect the appearance of the cell membrane. The MV became more numerous and thicker and frequently, membrane vesicles were found in the interspace between the membrane and the envelope. Altogether, these changes suggest a fibre/membrane interaction potentially capable of modifying the oocyte functions, as confirmed with our electrophysiological recordings. The literature shows that XLOs are able to endocytose materials, but this process is scanty in resting cells (Sardet *et al.*, 2002). Significant amounts of ligands can be taken up after at least 30 min of incubation (Mukhopadhyay *et al.*, 1997; Wall and Patel, 1987) and endocytic vesicles can be formed for recycling the membrane following the exocytosis of cortical granules (Sokac *et al.*, 2003). In our hands, despite the sporadic extrusion of some cortical granules and pigmented granules which could be confused with an endocytic event, treated oocytes did not show any sign of an ongoing endocytic or phagocytic process even after 60 min of incubation with asbestos fibres (not shown). Despite a careful analysis, we did not observe any microscopic evidence of fibre ingestion nor of fibre-induced passive piercing at the oocyte plasma membrane level, and we believe that the asbestos fibres can still passively pierce the external envelope, reach the underneath compartment, interact with MV and possibly modify the intracellular properties of the cell. However, it is noteworthy that intracellular microinjection of asbestos inside the XLOs in our experiments did not alter their electrical membrane properties, at least in the short-term. Presently, we do not have an explanation for the observed changes in oocyte morphology found at the envelope surface level; we can speculate that the evident change in pore-like structures found after asbestos fibre treatment could derive from the modification of MV activity. These protrusions are in fact in contact with the inner surface of the envelope

and may have the capacity of modulating its function. We believe that the MV–envelope interaction deserves to be further investigated from this point of view because it may help to reveal the possible different cellular effects of different type of asbestos fibres.

In conclusion, we have demonstrated for the first time that oocytes can represent a suitable model to study in detail the interaction between asbestos fibres and biological cell membranes at the electrophysiological and morphological level. Using aqueous suspensions of two common asbestos fibre types, Amos and Croc, we found that such an interaction significantly affected the electrical membrane properties as well as the morphology of the cells, and we propose that the fibres, either by adsorbing onto the cell surface and/or traversing the membrane, somehow create a non-specific "pore" through which ion fluxes can occur to change the RP and R_m. As cells were invariably depolarized with a conductance increase following asbestos exposure (equilibrium potential close to E_{Cl}), and in view of the appearance of an augmented slow, time-dependent outward rectification with an inward tail current following step voltage protocols, we suggest that these conductances could primarily involve an enhanced flux of Cl^- ions across the cell membrane; this however, would need to be confirmed in further experiments. Alternatively, our results could also be explained by a surface activation/modulation of ion channels already present in the oocyte membrane by asbestos, to alter their permeability characteristics. The fact that the effects of asbestos were annulled by chelator screening of the fibre surface charges contributed by molecular iron strongly suggests that such surface interactions to alter membrane permeability are feasible. How these observed permeability changes in XLOs relate to asbestos toxicity is also presently unclear, but they could be an important lead for obtaining a better understanding of the relevant underlying processes. Our findings suggest that the effects induced by asbestos fibres on XLOs are independent of fibre ingestion and that an involvement of asbestos with the intracellular compartments is not likely to be involved, even if we cannot completely exclude it. We think that an interaction between asbestos fibres and surface membrane components, whose nature remains to be defined, is very likely. Finally, as modification of the surface iron content in the Croc structure also significantly inhibits asbestos toxicity in cell cultures (Gulumian, 2005), we suggest that our method could be employed as a convenient assay for evaluating the potential cytotoxicity of asbestos-containing material whose industrial thermal inertization is commonly evaluated using physical tools (Leonelli *et al.*, 2006) but, only rarely by biological means (Giantomassi *et al.*, 2010; Valentine *et al.*, 1983). Noteworthy, asbestos has been reported to induce sex-chromosome aneuploidy in Drosophila oocytes (Osgood, 1994; Osgood and Sterling, 1991). Our method offers a very rapid outcome, avoiding time consuming, costly, and cumbersome cell culture methods.

It will also be interesting in the future, to compare the very early XLO–asbestos interaction we describe (both functionally and morphologically) for all types of asbestos fibres, in parallel with the long-term effects they produce on the viability of mammalian epithelial cell cultures.

FUNDING

Fondazione Benefica Kathleen Foreman-Casali (Italy) and Beneficentia Stiftung (Liechtenstein).

ACKNOWLEDGMENTS

The authors thank Mr Claudio Gamboz and Michele Zabucchi for their technical assistance.

REFERENCES

Andolfi, L., Trevisan, E., Zweyer, M., Prato, S., Troian, B., Vita, F., Borelli, V., Soranzo, M. R., Melato, M., and Zabucchi, G. (2013). The crocidolite fibres interaction with human mesothelial cells as investigated by combining electron microscopy, atomic force and scanning near-field optical microscopy. *J. Microsc.* **249,** 173–183.

Aust, A. E., Cook, P. M., and Dodson, R. F. (2011). Morphological and chemical mechanisms of elongated mineral particle toxicities. *J. Toxicol. Environ. Health B Crit. Rev.* **14,** 40–75.

Bernareggi, A., Reyes-Ruiz, J. M., Lorenzon, P., Ruzzier, F., and Miledi, R. (2011). Microtransplantation of acetylcholine receptors from denervated rat skeletal muscles to frog oocytes. *J. Physiol.* **589,** 1133–1142.

Blake, D. J., Bolin, C. M., Cox, D. P., Cardozo-Pelaez, F., and Pfau, J. C. (2007). Internalization of Libby amphibole asbestos and induction of oxidative stress in murine macrophages. *Toxicol. Sci.* **99,** 277–288.

Boulanger, G., Andujar, P., Pairon, J. C., Billon-Galland, M. A., Dion, C., Dumortier, P., Brochard, P., Sobaszek, A., Bartsch, P., Paris, C., *et al.* (2014). Quantification of short and long asbestos fibers to assess asbestos exposure: A review of fiber size toxicity. *Environ. Health* **13,** 59.

Brody, A. R., and Hill, L. H. (1983). Interactions of chrysotile asbestos with erythrocyte membranes. *Environ. Health Perspect.* **51,** 85–89.

Brody, A. R., George, G., and Hill, L. H. (1983). Interactions of chrysotile and crocidolite asbestos with red blood cell membranes. *Chrysotile binds to sialic acid.* Lab. Invest. **49,** 468–475.

Costa, P. F., Emilio, M. G., Fernandes, P. L., Ferreira, H. G., and Ferreira, K. G. (1989). Determination of ionic permeability coefficients of the plasma membrane of *Xenopus laevis* oocytes under voltage clamp. *J. Physiol.* **413,** 199–211.

Dascal, N., Landau, E. M., and Lass, Y. (1984). Xenopus oocyte resting potential, muscarinic responses and the role of calcium and guanosine 3',5'-cyclic monophosphate. *J. Physiol.* **352,** 551–574.

Duprat, F., Guillemare, E., Romey, G., Fink, F., Lesage, F., Lazdunski, M., and Honore, E. (1995). Susceptibility of cloned K^+ channels to reactive oxygen species. *Proc. Natl. Acad. Sci. U.S.A.* **92,** 11796–11800.

Elferink, J. G., and Kelters, I. (1991). Chrysotile asbestos-induced membrane damage in human erythrocytes. *Res. Commun. Chem. Pathol. Pharmacol.* **73,** 355–365.

Englund, U. H., Gertow, J., Kågedal, K., and Elinder, F. (2014). A voltage dependent non-inactivating Na^+ channel activated during apoptosis in Xenopus oocytes. *PLos One* **9,** e88381.

Gendek, E. G., and Brody, A. R. (1990). Changes in lipid ordering of model phospholipid membranes treated with chrysotile and crocidolite asbestos. *Environ. Res.* **53,** 152–167.

Giantomassi, F., Gualtieri, A. F., Santarelli, L., Tomasetti, M., Lusvardi, G., Lucarini, G., Governa, M., and Pugnaloni, A.. (2010). Biological effects and comparative cytotoxicity of thermal transformed asbestos-containing materials in a human alveolar epithelial cell line. *Toxicol. In Vitro* **24,** 1521–1531.

Gormley, I. P., and Wright, M. O. (1980). Electrophysiological changes induced by asbestos in macrophage-like cells during long-term culture. *IARC Sci. Publ.* **30,** 435–439.

Gormley, I. P., Wright, M. O., and Ottery, J. (1978). The effect of toxic particles on the electrophysiology of macrophage. *Ann. Occup. Hyg.* **21,** 141–149.

Governa, M., Amati, M., Fontana, S., Visona, I., Botta, G. C., Mollo, F., Bellis, D., and Bo, P. (1999). Role of iron in asbestos-body-induced oxidant radical generation. *J. Toxicol. Environ. Health A* **58,** 279–287.

Governa, M., Camillucci, L., Amati, M., Visonà, I., Valentino, M., Botta, G. C., Campopiano, A., and Fanizza, C. (1998). Wollastonite fibers in vitro generate reactive oxygen species able to lyse erythrocytes and activate the complement alternate pathway. *Toxicol. Sci.* **44,** 32–38.

Gulumian, M. (2005). An update on the detoxification processes for silica particles and asbestos fibers: Successes and limitations. *J. Toxicol. Environ. Health B Crit. Rev.* **8,** 453–483.

Iguchi, H., and Kojo, S. (1989). Possible generation of hydrogen peroxide and lipid peroxidation of erythrocyte membrane by asbestos: Cytotoxic mechanism of asbestos. *Biochem. Int.* **18,** 981–990.

Johnson, N. F., and Davies, R. (1983). Effect of asbestos on the P388D1 macrophage-like cell line: Preliminary ultrastructural observations. *Environ. Health Perspect.* **51,** 109–117.

Kohyama, N., Shinohara, Y., and Suzuki, Y.. (1996). Mineral phases and some reexamined characteristics of the International Union Against Cancer standard asbestos samples. *Am. J. Ind. Med.* **30,** 515–528.

Larabell, C. A., and Chandler, D. E. (1989). The coelomic envelope of *Xenopus laevis* eggs: A quick-freeze, deep-etch analysis. *Dev. Biol.* **131,** 126–135.

Leonelli, C., Veronesi, P., Boccaccini, D. N., Rivasi, M. R., Barbieri, L., Andreola, F., Lancellotti, I., Rabitti, D., and Pellacani, G. C. (2006). Microwave thermal inertisation of asbestos containing waste and its recycling in traditional ceramics. *J. Hazard. Mater.* **135,** 149–155.

Liu, G., Cheresh, P., and Kamp, D. W. (2013). Molecular basis of asbestos-induced lung disease. *Annu. Rev. Pathol.* **8,** 161–187.

Liu, W., Ernst, J. D., and Broaddus, V. C. (2000). Phagocytosis of crocidolite asbestos induces oxidative stress, DNA damage, and apoptosis in mesothelial cells. *Am. J. Respir. Cell. Mol. Biol.* **23,** 371–378.

Lu, L., Montrose-Rafizadeh, C., and Guggino, W. B. (1990). Ca^{2+}-activated K^{+} channels from rabbit kidney medullary thick ascending limb cells expressed in Xenopus oocytes. *J. Biol. Chem.* **265,** 16190–16194.

Malorni, W., Iosi, F., Falchi, M., and Donelli, G. (1990). On the mechanism of cell internalization of chrysotile fibers: An immunocytochemical and ultrastructural study. *Environ. Res.* **52,** 164–177.

Maxim, L. D., and McConnell, E. E. (2005). A review of the toxicology and epidemiology of Wollastonite. *Inhal. Toxicol.* **17,** 451–466.

Miledi, R. (1982). A calcium-dependent transient outward current in *Xenopus laevis* oocytes. *Proc. R. Soc. Lond. B Biol. Sci.* **215,** 491–497.

Miledi, R., Palma, E., and Eusebi, F. (2006). Microtransplantation of neurotransmitter receptors from cells to Xenopus oocyte membranes: New procedure for ion channel studies. *Methods Mol. Biol.* **322,** 347–355.

Mukhopadhyay, A., Barbieri, A. M., Funato, K., Roberts, R., and Stahl, P. D. (1997). Sequential actions of Rab5 and Rab7 regulate endocytosis in the Xenopus oocyte. *J. Cell Biol.* **136,** 1227–1237.

Osgood, C. J. (1994). Refractory ceramic fibers (RCFs) induce germline aneuploidy in Drosophila oocytes. Mutat. Res. **324,** 23–27.

Osgood, C., and Sterling, D. (1991). Chrysotile and amosite asbestos induce germ-line aneuploidy in Drosophila. *Mutat. Res.* **261,** 9–13.

Palomäki, J., Välimäki, E., Sund, J., Vippola, M., Clausen, P. A., Jensen, K. A., Savolainen, K., Matikainen, S., and Alenius, H. (2011). Long, needle-like carbon nanotubes and asbestos activate the Nlrp3 inflammasome through a similar mechanism. *ACS Nano.* **5,** 6861–6870.

Pollastri, S., Gualtieri, A. F., Gualtieri, M. L., Hanuskova, M., Cavallo, A., and Gaudino, G. (2014). The zeta potential of mineral fibers. *J. Hazard. Mater.* **276,** 469–479.

Sardet, C., Prodon, F., Dumollard, R., Chang, P., and Chênevert, J. (2002). Structure and function of the egg cortex from oogenesis through fertilization. *Dev. Biol.* **241,** 1–23.

Sokac, A. M., Co, C., Taunton, J., and Bement, W. (2003). Cdc42-dependent actin polymerization during compensatory endocytosis in Xenopus eggs. *Nat. Cell Biol.* **5,** 727–732.

Trevisan, E., Vita, F., Medic, N., Soranzo, M. R., Zabucchi, G., and Borelli, V. (2014). Mast cells kill *Candida albicans* in the extracellular environment but spare ingested fungi from death. *Inflammation* **37,** 2174–2189.

Valentine, R., Chang, M. J., Hart, R. W., Finch, G. L., and Fisher, G. L. (1983). Thermal modification of chrysotile asbestos: Evidence for decreased cytotoxicity. *Environ. Health Perspect.* **51,** 357–368.

Voets, T., Buyse, G., Tytgat, J., Droogmans, G., Eggermont, J., and Nilius, B. (1996). The chloride current induced by expression of the protein pICIn in Xenopus oocytes differs from the endogenous volume-sensitive chloride current. *J. Physiol.* **495,** 441–447.

Wall, D. A., and Patel, S. (1987). The intracellular fate of vitellogenin in Xenopus oocytes is determined by its extracellular concentration during endocytosis. *J. Biol. Chem.* **262,** 14779–14789.

NOTE

During the accomplishment of this thesis, the following papers and abstracts have been published and presented.

Full-text papers

- Annalisa Bernareggi, **Elisa Ren**, Violetta Borelli, Francesca Vita, Andrew Constanti, Giuliano Zabucchi. *Xenopus laevis oocytes as a model system for studying the interaction between asbestos fibers and cell membranes.* Toxicol Sci, 2015. **145**: p. 263-72.

Abstracts

- **Elisa Ren**, Elisa Luin, Giulia Parato, Paola Lorenzon, Marina Sciancalepore, Barbara Pavan and Annalisa Bernareggi. *Adenosine receptors modulate the autocrine nAChr-driven [Ca^{2+}] spiking activity of in vitro contracting myoutubes.* 64° National Meeting of Italian Society of Physiology, Portonovo (Italy), 18-20 September 2013.

- Paola Lorenzon, **Ren Elisa**, Luin Elisa, Ziraldo Gaia, Sciancalepore Marina, Bernareggi Annalisa. *The P1-purinergic receptor modulation of nAChR-channel activity at the endplate region.* 66° National Meeting of Italian Society of Fisiology, Genoa (Italy), 16-18 September 2015.

- **Elisa Ren**, Barbara Pavan, Marina Sciancalepore, Paola Lorenzon, Annalisa Bernareggi. *Adenosine-mediated modulation of ACh-evoked currents induced in Xenopus oocytes following embryonic skeletal muscle membrane*

microtransplantation. 44° European Muscle Conference, Warsaw (Poland), 21-25 September 2015.

- **Elisa Ren**, Davide Barbetta, Marco Stebel, Paola Zarattini, Annalisa Bernareggi. *Electrical membrane properties of oocytes isolated from Xenopus laevis following multiple laparotomies.* 22° Meeting AISAL, Naples (Italy), 22-23 October 2015.

ACKNOWLEDGEMENTS

I would like to thank the Biophysics and Cellular Neurobiology Laboratory of professors Annalisa Bernareggi, Paola Lorenzon and Marina Sciancalepore, I am especially grateful for giving me the possibility to attend my PhD in a productive, stimulating and peaceful environment. In particular, I want to thank my supervisor Annalisa Bernareggi for everything she taught me. She was an excellent example for me; I very much appreciated her professionalism, enthusiasm and joy for the research as well as for life.

I am thankful to all the people I have met in these past three years for sharing their experience, time and ideas with me, in particular Elisa Luin, Gaia Ziraldo, Pierpaolo Busan, Michele Zabucchi and Moreno Cocchietto.

It was a real pleasure to personally work with Prof. Giuliano Zabucchi from the University of Trieste and Barbara Pavan from the University of Ferrara. Thanks for the collaboration to Dr. Arthur Giniatullin from the University of Kazan and Prof. Rashid Giniatullin of the University of Eastern Finland, Kuopio.

At the top of my thoughts there is my lovely family, always present in my life, in other words my roots and example.

Another special thought goes to my great friends Cinzia, Giuliana, Karin, Viviana, Filippo, Alessio and in particular to Giulia and Federica, the best friends I could ever have.

Thank you Giorgio for making me smile every day.

REFERENCES

1. Naguib M, Flood P, McArdle JJ, Brenner HR. *Advances in neurobiology of the neuromuscular junction: Implications for the anesthesiologist.* Anesthesiology, 2002. **96**: p. 202.
2. Edwards FA. *Anatomy of fast central synapses lead to a structural model for long-term potentiation.* Physiol Rev, 1995. **75**: p. 759-787.
3. Bargmann C. *Neuroscience: genomics reaches the synapse.* Nature, 2014. **436**: p. 473-474.
4. Wess J, Eglen RM, Gautam D. *Muscarinic acetylcholine receptors: mutant mice provide new insights for drug development.* Nat Rev Drug Discov, 2007. **6**: p. 721-733.
5. Caulfield MP, Birdsall NJM. *International union of pharmacology. XVII. Classification of muscarinic acetylcholine receptors.* Pharmacol Rev, 1998. **50**: p. 279-290.
6. Wess J. *Molecular biology of muscarinic acetylcholine receptors.* Crit Rev Neurobiol, 1996. **10**: p. 69-99.
7. Furlan I, Godinho RO. *Developing skeletal muscle cells express functional muscarinic acetylcholine receptors coupled to different intracellular signaling systems.* Br J Pharmacol, 2005. **146**: p. 389-396.
8. Karlin A. *Emerging structure of the nicotinic acetylcholine receptors.* Nat Rev Neurosci, 2002. **3**: p. 102-114.
9. Barrantes FJ. *Structural basis for lipid modulation of nicotinic acetylcholine receptor function.* Brain Res Brain Res Rev, 2004. **47**: p. 71-95.
10. Unwin N. *Refined structure of the nicotinic acetylcholine receptor at 4A resolution.* J Mol Bio, 2005. **346**: p. 967-989.
11. Kalamida D, Poulas K, Avramopoulou V, Fostieri E, Lagoumintzis G, Lazaridis K, Sideri A, Zouridakis M, Tzartos SJ. *Muscle and neuronal nicotinic acetylcholine receptors Structure, function and pathogenicity.* FEBS J, 2007. **274**: p. 3799–3845.
12. Millar NS, Gotti C. *Diversity of vertebrate nicotinic acetylcholine receptors.* Neuropharmacology, 2009. **56**: p. 237-246.
13. Araud T, Wonnacott S, Bertrand D. *Associated proteins: The universal toolbox controlling ligand gated ion channel function.* Biochem Pharmacol, 2010. **80**: p. 160-169.
14. Li S, Wong AH, Liu F. *Ligand-gated ion channel interacting proteins and their role in neuroprotection.* Front Cell Neurosci, 2014. **8**: p. 125.
15. Martyn JA, White DA, Gronert GA, Jaffe RS, Ward JM. *Up-and-down regulation of skeletal muscle acetylcholine receptors* Anesthesiology, 1992. **76**: p. 822.
16. Hoffmann K, Muller J, Stricker S, Megarbane A, Rajab A, Lindner T, Cohen M, Chouery E, Adaimy L, Ghanem I, Delague V, Boltshauser E, Talim B, Horvath R, Robinson P, Lochmu¨ller H, Hubner C, Mundlos S. *Escobar syndrome is a prenatal myasthenia caused by disruption of the acetylcholine receptor fetal g subunit.* Am J Hum Genet, 2006. **79**: p. 303-312.
17. Schuetze S, Role L. *Developmental regulation of nicotinic acetylcholine receptors.* Annu Rev Neurosci, 1987. **10**: p. 403-457.
18. Entwistle A, Zalin RJ, Bevan S, Warner AE. *The control of chick myoblast fusion by ion channels operated by prostaglandins and acetylcholine.* J Cell Biol, 1988. **106**: p. 1693-1702.
19. Entwistle A, Zalin RJ, Warner AE, Bevan S. *A role for acetylcholine receptors in the fusion of chick myoblasts.* J Cell Biol, 1988. **106**: p. 1703-1012.
20. Krause RM, Hamann M, Bader CR, Liu JH, Baroffio A, Bernheim L. *Activation of nicotinic acetylcholine receptors increases the rate of fusion of cultured human myoblasts.* J Physiol 1995. **489**: p. 779-790.

21. Yang X, Arber S, William C, Li L, Tanabe Y, Jessell TM, Birchmeier C, Burden SJ. *Patterning of muscle acetylcholine receptor gene expression in the absence of motor innervation.* Neuron, 2001. **30**: p. 399-410.
22. Nakajima Y, Glavinoviæ MI, Miledi R. *In vitro formation of neuromuscular junctions between adult Rana muscle fibres and embryonic Xenopus neuron.* Proc R Soc Lond B Biol, 1987. **230**: p. 425-441.
23. Brehm P, Henderson L. *Regulation of acetylcholine receptor channel function during development of skeletal muscle.* Dev Biol, 1988. **129**: p. 1-11.
24. Lin W, Burgess RW, Dominguez B, Pfaff SL, Sanes JR, Lee KF. *Distinct roles of nerve and muscle in postsynaptic differentiation of the neuromuscular synapse.* Nature, 2001. **410**: p. 1057-1064.
25. Bandi E, Bernareggi A, Grandolfo M, Mozzetta C, Augusti-Tocco G, Ruzzier F, Lorenzon P. *Autocrine activation of nicotinic acetylcholine receptors contributes to Ca2+ spikes in mouse myotubes during myogenesis.* J Physiol, 2005. **568**: p. 171-180.
26. Bernareggi A, Luin E, Formaggio E, Fumagalli G, Lorenzon P. *Novel role for prepatterned nicotinic acetylcholine receptors during myogenesis.* Muscle Nerve 2012. **46**: p. 112-121.
27. Sanes JR, Lichtman JW. *Induction, assembly, maturation and maintenance of a postsynaptic apparatus.* Nat Rev Neurosci, 2001. **2**: p. 791-805.
28. Magleby KL, Stevens CF. *A quantitative description of end-plate currents.* J Physiol, 1972. **223**: p. 173-197.
29. Katz B, Thesleff S. *A study of 'desensitization' produced by acetylcholine at the motor end-plate.* J Physiol, 1957. **138**: p. 63-80.
30. Corringer PJ, Le Novère N, Changeux JP. *Nicotinic receptors at the amino acid level.* Annu Rev Pharmacol Toxicol, 2000. **40**: p. 431-458.
31. Jackson MB. *Spontaneous openings of the acetylcholine receptor channel.* PNAS, 1984. **1984**: p. 3901-3904.
32. Magleby KL, Pallotta BS. *A study of desensitization of acetylcholine receptors using nerve-released transmitter in the frog.* J Physiol, 1981. **316**: p. 225-250.
33. Changeux JP. *The TiPS lecture. The nicotinic acetylcholine receptor: an allosteric protein prototype of ligand-gated ion channels.* Trends Pharmacol Sci, 1990. **11**: p. 485-492.
34. Giniatullin R, Nistri A, Yakel JL. *Desensitization of nicotinic ACh receptors: shaping cholinergic signaling.* Trends Neurosci, 2005. **28**: p. 371-378.
35. Quick MW, Lester RA. *Desensitization of neuronal nicotinic receptors.* 2002. **53**: p. 457-478.
36. Jahn K, Mohammadi B, Krampfl K, Abicht A, Lochmuller H, Bufler J. *Deactivation and desensitization of mouse embryonic- and adult-type nicotinic receptor channel currents.* Neurosc Lett, 2001. **307**: p. 89-92.
37. Shankaran H, Wiley HS, Resat H. *Receptor downregulation and desensitization enhance the information processing ability of signalling receptors.* BMC Syst Biol, 2007. **1**: p. 48.
38. Huganir R, Greengard P. *Regulation of transmitter desensitization by protein phosphorilation.* Neuron, 1990. **5**: p. 555-567.
39. Caratsch CG, Grassi F, Eusebi F. *Functional regulation of nicotinic receptor-channels in muscle. In T. Narahashi (ed): "Ion channels" vol 3. New York: Plenum.* 1992.
40. Talwar S, Lynch JW. *Phosphorylation mediated structural and functional changes in pentameric ligand-gated ion channels: implications for drug discovery.* Int J Biochem Cell Biol, 2014. **53**: p. 218-223.
41. Huganir RL, Greengard P. *Regulation of receptor function by protein phosphorilation.* Trends Pharmacol Sci, 1987. **8**: p. 472-477.
42. Safran A, Sagi-Eisenberg R, Neumann D, Fuchs S. *Phosphorylation of the acetylcholine receptor by protein kinase C and identification of the phosphorylation site within the receptor delta subunit.* J Biol Chem, 1987. **262**: p. 10506-10510.

43. Huganir RL, Greengard P. *cAMP-dependent protein kinase phosphorylates the nicotinic acetylcholine receptor.* PNAS, 1983. **80**: p. 1130-1134.
44. Yee GH, Huganir RL. *Determination of the sites of cAMP-dependent phosphorylation on the nicotinic acetylcholine receptor.* J Biol Chem, 1987. **262**: p. 16748-16753.
45. Huganir RL, Delcour AH, Greengard P, Hess GP. *Phosphorylation of the nicotinic acetylcholine receptor regulates its rate of desensitization.* Nature, 1986. **321**: p. 774-776.
46. Albuquerque EX, Deshpande SS, Aracava Y, Alkondon M, Daly JW. *A possible involvement of cyclic AMP in the expression of desensitization of the nicotinic acetylcholine receptor. A study with forskolin and its analogs.* FEBS Lett, 1986. **199**: p. 113-120.
47. Zani BM, Grassi F, Molinaro M, Monaco L, Eusebi F. *Cyclic AMP regulates the life time of acetylcholine-activated channels in cultured myotubes.* Biochem Biophys Res Commun, 1986. **140**: p. 243-249.
48. Eusebi F, Molinaro M, Zani BM. *Agents that activate protein kinase C reduce acetylcholine sensitivity in cultured myotubes.* J Cell Biol, 1985. **100**: p. 1339-1342
49. Eusebi F, Grassi F, Nervi C, Caporale C, Adano S, Zabi BM, Molinaro M. *Acetycholine may regulate its own nicotinic receptor-channel trough the C-kinase system.* Proc R Soc Lond B Biol Sci, 1987. **230**: p. 355-365.
50. Huganir RL, Miles K, Greengard P. *Phosphorylation of the nicotinic acetylcholine receptor by an endogenous tyrosinespecific protein kinase.* PNAS, 1984. **81**: p. 6968-6972.
51. Caratsch CG, Knoflach F, Grassi F, Eusebi F. *Regulation of acetylcholine receptor function by the phorbol ester TPA in rat skeletal muscle.* Naunyn Schmiedebergs Arch Pharmacol, 1989. **340**: p. 82-86.
52. Adamo S, Zani BM, Nerri C, Senni MI, Eusebi F. *Acetylcholine stimulates phosphatidylinositol turnover at nicotinic receptors of cultured myotubes.* FEBS Lett, 1985. **190**: p. 161-164.
53. Smith MM, Merlie JP, Lawrence JC Jr. *Regulation of phosphorylation of nicotinic acetylcholine receptors in mouse BC3H1 myocytes.* PNAS, 1987. **84**: p. 6601-6605.
54. Miles K, Greengard P, Huganir RL. *Calcitonin gene-related peptide regulates phosphorylation of the nicotinic acetylcholine receptor in rat myotubes.* Neuron, 1989. **2**: p. 1517-1524.
55. Giniatullin RA, Talantova M, Vyskocil F. *Desensitization shortens the high-quantal-content endplate current time course in frog muscle with intact cholinesterase.* J Physiol, 1997. **502**: p. 641-648.
56. Mulle C, B.P., Pinset C, Roa M, Changeus JP. *Calcitonin gene-related peptide enhances the rate of desensitization of the nicotinic acetylcholine receptor in cultured mouse muscle cells.* PNAS, 1988. **85**: p. 5728-5732.
57. Chatzidaki A, Millar NS. *Allosteric modulation of nicotinic acetylcholine receptors.* Biochem Pharmacol, 2015. **97**: p. 408-417.
58. Verkhratsky A, Burnstock G. *Biology of purinergic signalling: its ancient evolutionary roots, its omnipresence and its multiple functional significance.* Bioessays, 2014. **36**: p. 697-705.
59. Burnstock G, Verkhratsky A. *Purinergic signalling and the nervous system. Heidelberg: Springer.* 2012.
60. Ralevic V, Burnstock G. *Receptors for purines and pyrimidines.* Pharmacol Rev, 1998. **50**: p. 413-492.
61. Thimm D, Knospe M, Abdelrahman A, Moutinho M, Alsdorf BB, von Kügelgen I, Schiedel AC, Müller CE. *Characterization of new G protein-coupled adenine receptors in mouse and hamster.* Purinergic Signal, 2013. **9**: p. 415-426.
62. Volontè C, D'Ambrosi N. *Membrane compartments and purinergic signalling: the purinome, a complex interplay among ligands, degrading enzymes, receptors and transporters.* Febs J, 2009. **276**: p. 318-329.

63. Sachdeva S, Gupta M. *Adenosine and its receptors as therapeutic targets: An overview.* Saudi Pharm J, 2013. **21**: p. 245-253.
64. Drury AN, Szent-Gyorgy A. *The physiological activity of adenine compounds with special reference to their action upon the mammalian heart.* J Physiol (Lond), 1929. **68**: p. 47-61.
65. Haskò G, Linden J, Cronstein B, Pacher P. *Adenosine receptors: therapeutic aspects for inflammmatory and immune diseases.* Nat Rev Drug Discov, 2008. **7**: p. 759-770.
66. Haskò G, Cronstein BN. *Adenosine: an endogenous regulator of innate immunity.* Trends Immunol, 2004. **25**: p. 33-39.
67. Newby AC. *Adenosine and the concept of 'retaliatory metabolites'.* Trends Biochem Sci, 1984. **9**: p. 42-44.
68. Sebastião AM, Ribeiro JA. *Tuning and fine-tuning of synapses with adenosine.* Curr Neuropharmacol, 2009. **7**: p. 180-194.
69. Cronstein BN. *Adenosine, en endogenous anti-inflammatory agent.* J Appl Physiol, 1994. **75**: p. 5-13.
70. Linden J. *Cloned adenosine A_3 receptors: pharmacological properties, species differences and receptors functions* Trends Pharmacol Sci, 1994. **15**: p. 298-306.
71. Forsythe P, Ennis M. *Adenosine, mast cell and asthma.* Inflamm Res, 1999. **48**: p. 301-307.
72. Ham J, Evans BA. *An emerging role for adenosine and its receptors in bone homeostasis.* Front Endocrinol (Lausanne), 2012. **3**: p. 113.
73. Eltzschig HK. *Adenosine: an old drug newly discovered.* Anesthesiology, 2009. **111**: p. 904-914.
74. Boison D, Singer P, Shen HY, Feldon J, Yee BK. *Adenosine hypothesis of schizophrenia--opportunities for pharmacotherapy.* Neuropharmacology, 2012. **62**: p. 1527-1543.
75. Livingston M, Heaney LG, Ennis M. *Adenosine, inflammation and asthma--a review.* Inflamm Res, 2004. **53**: p. 171-178.
76. Zhou Y, Schneider DJ, Blackburn MR. *Adenosine signaling and the regulation of chronic lung disease.* Pharmacol Ther, 2009. **123**: p. 105-116.
77. Williams TC, Jarvis SM. *Multiple sodium-dependent nucleoside transport system in bovine renal brush-border membrane vescicles* Biochem J, 1991. **274**: p. 27-33.
78. Chiavegatti T, Costa Vl Jr, Araùjo MS, Godinho RO. *Skeletal muscle expresses the extracellular cyclicAMP–adenosine pathway.* Br J Pharmacol, 2008. **153**: p. 1331-1340.
79. Linden J. *Adenosine in tissue protection and tissue regeneration.* Mol Pharmacol, 2005. **67**: p. 1385-1387.
80. Ballarin M, Fredholm BB, Ambrosio S, Mahy N. *Extracellular level of adenosine in its metabolites in the striatum of awake rats: inhibition of uptake and metabolism.* Acta Physiol Scand, 1991. **142**: p. 97-103.
81. Van Calker D, Müller M, Hamprecht B. *Adenosine regulates, via two different types of receptors, the accumulation of cyclic AMP in cultured brain cells.* J Neurochem, 1979. **33**: p. 999-1005.
82. Jacobson KA, Gao ZG. *Adenosine receptors as therapeutic targets.* Nat Rev Drug Discov, 2006. **5** p. 247–264.
83. Fredholm BB, Ijzerman AP, Jacobson KA, Linden J, Müller CE. *International Union of Basic and Clinical Pharmacology. LXXXI. Nomenclature and classification of adenosine receptors-an update.* Pharmacol Rev, 2011. **63**: p. 1-34.
84. Cieślak M, Komoszyński M, Wojtczak A. *Adenosine A_{2A} receptors in Parkinson's disease treatment.* Purinergic Signal, 2008. **4**: p. 305-312.
85. Linden J. *Structure and function of A_1 adenosine receptors.* FASEB J, 1991. **5**: p. 2668-2676.
86. Zimmermann H. *Ectonucleotidases in the nervous system.* Novartis Found Symp, 2006. **276**: p. 113–128.

87. Benarroch EE. *Adenosine and its receptors: multiple modulatory functions and potential therapeutic targets for neurologic disease.* Neurology, 2008. **70**: p. 231-236.
88. Rose JB, Coe IR. *Physiology of nucleoside transporters: back to the future.* Physiology (Bethesda), 2008. **23**: p. 41-48.
89. Novak I. *ATP as a signaling molecule: the exocrine focus.* News Physiol Sci, 2003. **18**: p. 12-17.
90. Olah ME, Stiles GL. *Adenosine receptor subtypes: characterization and therapeutic regulation.* Annu Rev Pharmacol Toxicol, 1995. **35**: p. 581-606.
91. Chen JF, Eltzschig HK, Fredholm BB. *Adenosine receptors as drug targets--what are the challenges?* Nat Rev Drug Discov, 2013. **12**: p. 265-286.
92. Libert F, Parmentier M, Lefort A, Dinsart C, Van Sande J, Maenhaut C, Simons MJ, Dumont JE, Vassart G. *Selective amplification and cloning of four new members of the G protein-coupled receptor family.* Science, 1989. **244**: p. 569-572.
93. Fredholm BB. *Purinoceptors in the nervous system.* Pharmacol Toxicol, 1995. **76**: p. 228-239.
94. Fredholm BB, Cunha RA, Svenningsson P. *Pharmacology of adenosine A_{2A} receptors and therapeutic applications.* Curr Top Med Chem, 2002. **3**: p. 413-426.
95. Ohta A, Sitkovsky M. *Role of G-protein-coupled adenosine receptors in downregulation of inflammation and protection from tissue damage.* Nature, 2001. **414**: p. 916-920.
96. Marala RB, Mustafa SJ. *Direct evidence for the coupling of A2-adenosine receptor to stimulatory guanine nucleotide-binding-protein in bovine brain striatum.* J Pharmacol Exp Ther, 1993. **266**: p. 294-300.
97. Ferré S, Karcz-Kubicha M, Hope BT, Popoli P, Burgueño J, Gutiérrez MA, Casadó V, Fuxe K, Goldberg SR, Lluis C, Franco R, Ciruela F. *Synergistic interaction between adenosine A_{2A} and glutamate mGlu5 receptors: implications for striatal neuronal function.* PNAS, 2002. **99**: p. 11940-11945.
98. Corset V, Nguyen-Ba-Charvet KT, Forcet C, Moyse E, Chédotal A, Mehlen P. *Netrin-1-mediated axon outgrowth and cAMP production requires interaction with adenosine A_{2B} receptor.* Nature, 2000. **407**: p. 747-750.
99. Borrmann T, Hinz S, Bertarelli DC, Li W, Florin NC, Scheiff AB, Müller CE. *1-alkyl-8-(piperazine-1-sulfonyl)phenylxanthines: development and characterization of adenosine A_{2B} receptor antagonists and a new radioligand with subnanomolar affinity and subtype specificity.* J Med Chem, 2009. **52**: p. 3994-4006.
100. Ryzhov S, Novitskiy SV, Zaynagetdinov R, Goldstein AE, Carbone DP, Biaggioni I, Dikov MM, Feoktistov I. *Host $A_{(2B)}$ adenosine receptors promote carcinoma growth.* Neoplasia, 2008. **10**: p. 987-995.
101. Cacciari B, Pastorin G, Bolcato C, Spalluto G, Bacilieri M, Moro S. *A_{2B} adenosine receptor antagonists: recent developments.* Mini Rev Med Chem, 2005. **5**: p. 1053-1060.
102. Zhou QY, Li C, Olah ME, Johnson RA, Stiles GL, Civelli O. *Molecular cloning and characterization of an adenosine receptor: the A_3 adenosine receptor.* PNAS, 1992. **89**: p. 7432-7436.
103. Fishman P, Bar-Yehuda S, Liang BT, Jacobsonc KA. *Pharmacological and Therapeutic Effects of A_3 Adenosine Receptor (A_3AR) Agonists.* Drug Discov Today, 2012. **17**: p. 359-366.
104. Cinalli AR, Guarracino JF, Fernandez V, Roquel LI, Losavio AS. *Inosine induces presynaptic inhibition of acetylcholine release by activation of A_3 receptors at the mouse neuromuscular junction.* Br J Pharmacol, 2013. **169**: p. 1810-1823.
105. Ciruela F, Ferré S, Casadó V, Cortés A, Cunha RA, Lluis C, Franco R. *Heterodimeric adenosine receptors: a device to regulate neurotransmitter release.* Cell Mol Life Sci, 2006. **63** p. 2427–2431.
106. Sichardt K, Niebern K. *Adenosine A_1 receptor: Functional receptor-receptor interactions in the brain.* Purinergic Signalling, 2007. **3**: p. 285–298.
107. Niebera K, Michaelb S. *Adenosine receptors: Intermembrane receptor–receptor interactions in the brain.* Synergy, 2014. **1**: p. 83–91.

108. Rådegran G, Hellsten Y. *Adenosine and nitric oxide in exercise-induced human skeletal muscle vasodilatation.* Acta Physiol Scand, 2000. **168**: p. 575-591.
109. Vergauwen L, Hespel P, Richter EA. *Adenosine receptors mediate synergistsic stimulation of glucose uptake and transport by insulin and by contractions in rat skeletal muscle.* J Clin Inves, 1994. **93**: p. 974-981.
110. Clark KI, Barry SR. *Aminophylline enhances resting Ca^{2+} concentrations and twitch tension by adenosine receptor blockade in Rana pipiens.* J Physiol, 1994. **481**: p. 129-137.
111. Warren GL, Hulderman T, Liston BSA, Simeonova PP. *Toll-like and adenosine receptor expression in injured skeletal muscle.* Muscle Nerve, 2011. **44**: p. 85-92.
112. Urso ML, Wang R, Zambraski EJ, Liang BT. *Adenosine A_3 receptor stimulation reduces muscle injury following physical trauma and is associated with alterations in the MMP/TIMP response.* J Appl Physiol, 2012. **112**: p. 658-670.
113. Lynge J, Hellsten Y. *Distribution of adenosine A_1, A_{2A} and A_{2B} receptors in human skeletal muscle.* Acta Physiol Scand, 2000. **169**: p. 283-290.
114. Lynge J, Juel C, Hellsten Y. *Extracellular formation and uptake of adenosine during skeletal muscle contraction in the rat: role of adenosine transporters.* J Physiol, 2001. **537** p. 597-605.
115. Pitchford S, Day JW, Gordon A, Mochly-Rosen D. *Nicotinic acetylcholine receptor desensitization is regulated by activation-induced extracellular adenosine accumulation.* J Neurosci, 1992. **12**: p. 4540-4544.
116. Bernareggi A, Luin E, Pavan B, Parato G, Sciancalepore M, Urbani R, Lorenzon P. *Adenosine A_{2B} receptors enhance nAChR single channel activity and spontaneous intracellular calcium spiking occurring in mouse skeletal myotubes.* Acta Physiol (Oxf), 2015. **214**: p. 467-480.
117. Henning RH. *Purinoreceptors in neuromuscular transmission.* Pharmacol Ther, 1997. **74**: p. 115-128.
118. Smith DO. *Sources of adenosine released during neuromuscular transmission in the rat.* J Physiol (Lond), 1991. **432**: p. 343-354.
119. Cunha RA, Sebastiao AM. *Adenosine and adenine nucleotides are indipendently released from both the nerve terminals and the muscle fibers upon electrical stimulation of the innervated skeletal muscle of the frog.* Pflugers Arch, 1993. **424**: p. 503-510.
120. Garcia N, Priego M, Obis T, Santafe MM, Tomàs M, Besalduch N, Lanuza MA, Tomàz J. *Adenosine A_1 and A_{2A} receptors-mediated modulation of acetylcholine release in the mice neuromuscular junction.* Eur J Neurosci, 2013. **38**: p. 2229-2241.
121. Garcia N, Priego M, Hurtado E, Obis T, Santafe MM, Tomàs M, Lanuza MA, Tomàs J. *Adenosine A_{2B} and A_3 receptor location at the mouse neuromuscular junction.* J Anat, 2014. **225**: p. 109-117.
122. Santafé MM, Salon I, Garcia N, Lanuza MA, Uchitel OD, Tomàs J. *Modulation of ACh release by presynaptic muscarinic autoreceptors in the neuromuscular junction of the newborn and adult rat.* Eur J Neurosci, 2003. **17**: p. 119-127.
123. Adámek S, Shakirzyanova AV, Malomouzh AI, Naumenko NV, Vyskočil F. *Interaction of glutamate- and adenosine-induced decrease of acetylcholine quantal release at frog neuromuscular junction.* Physiol Res, 2010. **59**: p. 803-810.
124. Pousinha PA, Correia AM, Sebastião AM, Ribeiro JA. *Predominance of adenosine excitatory over inhibitory effects on transmission at the neuromuscular junction of infant rats.* J Pharmacol Exp Ther, 2010. **332**: p. 153-163.
125. Veggetti M, Muchnik S, Losavio A. *Effect of purines on calcium-independent acetylcholine release at the mouse neuromuscular junction.* Neuroscience, 2008. **154**: p. 1324-1336.
126. Muller CE, Jacobson KA. *Recent developments in adenosine receptor ligands and their potential as novel drugs.* Biochim Biophys Acta, 2011. **1808**: p. 1290–1308.
127. Dalpiaz A, Cacciari B, Vicentini CB, Bortolotti F, Spalluto G, Federico S, Pavan B, Vincenzi F, Borea PA, Varani K. *A novel conjugated agent between dopamine and an*

A_{2A} adenosine receptor antagonist as a potential anti-Parkinson multitarget approach. Mol Pharmacol, 2012. **9**: p. 591-604.
128. Dungo R, Deeks ED. *Istradefylline: first global approval.* Drugs, 2013. **73**: p. 875-882.
129. Ghimire G, Hage FG, Heo J, Iskandrian AE. *Regadenoson: a focused update.* J Nucl Cardiol, 2012. **20**: p. 284-288.
130. Gessi S, Merighi S, Fazzi D, Stefanelli A, Varani K, Borea PA. *Adenosine receptor targeting in health and disease.* Expert Opin Investig Drugs, 2011. **20**: p. 1591-1609.
131. Garvey N. *"Xenopus laevis" (On-line), Animal Diversity Web*. 2000; Available from: http://animaldiversity.org/accounts/Xenopus_laevis/.
132. Green SL. *Factors affecting oogenesis in the South African Clawed frog (Xenopus laevis).* Comp Med, 2002. **52**: p. 307-312.
133. Yao SYM, Cass CE, Young JD. *The Xenopus oocyte expression system for the cDNA cloning and characterization of plasma membrane transport proteins. In:Membrane transport: A Practical Approach. Baldwin SA, editor. Oxford University Press, Oxford, pp. 47-78*. 2000.
134. Goldin AL. *Maintenance of Xenopus laevis and oocyte injection. Methods in Enzmology, Vol. 207. Ion Channels. Rudy B, Iverson LE, editors. London: Academic Press; pp. 266–279.* 1992.
135. Dascal N, Landau EM, Lass Y. *Xenopus oocyte resting potential, muscarinic responces and the role of calcium and guanosine 3',5'-cyclic monophosphate.* J Physiol, 1984. **352**: p. 551-574.
136. Dumont JN. *Oogenesis in Xenopus laevis (Daudin). I. Stages of oocyte development in laboratory maintained animals. .* J Morphol, 1972. **136**: p. 153-180.
137. Hausen P, Riebesell M. *The early development of Xenopus laevis: an atlas of the histology*, ed. B. Springer-Verlag. 1991.
138. Bossi E, Fabbrini MS, Ceriotti A. *Exogenous protein expression in xenopus oocytes. Basic procedures.* Methods Mol Biol, 2007. **375**: p. 107-131.
139. Weber WM. *Endogenous ion channels in oocytes of xenopus laevis: recent developments* J Membr Biol, 1999. **170**: p. 1-12.
140. Fraser SP, Djamgoz MBA. *Xenopus oocytes: endogenous electrophysiological characteristics Current Aspects of the Neurosciences London: Macmillan Press; 267–315 vol. 4. ed. Osborne, N. N. pp.* 1992.
141. Vasilets LA, Schmalzing G, Mädefessel K, Haase W, Schwarz W. *Activation of protein kinase C by phorbol ester induces downregulation of the $Na^+/K(^+)$-ATPase in oocytes of Xenopus laevis.* J Membr Biol, 1990. **118**: p. 131-142.
142. Sigel E. *Use of Xenopus oocytes for the functional expression of plasma membrane proteins.* J Membr Biol, 1990. **117**: p. 201-221.
143. Weber WM, Cuppens H, Cassiman JJ, Clauss W, Van Driessche W. *Capacitance measurements reveal different pathways for the activation of CFTR.* Pflugers Arch, 1999. **438**: p. 561-569.
144. Lafaire AV, Schwarz W. *Voltage dependence of the rheogenic Na^+/K^+ ATPase in the membrane of oocytes of Xenopus laevis.* J Membr Biol, 1986. **91**: p. 46-51.
145. Wallace RA, Steinhardt RA. *Maturation of Xenopus oocytes. II. Observations on membrane potential.* Dev Biol, 1977. **57**: p. 305-316.
146. Kusano K, Miledi R, Stinnakre J. *Cholinergic and catecholaminergic receptors in the Xenopus oocyte membrane.* J Physiol, 1982. **328**: p. 143-170.
147. Dascal N. *The use of Xenopus oocytes for the study of ion channels.* CRC Crit Rev Biochem, 1987. **22**: p. 317-387.
148. Weber WM. *Ion currents of Xenopus laevis oocytes: state of the art.* Biochim Biophys Acta, 1999. **1421**: p. 213-233.
149. Dumont JN, Brummett AN. *Oogenesis in Xenopus laevis (Daudin). V. Relationship between developing oocytes and their investing tissues.* J Morphol, 1978. **155**: p. 73-98.
150. Lotan I, Dascal N, Cohen S, Lass Y. *Adenosine-induced slow ionic currents in the Xenopus oocyte.* Nature, 1982. **298**: p. 572-574.

151. Stinnakre J, Van Renterghem C. *Cyclic adenosine monophosphate, calcium, acetylcholine and the current induced by adenosine in the Xenopus oocyte.* J Physiol, 1986. **374**: p. 551-569.
152. Greenfield LJ, Jr Hackett JT, Linden J. *Xenopus oocyte K^+ current. I. FSH and adenosine stimulate follicle cell-dependent currents.* Am J Physiol Cell Physiol, 1990. **259**: p. C775–C783.
153. Greenfield LJ, Jr Hackett JT, Linden J. *Xenopus oocyte K^+ current. II. Adenylyl cyclase-linked receptors on follicle cells.* Am J Physiol Cell Physiol, 1990. **259**: p. C784–C791.
154. Honoré E, Lazdunski M. *Hormone-regulated K^+ channels in follicle-enclosed oocytes are activated by vasorelaxing K^+ channel openers and blocked by antidiabetic sulfonylureas.* PNAS, 1991. **88**: p. 5438-5442.
155. Arellano RO, Woodward RM, Miledi R. *in Ion Channels, Ion channels and membrane receptors in follicle-enclosed Xenopus oocytes, ed Narahashi T (Plenum Press, New York), 4.* 1996.
156. Arellano RO, Garay E, Miledi R. *Cl^- currents activated via purinergic receptors in Xenopus follicles.* Am J Physiol Cell Physiol 1998. **274**: p. C333–C340.
157. King BF, Pintor J, Wang S, Ziganshin AU, Ziganshina LE, Burnstock G. *A novel P1 purinoceptor activates an outward K^+ current in follicular oocytes of Xenopus laevis.* J Pharmacol Exp Ther 1996. **276**: p. 93–100.
158. Matsuoka T, Nishizaki T, Nomura T, Mori M, Okada Y. *ATP produces potassium currents via P3 purinoceptor in the follicle cell layer of Xenopus oocytes.* Neurosc Lett, 1998. **248**: p. 130-132.
159. Miledi R, Woodward RM. *Effects of defolliculation on membrane current responses of Xenopus oocytes.* J Physiol (Lond), 1989. **416**: p. 601-621.
160. Gelerstein S, Shapira H, Dascal N, Yekuel R, Oron Y. *Is a decrease in cyclic AMP a necessary and sufficient signal for maturation of amphibian oocytes?* Dev Biol, 1988. **127**: p. 25-32.
161. Finidori J, Hanoune J, Baulieu EE. *Adenylate cyclase in Xenopus laevis oocytes: characterization of the progesterone-sensitive, membrane-bound form.* Mol Cell Endocrinol, 1982. **28**: p. 211-227.
162. Kobayashi T, Ikeda K, Kumanishi T. *Functional characterization of an endogenous Xenopus oocyte adenosine receptor.* Br J Pharmacol, 2002. **135**: p. 313-322.
163. Gurdon JB, Lane CD, Woodland HR, Marbaix G. *Use of frog eggs and oocytes for the study of messenger RNA and its translation in living cells.* Nature, 1971. **233**: p. 177-182.
164. Miledi R, Parker I, Sumikawa K. *Properties of acetylcholine receptors translated by cat muscle mRNA in Xenopus oocytes.* EMBO J, 1982. **1**: p. 1307-1312.
165. Barnard EA, Miledi R, Sumikawa K. *Translation of exogenous messenger RNA coding for nicotinic acetylcholine receptor produces functional receptors in Xenopus oocytes.* PNAS, 1982. **215**: p. 241-246.
166. Gundersen CB, Miledi R, Parker I. *Messenger RNA from human brain induces drug- and voltage-operated channels in Xenopus oocytes.* Nature, 1984. **308**: p. 421-424.
167. Gundersen CB, Miledi R, Parker I. *Glutamate and kainate receptors induced by rat brain messenger RNA in Xenopus oocytes.* Proc R Soc Lond B Biol Sci, 1984. **221**: p. 127-143.
168. Miledi R, Palma E, Eusebi F. *Microtransplantation of neurotransmitter receptors from cells to Xenopus oocyte membranes: new procedure for ion channel studies* Methods Mol Biol, 2006. **322**: p. 347-355.
169. Miledi R, Eusebi F, Martínez-Torres A, Palma E, Trettel F. *Expression of functional neurotransmitter receptors in Xenopus oocytes after injection of human brain membranes.* PNAS, 2002. **99**: p. 13238-13242.
170. Le Cahérec F, Bron P, Verbavatz JM, Garret A, Morel G, Cavalier A, Bonnec G, Thomas D, Gouranton J, Hubert JF. *Incorporation of proteins into (Xenopus) oocytes by*

proteoliposome microinjection: functional characterization of a novel aquaporin. J Cell Sci, 1996. **109**: p. 1285-1295.
171. Baker G, Dunn S, Holt A. *Handbook of neurochemistry and molecular neurobiology: practical neurochemistry methods. Springer Science & Business Media*. Vol. 6. 2007.
172. Eusebi F, Palma E, Amici M, Miledi R. *Microtransplantation of ligand-gated receptor-channels from fresh or frozen nervous tissue into Xenopus oocytes: A potent tool for expanding functional information.* Prog Neurobiol, 2009. **88**: p. 32-40.
173. Palma E, Trettel F, Fucile S, Renzi M, Miledi R, Eusebi F. *Microtransplantation of membranes from cultured cells to Xenopus oocytes: a method to study neurotransmitter receptors embedded in native lipids.* PNAS, 2003. **100**: p. 2896-2900.
174. Bernareggi A, Dueñas Z, Reyes-Ruiz JM, Ruzzier F, Miledi R. *Properties of glutamate receptors of Alzheimer's disease brain transplanted to frog oocytes.* PNAS, 2007. **104**: p. 2956-2960.
175. Limon A, Reyes-Ruiz JM, Miledi R. *Microtransplantation of neurotransmitter receptors from postmortem autistic brains to Xenopus oocytes.* PNAS, 2008. **105**: p. 10973-10937.
176. Marsal J, Tigyi G, Miledi R. *Incorporation of acetylcholine receptors and Cl- channles in Xenopus oocytes injected with Torpedo electroplaque membranes.* PNAS, 1995. **92**: p. 5224-5228.
177. Limon A, Reyes-Ruiz JM, Miledi R. *GABA and glutamate receptors of the autistic brain. In: Autism- A Neurodevelopmental Journey from Genes to Behavior. Ed. Intech. ISBN 978-953-307-493-1.* 2011.
178. Miledi R, Palma E, Eusebi F. *Microtransplantation of neurotransmitter receptors from cells to Xenopus oocyte membranes: new procedure for ion channel studies.* Methods Mol Biol, 2006. **322**: p. 347-355.
179. Gal B, Ivorra I, Morales A. *Functional incorporation of exogenous proteins into the Xenopus oocyte membrane does not depend on intracellular calcium increase.* Plugers Arch-Eur J Physiol 2000. **440**: p. 852-857.
180. Morales A, Aleu J, Ivorra I, Ferragut JA, Gonzalez-Ros JM, Miledi R. *Incorporation of reconstituted acetylcholine receptors from Torpedo into the Xenopus oocyte membrane.* PNAS, 1995. **95**: p. 8468–8472.
181. Guan B, Chen X, Zhang H. *Two-Electrode Voltage Clamp.* Methods Mol Biol, 2013. **998**: p. 79-89.
182. Miledi R. *A calcium-dependent transiet outward current in Xenopus laevis oocytes.* Proc R Soc Lond B Biol Sci, 1982. **215**: p. 491-497.
183. Bufler J, Franke C, Witzemann V, Ruppersberg JP, Merlitze S, Dudel J. *Desensitization of embryonic nicotinic acetylcholine receptors expressed in Xenopus oocytes.* Neurosci Lett 1993. **152**: p. 77-80.
184. Grassi F, Palma E, Mileo AM, Eusebi F. *The desensitization of the embryonic mouse muscle acetylcholine receptor depends on the cellular environment.* Pflugers Arch, 1995. **430**: p. 787-794.
185. Mileo AM, Palma E, Polenzani L, Limatola C, Grassi F, Eusebi F. *Protein kinase C modulates exogenous acetylcholine current in Xenopus oocytes.* J Neurosci Res, 1995. **41**: p. 443-451.
186. Bernareggi A, Ren E, Borelli V, Vita F, Constanti A, Zabucchi G. *Xenopus laevis oocytes as a model system for studying the interaction between asbestos fibres and cell membranes.* Toxicol Sci, 2015. **145**: p. 263-272.
187. Bernareggi A, Reyes-Ruiz JM, Lorenzon P, Ruzzier F, Miledi R. *Microtransplantation of acetylcholine receptors from normal or denervated rat skeletal muscles to frog oocytes.* J Physiol, 2011. **589**: p. 1133-1142.
188. Irintchev A, Langer M, Zweyer M, Theisen R, Wernig A. *Functional improvement of damaged adult mouse muscle by implantation of primary myoblasts.* J Physiol, 1997. **500**: p. 775–785.
189. Waterborg JH, Matthews HR. *The Lowry method for protein quantitation.* Methods Mol Biol, 1994. **32**: p. 1-4.

190. Dalpiaz A, Scatturin A, Pavan B, Biondi C, Vandelli MA, Forni F. *Poly(lactic acid) microspheres for the sustained release of a selective A_1 receptor agonist.* J Control Release, 2001. **73**: p. 303-313.
191. Delpire E, Gagnon KB, Ledford JJ, Wallace JM. *Housing and husbandry of Xenopus laevis affect the quality of oocytes for heterologous expression studies.* J Am Assoc Lab Anim Sci, 2011. **50**: p. 46-53.
192. Elsner HA, Honck HH, Willmann F, Kreienkamp Hj, Iglauer F. *Poor quality of oocytes from Xenopus laevis used in laboratory experiments: prevention by use of antiseptic surgical technique and antibiotic supplementation* Comp Med, 2000. **50**: p. 206-211.
193. Dascal N, Landau EM. *Types of muscarinic response in Xenopus oocytes.* Life Sciences, 1980. **27**: p. 1423-1428.
194. Ogden DC, Colquhoun D. *Ion channel block by acetylcholine, carbachol and suberyldicholine at the frog neuromuscular junction.* Proc R Soc Lond B Biol Sci, 1985. **225**: p. 329-355.
195. St John PA, Gordon H. *Agonists cause endocytosis of nicotinic acetylcholine receptors on cultured myotubes.* J Neurobiol, 2001. **49**: p. 212-223.
196. Bahima L, Aleu J, Martìn-Satué M, Muhaisen A, Blasi J, Marsal J, Solsona C. *Endogenous hemichannels play a role un the release of ATP from Xenopus oocyte.* J Cell Physiol, 2006. **209**: p. 95-102.
197. Phelps PT, Anthes JC, Correll CC. *Characterization of adenosine receptors in the human bladder carcinoma T24 cell line.* Eur J Pharmacol 2006. **536**: p. 28–37.
198. Xu Y, Ravid K, Smith BD. *Major histocompatibility class II transactivator expression in smooth muscle cells from A_{2b} adenosine receptor knock-out mice: crosstalk between the adenosine and interferon-gamma signaling.* J Biol Chem, 2008. **283**: p. 14213–14220.
199. Van der Hoeven D, Wan TC, Gizewski ET, Kreckler LM, Maas JE, Van Orman J, Ravid K, Auchampach JA. *A role for the low-affinity A_{2B} adenosine receptor in regulating superoxide generation by murine neutrophils.* J Pharmacol Exp Ther, 2011. **338**: p. 1004–1012.
200. Roseti C, Palma E, Martinello K, Fucile S, Morace R, Esposito V, Cantore G, Arcella A, Giangaspero F, Aronica E, Mascia A, Di Gennaro G, Quarato PP, Manfredi M, Cristalli G, Lambertucci C, Marucci G, Volpini R, Limatola C, Eusebi F.. *Blockage of A_{2A} and A_3 adenosine receptors decreases the desensitization of human GABA(A) receptors microtransplanted to Xenopus oocytes.* PNAS, 2009. **106**: p. 15927-15931.
201. Son YK, Park WS, Ko JH, Han J, Kim N, Earm YE. *Protein kinase A-dependent activation of inward rectifier potassium channels by adenosine in rabbit coronary smooth muscle cells.* Biochem Biophys Res Commun, 2005. **337**: p. 1145-1152.
202. Liu IM, Lai TY, Tsai CC, Cheng JT. *Characterization of adenosine A_1 receptor in cultured myoblast C2C12 cells of mice.* Auton Neurosci, 2001. **87**: p. 59–64.
203. Olah ME, Gallo-Rodriguez C, Jacobson KA, Stiles GL. *125I-4-aminobenzyl-5'-N-methylcarboxamidoadenosine, a high affinity radioligand for the rat A_3 adenosine receptor.* Mol Pharmacol, 1994. **45**: p. 978–982.
204. Yang Z, Sun W, Hu K. *Adenosine A_1 receptors selectively target protein kinase C isoforms to the caveolin-rich plasma membrane in cardiac myocytes.* Biochimica et Biophysica Acta, 2009. **1793**: p. 1868–1875.
205. Onda T, Hashimoto Y, Nagai M, Kuramochi H, Saito S, Yamazaki H, Toya Y, Sakai I, Homcy CJ, Nishikawa K, Ishikawa Y. *Type-specific regulation of adenylyl cyclase. Selective pharmacological stimulation and inhibition of adenylyl cyclase isoforms.* J Biol Chem, 2001. **276**: p. 47785-47793.
206. Aldehni F, Tang T, Madsen K, Plattner M, Schreiber A, Friis UG, Hammond HK, Han PL, Schweda F. *Stimulation of renin secretion by catecholamines is dependent on adenylyl cyclase AC5 and AC6.* Hypertension, 2011. **57**: p. 460–468.
207. Hu CL, Chandra R, Ge H, Pain J, Yan L, Babu G, Depre C, Iwatsubo K, Ishikawa Y, Sadoshima J, Vatner SF, Vatner DE. *Adenylyl cyclase type 5 protein expression during*

cardiac development and stress. Am J Physiol Heart Circ Physiol, 2009. **297**: p. H1776-1782.
208. Guzmán L, Romo X, Grandy R, Soto X, Montecino M, Hinrichs M, Olate J. *A Gbetagamma stimulated adenylyl cyclase is involved in Xenopus laevis oocyte maturation.* J Cell Physiol, 2005. **202**: p. 223-229.
209. Sadana R, Dessauer CW. *Physiological roles for G protein-regulated adenylyl cyclase isoforms: Insights from Knockout and overexpression studies.* Neurosignals, 2009. **17**: p. 5–22.
210. Lotan I, Dascal N, Oron Y, Cohen S, Lass Y. *Adenosine-induced K+ current in the Xenopus oocyte and the role of adenosine 3',5'-monophosphate.* Mol Pharmacol, 1985. **28**: p. 107-177.
211. Hoffman PW, Ravindran A, Huganir RL. *Role of phosphorylation in desensitization of acetylcholine receptors expressed in Xenopus oocytes.* J Neurosci, 1994. **14**: p. 4185-4195.
212. Arellano RO, Garay E, Vázquez-Cuevas F. *Functional interaction between native G protein-coupled purinergic receptors in Xenopus follicles.* Proc Natl Acad Sci U S A, 2009. **106**: p. 16680-16685.
213. Klotz KN. *Adenosine receptors and their ligands.* Naunyn Schmiedebergs Arch Pharmacol, 2000. **362**: p. 382-391.
214. Shakirzyanova AV, Bukharaeva EA, Nikolsky EE, Giniatullin RA. *Negative cross-talk between presynaptic adenosine and acetylcholine receptors.* Eur J Neurosci, 2006. **24**: p. 105-115.
215. Silinsky EM, Ginsborg BL. *Inhibition of acetylcholine release from preganglionic frog nerves by ATP but not adenosine.* Nature, 1983. **305**: p. 327-328.
216. Tomàs J, Santafé MM, Garcia N, Lanuza MA, Tomàs M, Besalduch N, Obis T, Priego M, Hurtado E. *Presynaptic membrane receptors in acetylcholine release modulation in the neuromuscular synapse.* J Neurosci Res, 2014. **92**: p. 543-554.
217. Lanuza MA, Gizaw R, Viloria A, González CM, Besalduch N, Dunlap V, Tomàs J, Nelson PG. *Phosphorylation of the nicotinic acetylcholine receptor in myotube-cholinergic neuron cocultures.* J Neurosci Res, 2006. **83**: p. 1407–1414.
218. Martinez-Pena y Valenzuela I, Pires-Oliveira M, Akaaboune M. *PKC and PKA regulate AChR dynamics at the neuromuscular junction of living mice.* PLoS One, 2013. **8**: p. e81311.
219. Park A, Stacy M. *Istradefylline for the treatment of Parkinson's disease.* Expert Opin Pharmacother, 2012. **13**: p. 111-114.